



Norwegian University of  
Science and Technology

# Modeling and Simulation of Hydropower Plant in Scilab

**Erik Rognaldsen**

Master of Energy Use and Energy Planning

Submission date: June 2017

Supervisor: Bjørnar Svingen, EPT

Norwegian University of Science and Technology  
Department of Energy and Process Engineering



EPT-M-2017- XX

**MASTEROPPGAVE**

for

Student Erik Rognaldsen

Våren 2017

Modellering og simulering av vannkraftverk i Scilab

*Modeling and simulation of hydropower plant in Scilab***Bakgrunn og målsetting**

Høsten 2016 har studenten modellert og simulert et kraftverk i Xcos i Scilab ([www.scilab.org](http://www.scilab.org)). Kraftverket bestod av en turbin tilkoblet trykksjakt, overvann og undervann. Turbinmodellen som ble brukt er en linearisert versjon av Torbjørn Nielsens analytiske turbinmodell, der lineariserings-parameterne er gjort som beskrevet i diverse paper fra IEEE. Resultatene er meget lovende, og studenten skal arbeide videre med denne modellen.

Modellen av vannvegene skal inkludere en svingesjakt og tilløpstunnel, og det skal sees på mulighetene for å modellere elastisk trykksjakt. Svingesjakt-modellen skal verifiseres av kandidaten med eksperimenter i Vannkraft-laboratoriet. Eksperimentene skal gjøres på den nye riggen for u-rør-svingning.

Det ønskelig at Scilab/Xcos-modellen knyttes nærmere opp til Torbjørn Nielsens modell på et teoretisk grunnlag, slik at utledninger for de partiell-deriverte blir gjort med utgangspunkt i Torbjørn Nielsens modell. Videre er det ønskelig at modellen kan kjøres på isolernett slik som nå, og at den også kan kjøre på felles nett. På felles nett skal frekvens(turtall) gis inn som en parameter. Modellen(e) av kraftverk skal sammenlignes med tilsvarende modell i LVTrans. Det skal også ses på hvilke muligheter man har for frekvensplananalyse i Scilab/Xcos med modellen.

## Oppgaven bearbeides ut fra følgende punkter

- 1 Legge til svingesjakt og tilførselstunnel på eksisterende modell
- 2 Verifisere svingesjaktmodell med tester på rig i laboratoriet
- 3 Se på mulighetene for elastisk trykksjakt og legge til dette hvis mulig og praktisk.
- 4 Teoretisk utledning av partiell-deriverte til bruk i Xcos-modellen, basert på Torbjørn Nielsens turbinmodell.
- 5 Simulere både på isolert nett og på felles nett, og sammenligne med LVTrans
- 6 Se på muligheter for frekvensplananalyse i Scilab/Xcos
- 7 Det forutgående prosjektarbeid og framtidig arbeid i denne master skal beskrives i et faginnlegg, "paper", som skal presenteres ved 7th International Symposium on Current Research in Hydraulic Turbines (CRHT-VII) at Katmandu University, april 2017.
- 8 Skrive en rapport.

” - ”

Senest 14 dager etter utlevering av oppgaven skal kandidaten levere/sende instituttet en detaljert fremdrift- og eventuelt forsøksplan for oppgaven til evaluering og eventuelt diskusjon med faglig ansvarlig/veiledere. Detaljer ved eventuell utførelse av dataprogrammer skal avtales nærmere i samråd med faglig ansvarlig.

Besvarelsen redigeres mest mulig som en forskningsrapport med et sammendrag både på norsk og engelsk, konklusjon, litteraturliste, innholdsfortegnelse etc. Ved utarbeidelsen av teksten skal kandidaten legge vekt på å gjøre teksten oversiktlig og velskrevet. Med henblikk på lesning av besvarelsen er det viktig at de nødvendige henvisninger for korresponderende steder i tekst, tabeller og figurer anføres på begge steder. Ved bedømmelsen legges det stor vekt på at resultatene er grundig bearbeidet, at de oppstilles tabellarisk og/eller grafisk på en oversiktlig måte, og at de er diskutert utførlig.

Alle benyttede kilder, også muntlige opplysninger, skal oppgis på fullstendig måte. For tidsskrifter og bøker oppgis forfatter, tittel, årgang, sidetall og eventuelt figurnummer.

Det forutsettes at kandidaten tar initiativ til og holder nødvendig kontakt med faglærer og veileder(e). Kandidaten skal rette seg etter de reglementer og retningslinjer som gjelder ved alle (andre) fagmiljøer som kandidaten har kontakt med gjennom sin utførelse av oppgaven, samt etter eventuelle pålegg fra Institutt for energi- og prosesssteknikk.

Risikovurdering av kandidatens arbeid skal gjennomføres i henhold til instituttets prosedyrer. Risikovurderingen skal dokumenteres og inngå som del av besvarelsen. Hendelser relatert til kandidatens arbeid med uheldig innvirkning på helse, miljø eller sikkerhet, skal dokumenteres og inngå som en del av besvarelsen. Hvis dokumentasjonen på risikovurderingen utgjør veldig mange sider, leveres den fulle versjonen elektronisk til veileder og et utdrag inkluderes i besvarelsen.

I henhold til ”Utfyllende regler til studieforskriften for teknologistudiet/sivilingeniørstudiet” ved NTNU § 20, forbeholder instituttet seg retten til å benytte alle resultater og data til undervisnings- og forskningsformål, samt til fremtidige publikasjoner.

Besvarelsen leveres digitalt i DAIM. Et faglig sammendrag med oppgavens tittel, kandidatens navn, veileders navn, årstall, institutt navn, og NTNUs logo og navn, leveres til instituttet som en separat pdf-fil. Etter avtale leveres besvarelse og evt. annet materiale til veileder i digitalt format.

Arbeid i laboratorium (vannkraftlaboratoriet, strømningsmekanisk, varmeteknisk)

Feltarbeid

NTNU, Institutt for energi- og prosesseteknikk, 15. januar 2017



Bjørnar Svingen

Faglig ansvarlig/veileder

Medveileder(e): Pål-Tore Selbo Storli

---

# Abstract

A hydro power plant is modeled in a computer application called Scilab, an open source MATLAB clone with capabilities to create block diagrams and do system simulations. The system is designed to do both frequency regulation when running in island operation and power regulation in a stiff power network. The conduit system are set up with a dynamic penstock model, surge shaft and a rigid head-race tunnel. Draft tube and a lower surge shaft are also been implemented. It is used a linear turbine model which utilize linearized turbine characteristics of a designed turbine to get a detailed description of the turbine behavior. The linearization are performed with a computer program based on modified Euler's turbine equations deduced by Torbjørn Nielsen. The model is then evaluated up against a hydro power simulation tool called LVTrans, a program coded in LabVIEW based on the method of characteristics.

The scilab model shows good performance for simulations around its operating point. Simulation in island mode shows a frequency deviation between the models during a 10% load drop of 0.25Hz, or 0.5%. Simulating in stiff grid both models responds similarly to a frequency change of +0.01Hz decreasing the turbine power output by 16.7% with a droop of 6%. The system simulation performance of mass oscillations and water hammer is also tested. The simulations was performed with a change in the friction factor to a more representative number for an turbulent and flow fluctuating situations. This gave good results compared to LVTrans simulations, but it gave too much friction at the end of the event as the mass flow fluctuations reaches zero.

The surge shaft model is evaluated up against a u-pipe test rig located at the water power laboratory. Comparing simulations to the rig tests gave indications that the model is suited for simulating transient pressure pulsations in form of mass oscillations. It also shows that the friction model brakes the pulsations too fast resulting in a decrease in amplitude and the time to reach steady state gets too short.

**Keywords:** Hydropower modeling, block diagram, linearized Francis turbine, dynamic penstock, model verification.

---

# Sammendrag

Modelering av et vannkraft verk er utført i et program kalt Scilab. Scilab gir mulighet for numerisk kalkulering og system-modellering likt som MATLAB, men er uten kostnader og har åpen kildekode. Det modelerte anlegget er designet for å utføre både frekvenssimuleringer i isolert nett samt effektregulering mot stivt nett. Systemet er modelert med en dynamisk rørgate, øvre og nedre svingesjakt, sugerør samt inngangstunnel. Det er benyttet en linearisert fransis turbin modell basert på modifiserte Euler turbin ligninger utviklet av Torbjørn Nielsen.

Modellen er blitt testet opp mot et program utviklet i labVIEW kalt LVTrans. Dette programmet er basert på karakteristikk metoden og er et utprøvd program av bla. statkraft med gode resultater. Dette vil fungere som en mal for hvordan scilab modellen presterer og blir evaluert der etter. Kjøringer i øydrift avslører at turbinen har et begrenset arbeidsområde der den gir gode resultater. Lastavslag fra 85% til 75% gir veldig liten forskjell i transient frekvens økning ( $0.25Hz$ ). Kjøringer med større last avslag som fra 100% til 50% gir en forskjell på 4Hz som er ca. halvparten av hva LVTrans simulerte. Simulering i stivt nett gir de beste resultatene der det er svært lite forskjell mellom modellene. Begge responderte likt ved en frekvensendring på  $+0.01Hz$  og strupet produksjonen med 16.7% ca 15.7MW med en statikk på 6%.

Systemets ytelse for trykktransienter og massesvinginger er også testet. Scilab modellen viser gode resultater, da på tross av enkel statisk friksjonsmodel, men ved bruk av reléer i modellen er det mulig å endre friksjonskoeffisienter under kjøringen noe som kompenserer for manglende samsvar mellom modellene. Det er også utført trykksjakt valitering med urør-rig ved vannkraft laboratoriet på NTNU. Kjøringene er validert opp mot trykksjakten på riggen og simuleringene vier tilfredsstillende resultater, men med noe avvik. Kjøringene syneligjør den enkle friksjonsmodellen som scilab modellen tar i bruk og avvik forkommer ved at simuleringer gir lavere trykkamplituder, og massesvingningene dør ut for kjapt.

Oppsummert, viser modellen lovende resultater sammenliknet med LVTrans, men den har sine restriksjoner da turbinen er linearisert og friksjonsmodellen er statisk.

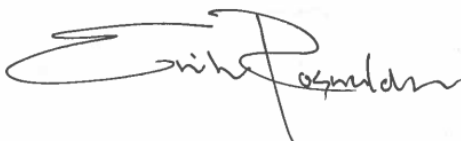
---

# Preface

The master thesis has been written at the Waterpower Laboratory under the Department of Energy and Process Engineering at the Norwegian University of Science and Technology. During the last semester, a simulation tool for hydropower simulations has been developed in a program called Scilab. The process of system modelling and increasing the quality of simulation has been some of the central challenges. The master thesis is a continuation and extension of the project work conducted during the autumn semester 2016.

I would like to thank my supervisor Bjørnar Svingen for supporting, and for motivating me during the whole last year at NTNU. Special thanks to PhD candidates at the lab for their availability and good discussions. Also special thanks to my girlfriend Kathrine who has been supportive and patient during the busy times working with the thesis. Thanks to my parents for being motivational, and supporting me in every way. Also thanks to the department of energy and process engineering for allowing me to write my master thesis at the water power laboratory.

Last but not least, thanks to all my fellow students at the Waterpower Laboratory for making the last semesters amazingly great, and the trip to Nepal unforgettable. Working in such competent and enjoyable environment has made the last year one of the best ones so far.

A handwritten signature in black ink, appearing to read 'Erik Rognaldsen', with a large, stylized initial 'E'.

Erik Rognaldsen

Trondheim, June 15, 2017



---

# Table of Contents

<b>Summary</b>	<b>i</b>
<b>Sammendrag</b>	<b>ii</b>
<b>Preface</b>	<b>iii</b>
<b>Table of Contents</b>	<b>ix</b>
<b>List of Tables</b>	<b>xi</b>
<b>List of Figures</b>	<b>xvi</b>
<b>Nomenclature</b>	<b>xvii</b>
<b>1 Introduction</b>	<b>1</b>
1.1 Motivation . . . . .	1
1.2 Thesis Description . . . . .	2
1.3 System Introduction . . . . .	3
<b>2 Previous Work</b>	<b>5</b>

---

2.1	Project Work . . . . .	5
2.2	Paper Presented at the 7th International Symposium on Current Research in Hydraulic Turbines . . . . .	6
<b>3</b>	<b>Theory</b>	<b>7</b>
3.1	General Equations . . . . .	8
3.2	Transient Fundamentals . . . . .	9
3.2.1	Pressure wave velocity . . . . .	9
3.2.2	Wave reflection time . . . . .	10
3.2.3	Mass Forces . . . . .	11
3.3	Friction Losses . . . . .	13
3.4	Surge shaft . . . . .	17
3.4.1	Surge shaft Oscillations . . . . .	17
3.4.2	Surge Shaft Transfer Function . . . . .	18
3.5	Penstock and Tunnels . . . . .	20
3.5.1	Dynamic penstock . . . . .	20
3.5.2	Approximation of Tanh . . . . .	20
3.5.3	RLC Penstock Model . . . . .	21
3.5.4	Static Tunnel Model . . . . .	23
<b>4</b>	<b>Modelling and Simulation Tools</b>	<b>25</b>
4.1	Scilab . . . . .	26
4.2	LVTrans . . . . .	27
<b>5</b>	<b>Hydropower Modelling</b>	<b>29</b>
5.1	Modeling scenarios . . . . .	31
5.2	Hydraulic System . . . . .	32

---

5.2.1	Penstock . . . . .	32
5.2.2	Head Race Tunnel and Draft Tube . . . . .	34
5.3	Surge Shaft . . . . .	36
5.4	Surgeshaft validation model . . . . .	37
5.5	Turbine . . . . .	38
5.6	PID - Regulator . . . . .	41
5.7	Servo System . . . . .	43
5.8	PID Tuning . . . . .	44
5.8.1	Method 1 . . . . .	44
5.8.2	PID tuning by frequency analysis . . . . .	45
<b>6</b>	<b>Simulation and Analysis</b>	<b>47</b>
6.1	System Setup . . . . .	48
6.1.1	Scilab Setup . . . . .	49
6.1.2	LVTrans Setup . . . . .	55
6.2	Functional Requirement . . . . .	56
6.3	Stability Analysis . . . . .	57
6.4	Evaluation of Hydraulic Systems in Scilab . . . . .	60
6.4.1	Comparing Dynamic and Static Penstock . . . . .	60
6.4.2	The Effect of Extending Penstock Length . . . . .	62
6.4.3	The effect of adding a draft tube and lower surge shaft . . . . .	63
6.5	Model Validation with LVTrans . . . . .	64
6.5.1	Frequency regulation in island mode. . . . .	64
6.5.2	Power Regulation in Stiff Grid Mode. . . . .	65
6.5.3	Water Hammer and Mass Oscillations . . . . .	67

---

---

<b>7</b>	<b>Laboratory Work</b>	<b>71</b>
7.1	Laboratory Setup . . . . .	72
7.2	Results From the Rig . . . . .	74
7.3	Rig results V.S Scilab model . . . . .	76
<b>8</b>	<b>Discussion</b>	<b>79</b>
8.1	Model Validation . . . . .	80
8.2	Model Stability . . . . .	81
8.3	Scilab VS LVTrans . . . . .	82
8.3.1	Frequency regulation in Island mode . . . . .	82
8.3.2	Power regulation in Stiff Grid Mode . . . . .	82
8.3.3	Mass oscillation and water hammer simulations . . . . .	83
8.4	Surgeshaft Verification With Test Rig . . . . .	84
<b>9</b>	<b>Conclusion</b>	<b>85</b>
<b>10</b>	<b>Further Work</b>	<b>87</b>
	<b>Bibliography</b>	<b>89</b>
	<b>Appendix</b>	<b>A</b>
<b>A</b>		<b>A-1</b>
<b>B</b>		<b>B-1</b>
<b>C</b>		<b>C-1</b>
<b>D</b>		<b>D-1</b>

---

**E**

**E-1**

**F**

**F-1**

**G**

**G-1**

---

# List of Tables

3.1	Typical surface roughness on different materials. [15]	14
3.2	RLC component description	23
5.1	Hydraulic system parameter values.	30
5.2	Turbine specifications	40
5.3	Proposal for PID tuning by frequency analysis [9]	45
6.1	Values from comparing dynamic and static penstock	62
6.2	Values inserted in the scilab model during the simulations	63
7.1	Losses in the test pipe under different flow scenarios.	73
7.2	Values inserted in the scilab model during the simulations	76
10.1	Parameter values for the head race tunnel	A-1
10.2	Parameter values for the penstock	A-3
10.3	Values for the parameters, a and b based on earlier experiences.	B-2



---

# List of Figures

1.1	General layout of the Norwegian island operated turbine. . . . .	3
1.2	Simulation set up for stiff grid mode. . . . .	4
2.1	Block diagram made in the project work fall 2016. . . . .	5
3.1	A representation of pressure propagation in a conduit.[5] . . . . .	10
3.2	Description of mass forces during transient state. . . . .	11
3.3	The moody diagram, used to obtain friction factor $f$ [10] . . . . .	14
3.4	Cross section of the inlet tunnel . . . . .	15
3.5	Cross section sketch of the conduit system at the susrge shaft and the forbay. . . . .	17
3.6	A penstock with lenght a $L$ can be represented with this equivalent circuit schematic . . . . .	22
4.1	Interface of scilab . . . . .	26
4.2	Interface of LVTrans . . . . .	27
5.1	Cross section of the system. . . . .	29
5.2	General layout for the system in grid mode with frequency regulation. . . . .	31

---

5.3	General layout for the system in stiff network mode with power regulation.	31
5.4	General layout for the hydraulic system used in the simulations with scilab.	32
5.5	Block diagram from scilab describing the penstock used in the simulations.	33
5.6	Transfer function block representing the RLC penstock model . . . . .	34
5.7	Transfer function block from scilab describing the head-race tunnel used in the simulations. . . . .	35
5.8	Transfer function block from scilab describing the draft tube tunnel used in the simulations. . . . .	35
5.9	Transfer function block from scilab describing the surge shaft used in the simulations. . . . .	36
5.10	Block diagram for simulation of the test rigg at the laboratory. . . . .	37
5.11	The model for surge shaft validation with scilab . . . . .	37
5.12	Picture of interface of the programe used to linearize the turbine characteristics. . . . .	39
5.13	Transfer function block from scilab describing the surge shaft used in the simulations. . . . .	40
5.14	PID regulator for speed regulation and power regulation, as modelled in scilab. [17] . . . . .	42
5.15	The ratelimiter block used for waterhammer simulations. . . . .	43
5.16	Examples of unstable and stable systems based on phase and gain margin [11]. . . . .	46
6.1	Layout of the block diagram for frequency regulation in island mode. . .	49
6.2	Layout of the block diagram for load regulation connected to a stiff load. .	50
6.3	The effect of three different droop settings . . . . .	50
6.4	The hydraulic system used in the simulations. . . . .	51
6.5	Analytic functions for scilab model . . . . .	52
6.6	Changes in the infrastructure due to water hammer simulations. . . . .	53
6.7	set context tool to inset system variables. . . . .	53

---

---

6.8	Analytic model with water hammer sim and friction modification. . . . .	54
6.9	System in LVTrans . . . . .	55
6.10	Bode plot for the open loop transfer function. $K_p = 3$ , $T_i = 7$ and time delay = 0.01s . . . . .	57
6.11	Gain and phase response due to changes in $K_p$ . . . . .	58
6.12	Gain and phase response due to changes in $T_i$ . . . . .	58
6.13	Frequency response for a load drop of 50% . . . . .	59
6.14	Gate opening, responding to a drop in load demand of 50% . . . . .	59
6.15	Comparing the frequency dynamics of two penstock models, when simulating a drop in load of 10 % in island-mode. . . . .	60
6.16	Comparing the pressure dynamics in front of the turbine when simulating a drop in load of 50 % in island-mode. . . . .	61
6.17	Simulation of pressure and frequency, comparing the penstock models isolated. . . . .	61
6.18	Pressure pulsation effect for different penstock lengths . . . . .	62
6.19	Frequency response of system start up and during a load rejection of 10% during full load. . . . .	63
6.20	Frequency regulation during a drop from 100% to 50% in load demand . . . . .	65
6.21	Frequency regulation during a drop from 85% to 75% in load. . . . .	65
6.22	Power regulation in stiff grid mode with a drop of 0.01% in grid frequency . . . . .	66
6.23	Power regulation in stiff grid mode with a increase of 0.01% in grid frequency . . . . .	66
6.24	Water hammer simulations done in scilab and LVTrans . . . . .	67
6.25	A close look at the first transient from figure 6.24. . . . .	67
6.26	Simulation of a full system stop, with changes in the internal friction factors in the scilab model. . . . .	68
7.1	Picture of the rig. . . . .	71
7.2	A scetch of the test ring at the laboratory . . . . .	72

---

---

7.3	Rig test result #1 . . . . .	74
7.4	Rig test result #2 . . . . .	74
7.5	Rig test result #3 . . . . .	75
7.6	Comparison of all three test results from the rig. . . . .	75
7.7	Comparing test 1 with the scilab model . . . . .	76
7.8	Comparing test 2 with the scilab model . . . . .	77
7.9	Comparing test 3 with the scilab model . . . . .	77
10.1	Cross section of the head race tunnel . . . . .	A-2
10.2	Cross section of the penstock . . . . .	A-3
10.3	Velocity triangles for a Francis turbine. [2] . . . . .	B-1
10.4	Calculations of transfer coefficients in reference to induced torque by the turbine . . . . .	C-1
10.5	Calculations of transfer coefficients in reference to flow through the turbine . . . . .	C-2
10.6	Power regulation in a stiff network. . . . .	D-2
10.7	Frequency regulation in island mode. . . . .	D-3
10.8	The hydraulic system used in the simulations. . . . .	D-4
10.9	Parameters used in the LVTrans simulations . . . . .	E-2
10.10	Risk assessment . . . . .	F-1

# Nomenclature

$\mu$  = Dynamic viscosity

$\rho$  = Mass density [ $\frac{kg}{m^3}$ ]

$\eta_{bep}$  = Efficiency at best point [-]

$\omega$  = Rotational speed [RPM]

$\epsilon$  = Signal deviation [pu]

$a$  = Wave Velocity [ $\frac{m}{s^2}$ ]

$A$  = Area [ $m^2$ ]

$A_t$  = Proportionality factor [-]

$A_s$  = Surge shaft area [m]

$A_p$  = Penstock area

$c_{fluid}$  = Velocity of sound in a fluid [ $\frac{m}{s}$ ]

$D = d$  = Pipe diameter [m]

$D_h$  = Hydraulic diameter

$D$  = Machine damping constant [-]

$e$  = typical surface roughness [m]

$E$  = Young's Modulus [ $\frac{N}{m^2}$ ]

---

$f$  = frequency [Hz], may also be defined in [%]

$f_n$  = Nominal frequency [Hz] or [pu]

$f_t$  = Thickness of the pipe wall [m]

$f_D$  = Friction coefficient [-]

$Re$  = Reynolds number

$F$  = Force [N]

$g$  = Acceleration of gravity [ $\frac{m}{s^2}$ ]

$G$  = Guide vane opening [%]

$h_f$  = Friction losses [ $m_{H_2O}$ ]

$H_r$  = Rated head [m]

$k_f$  = friction factor [-]

$K$  = Bulk Modulus [ $\frac{N}{m^2}$ ]

$K_p$  = Proportionality factor

$l = L$  = Length [m]

$m$  = Mass [kg]

$m_t$  = Mechanical torque [pu]

$M$  = Mannings number [ $\frac{m^{\frac{1}{3}}}{s}$ ]

$n$  = Speed [%]

$n_r$  = Rated speed [%], may be defined as [rpm] (rotations per minute)

$Nbep$  = Best efficiency speed [rpm]

$p$  = Whetted perimeter [m]

$P_m$  = Mechanical power [MW]

$p_r$  = Rated power [%], may be defined as [MW]

$p_e$  = Grid power [%], may be defined as [MW]

$p_t$  = Transient pressure [ $m_{H_2O}$ ]

---

$P_d$  = Power demand

$P_g$  = Power generation

$q$  = Flow [ $pu$ ]

$Q$  = Flow [ $\frac{m^3}{s}$ ]

$Q_1$  = Flow in the head race tunnel [ $\frac{m^3}{s}$ ]

$Q_2$  = Flow into the upper surge shaft [ $\frac{m^3}{s}$ ]

$Q_3$  = Flow in the penstock [ $\frac{m^3}{s}$ ]

$Q_{bep}$  = Best efficiency point flow [ $\frac{m^3}{s}$ ]

$Q_r$  = Rated flow [ $\frac{m^3}{s}$ ]

$r$  = Radius [ $m$ ]

$r_1$  = Inlet runner radius [ $m$ ]

$r_2$  = Outlet runner radius [ $m$ ]

$r_h$  = hydraulic resistance [-]

$Rq$  = Constant for RPT [-]

$Rm$  = Angular velocity damping constant [-]

$Rd$  = Design constant koeffisient [-]

$s$  = Laplace operator

$t$  = time [ $s$ ]

$T_{bep}$  = Best efficiency torque [ $Nm$ ]

$T_s$  = Surge shaft filling time [ $s$ ]

$T_e$  = Wave travel time

$T_w$  = Water time constant [ $s$ ]

$T_r$  = Pressure reflection time [ $s$ ]

$T_c$  = Closure time [ $s$ ]



---

$Td$  = Time derivative constant [s]

$Ti$  = Time integrate constant [s]

$u$  = output signal

$v$  = Speed [ $\frac{m}{s}$ ]

$z$  = Upper surge shaft water level [m]

$z_0$  = Head loss in the head race tunnel [m]

$Z_p$  = Hydraulic surge impedance of the penstock [-]

# Chapter 1

## Introduction

### 1.1 Motivation

To achieve a satisfying power system with a high security of supply, robustness and stability, power generation with good regulation and governing is necessary. Implemented in the production of active and reactive energy, governor systems capable of regulating voltage and frequency is a prerequisite to achieving the goals for stability and safety of supply [8].

Frequency variations on the grid are a direct consequence of a difference in energy demand and power generation. A common analogy is an example of riding a tandem bike. When the road suddenly gets steeper somebody must push harder, or the speed will decrease. The same counts for power systems, as load demand increases, the power generation must follow, or else the frequency will decrease. Depending on the size and type of system, all hydropower plants must have regulation where power and speed can be regulated to some extent.

In Norway aggregates larger than 10 MVA must have the opportunity to do frequency regulation, this is also applicable for smaller systems, where it is possible to do so. System's that have reserves to do frequency regulations must regulate within a 1% mark. So for power systems that are being supplied with a base frequency of 50Hz, the generation stay within a range of 49.5 to 50.5 Hz. This counts as 1% droop, or higher dependent on the energy reserves [20].

Due to these strict regulations, simulation of hydropower plants is a valuable and money saving process to anticipate the dynamics of the system, compared to real life experiment. When setting up a new power plant or making smaller parameter changes, predictability is important and can be achieved with system simulations.

## 1.2 Thesis Description

The thesis is based on the project work done in the first semester at the last year at NTNU. During the project work a simple model of a hydropower plant was made and a literature study of modelling turbines and hydraulic systems. The master thesis is based on the same system but has been heavily modified.

Seven primary objectives were given in the thesis:

1. Add a surge shaft and an inlet tunnel to the existing model.
2. Verify the surge shaft with experiments in the laboratory.
3. Research the opportunities to add an elastic penstock model to the system.
4. Theoretical deduction of the partial derivatives for use in the xcos model, based on Torbjørn Nielsen's turbine model.
5. Simulate the system with both an isolated and stiff grid.
6. Look for possibilities to do a frequency response analysis.
7. A short paper shall be written and presented at the 7th International Symposium on Current Research in Hydraulic Turbines (CRHT-VII) at Katmandu University, April 2017.
8. Write a report.

The plant is based on a Francis turbine with a rated power output of 94MW. It is designed for a gross head of 200m and a flow rate of  $50 \frac{m^3}{s}$ . The power plant is modelled in block diagrams based on mathematical models and transfer functions. The turbine is based on a linearized model, which gives an accurate description of the turbine behaviour for a given operating point. The plant is controlled by a PI regulator providing frequency stability and eliminates the deviation between process and reference values.

By increasing the level of detail in the model, better simulation results are expected. A more detailed system gives better flexibility which provides more simulation possibilities and situations. Four systems have been made in the thesis. Three in island mode with a single machine, single load, where the first one is build up with a block having a standard input configuration directly in the blocks. The second one is the one called analytic model where the equations are inserted in the different blocks, and the input values are defined through a context file. The third model is for water hammer simulation and is based on the analytic model but with relays forcing a fast closure of the guide vanes and changing the friction characteristics of the system. The fourth model is the stiff grid operation with turbine power regulation, and with frequency as an input variable.

All the simulation models share the same turbine model and hydraulic system. In this thesis, all the systems will be evaluated up against LVTrans, and the surge shaft model will be tested towards a test rig at the water power laboratory.

## 1.3 System Introduction

The plant design is based on a typical Norwegian layout represented in a block diagram seen in figure 1.1.

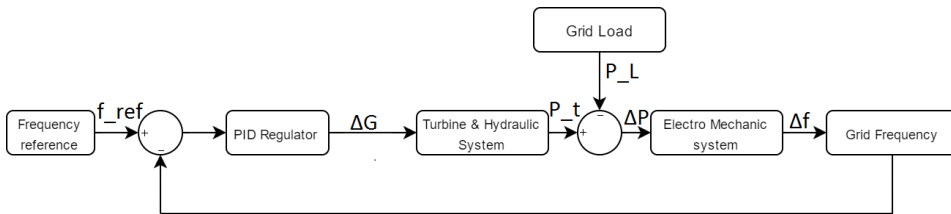


**Figure 1.1:** General layout of the Norwegian island operated turbine.

The block diagrams consist of a frequency reference value, sending the signal to a summation block. The summation block subtracts the process frequency value which becomes  $\epsilon$  and sends it into the PID regulator. The regulator then transfers the signal into what is then represented as the guide vane opening  $\Delta G$ . Through turbine dynamics, the amount of flow  $\Delta Q$  is then given by the guide vane opening and sent into the hydraulic system. The hydraulic system is then transferring the signal into pressure head,  $\Delta H$ . This pressure is then processed through turbine dynamics one last time giving turbine power as an output. The speed is then represented after the torque ( $T_t$ )/power ( $P_t$ ) signal has gone through the generator dynamics also called electromechanical system. The torque provided to the generator is turbine power subtracted with power demands ( $P_L$ ) giving  $\Delta P$  or  $\Delta T$ . Since the system is in per unit values, the values can easily get converted by multiplying with the base value of either torque or power. The same counts for the speed which can be multiplied with both the base value of the grid frequency (50Hz) or the rated generator speed (333,33RPM).

For simulations in a stiff grid environment, the model has to change some of the layouts as seen in figure 1.2.

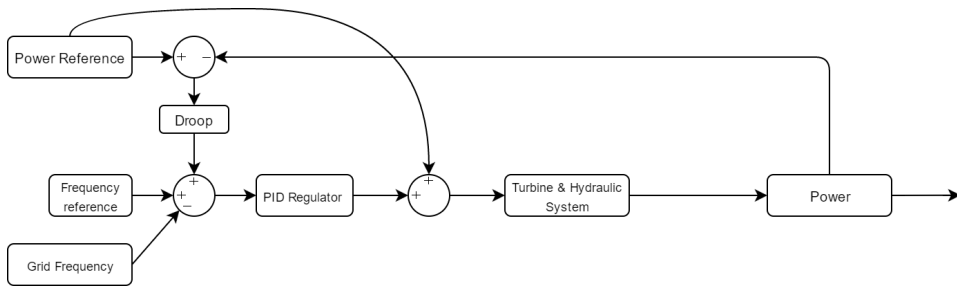


**Figure 1.2:** Simulation set up for stiff grid mode.

In the figure, 1.2 much of the same signal processing occurs but the regulator loop is power dependant, and the governor regulates towards a power reference and droop characteristics. Changing the value of grid frequency provides a change in the system stability. The system will then automatically regulate the power output from the turbine to the value decided by the droop.

# Previous Work

## 2.1 Project Work

During the fall of 2016 the project work called "comparison of block diagrams for hydropower plants" was done. It was a literature study combined with modelling and simulation of an elementary hydropower plant. The literature study gave insight and knowledge of system regulation, modelling of different components in a hydropower plant from a mathematical approach.

The model created in the project work consisted of a linear turbine model regulated by a simple PI regulator, a simple rigid penstock modelled as a static water column, and generator. The system can be seen in figure 2.1

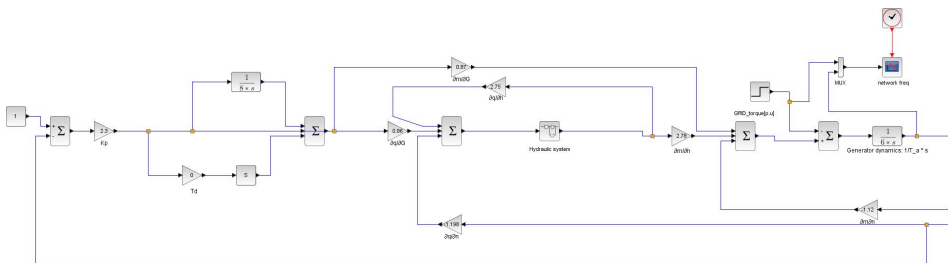


**Figure 2.1:** Block diagram made in the project work fall 2016.

The model was made to perform simulations in island mode with frequency regulation during load acceptance and rejection. Simulations gave reasonably good results compared to simulations conducted in LVTrans, but there were some deviations between them. Lack

of system dynamics and simulation flexibility made it desirable to develop the system further.

By giving the system more scenarios for simulation such as power regulation during frequency variation in a stiff network environment, and create systems for transient pressure simulations increases the usability.

## **2.2 Paper Presented at the 7th International Symposium on Current Research in Hydraulic Turbines**

During the last semester at NTNU, the students at the water power laboratory attended at the international symposium on current research in hydraulic turbines at Kathmandu University. In that occasion a presentation and a paper where to be delivered, presenting the thesis and the work to come.

In Appendix G, the paper provided to Kathmandu University is found. It was written in an early stage of the thesis and lacks extensively of system model and simulations.

Some of the larger improvements and implementations that have been done post paper delivery are:

- New turbine transfer coefficients are calculated.
- New friction coefficients
- New PI settings for the regulator
- Draft tube and lower surge shaft are implemented
- The "Analytic" model has been made

The presentation was performed during the trip to Nepal and was successfully conducted at the conference.

# Chapter 3

## Theory

This section includes different mathematical and physical definitions directly linked to understanding the modelling, and the various physical situations that could occur during simulation of a hydropower system. At first, some general equations for fluid mechanics as well as energy, and mass behaviour will be shown and is found in section 3.1. A method for calculating forces in transient states such as water hammer phenomenon are included in 3.2. Later in the chapter, different approaches for calculating friction, and the various parts of the hydropower plant will be presented, found in section 3.3 to 3.5. Most of the theory found in this chapter are found in books such as: "Modelling and controlling Hydropower plants" [12], "Vassdragsteknikk II" [5], and the paper by J. Riera [14].



### 3.1 General Equations

A string of water must comply with the equation of motion and the equation of continuity. The continuity equation constrains the law of mass flow inside a control volume. For a given amount of volume flow getting into the system. The same amount must come out plus the eventual rest inside the volume. The equation of continuity is defined mathematically as:

$$\frac{\partial H}{\partial t} + \frac{a^2}{g} \cdot \frac{\partial v}{\partial x} = 0 \quad (3.1)$$

Where  $a$  is the velocity of sound in water, approximately around  $1200 \frac{m}{s}$ . This velocity is defined in equation 3.6, and it is dependent on the thickness of the pipe walls, pipe diameter, the mass density of water, and the water compressibility module.

The equation of motion describes the forces acting on the control volume. All the forces on it must be zero which leads to the following equation:

$$g \cdot \frac{\partial H}{\partial t} + \frac{\partial v}{\partial t} + \lambda \cdot \frac{v |v|}{2D} = 0 \quad (3.2)$$

## 3.2 Transient Fundamentals

The hydraulic transients are recognised as the change in pressure or pressure fluctuations in a fluid caused by a change in flow conditions. Pressure waves travel with the velocity of sound which is given by:

$$c_{fluid} = \sqrt{\frac{K}{\rho}} \quad (3.3)$$

Where  $\rho$  is the density and  $K$  is the bulk modulus of the fluid given by:

$$K = \rho \cdot \frac{dP}{dV} \rightarrow K_{H_2O} = 2.2 \cdot 10^9 \frac{N}{m^2} \quad (3.4)$$

There are many different events that lead to a change in the mean flow of the system, and some of the more usual are: system start-up and shut down, changes in frequency, vibrations of a runner, and different sorts of dam failure.

### 3.2.1 Pressure wave velocity

$$a = \sqrt{\frac{K}{\rho(1 + \frac{DK}{f_t E})}} \quad (3.5)$$

Where  $D$  is the internal penstock diameter,  $f_t$  is the wall thickness of the penstock walls, and  $E$  is Young's modulus of pipe wall material. For steel this value is  $2.22 \cdot 10^{11} \frac{N}{m^2}$ . For a perfectly rigid penstock, assuming  $E$  to be infinite simplifies the equation to 3.3:

$$a = \sqrt{\frac{K}{\rho}} = c_{fluid} \quad (3.6)$$

### 3.2.2 Wave reflection time

After a rapid closure of the turbine valves, a high pressure occurs in front of the turbine as the water masses is forced to decelerate, ( $F=ma$ ). This overpressure will immediately propagate up towards the nearest water surface like a wave. The amount of time in seconds for the wave to reach the open surface is given by:

$$T_e = \frac{L}{a} \tag{3.7}$$

Where  $L$  is the length of the penstock [ $m$ ] and  $a$  is the wave speed [ $\frac{m}{s}$ ]. In figure 3.1 the pressure propagation in two cycles are shown. note that in the figure, the wave velocity is given by  $C$  and not  $a$ .

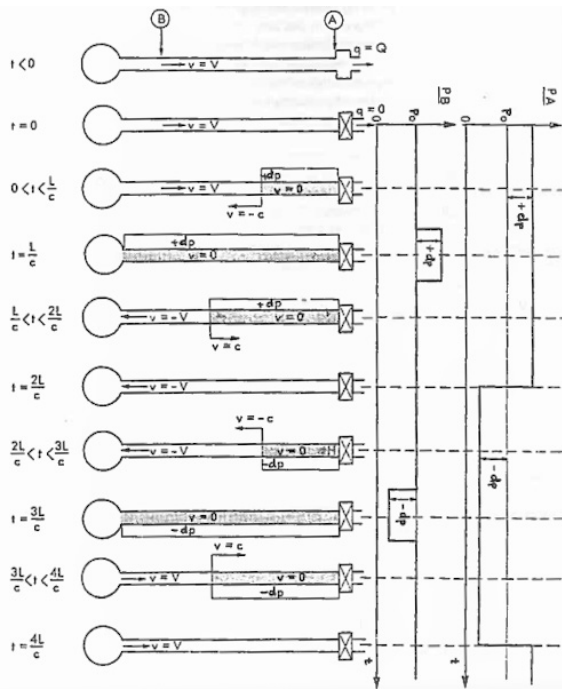


**Figure 3.1:** A representation of pressure propagation in a conduit.[5]

Pressure reflection time is given by the time for the wave to reach surface and back again to the closing valve. This naturally becomes that  $T_r = 2 \cdot T_e$ . To avoid damage to the turbine and the rest of the system, the closure time ( $T_c$ ) for the valve should always be larger than  $T_r$ . The closing time is seen as the simplest ways to avoid high-pressure transients, but again it's delimiting the power plans ability to regulate fast.

### 3.2.3 Mass Forces

Mass forces for the pressure transients in front of the turbine is essential to know when designing a power system. Pressure transients during rapidly closed valves could harm the pipelines and the penstock. In this subsection, the equation for the change in pressure given in mWC is deduced.

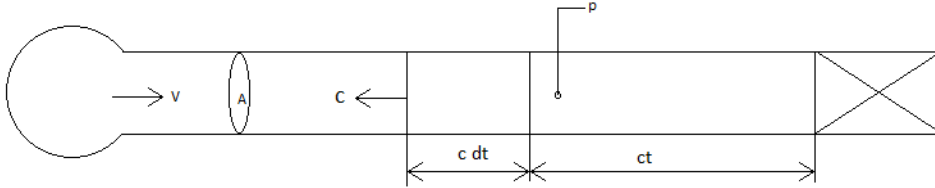


**Figure 3.2:** Description of mass forces during transient state.

Using pulse rate to the system:

$$F \cdot dt = d(mv) = m \cdot dv + v \cdot dm \quad (3.8)$$

Knowing that  $F = dp \cdot A$  and the changes in mass for the control volume is  $dm = \rho \cdot A \cdot c \cdot dt$  gives:

$$dp = \rho \cdot c \cdot dv + \rho \cdot v^2 \quad (3.9)$$

At an instantaneous change in mean flow gives  $dv = v$ . Also in practical scenarios wave velocity,  $c$  is in magnitude of  $100 \rightarrow 1000 \frac{m}{s}$ , which results in  $v \ll c$

Giving the simpler form:

$$dp = \rho \cdot c \cdot v \quad (3.10)$$

and in the form of height [m]:

$$dh = \frac{c \cdot \Delta v}{g} \quad (3.11)$$

This equation applies for instantaneously change in the fluid velocity. When using closure times to the turbine valves a modification to equation 3.11 is given by:

$$\Delta h = \frac{c\Delta v}{g} \cdot \frac{T_r}{T_c} = 2 \cdot \frac{\Delta Q}{T_c} \cdot \frac{L}{gA} \quad (3.12)$$

### 3.3 Friction Losses

Losses due to friction inside the conduit wall can be found by using Darcy Weisbach's empirical equation. There are other factors that lead to head losses in a hydro power plant, but in this thesis, only friction due to sheer forces inside the conduit is taken account.

$$h_f = f_D \cdot \frac{L}{D} \cdot \frac{V|v|}{2g} \quad (3.13)$$

Where:  $h_f$  = head loss,  $f_D$  = Darcy weisbach's friction factor,  $v$  = the average velocity of the fluid,  $D$  = hydraulic diameter,  $L$  = the length of the pipe.

For laminar flow with  $Re < 2320$  in a circular pipe, Darcy Weisbach's friction coefficient  $f_D$  is defines as follows:

$$f_D = \frac{64}{Re} \quad (3.14)$$

where Reynolds number is defined by:

$$Re = \frac{\rho \cdot v \cdot D_h}{\mu} \quad (3.15)$$

$\rho$  is the mass density of the fluid,  $v$  is the speed,  $L$  is the characteristic length and  $\mu$  is the dynamic viscosity.

For calculating friction during turbulent flow, the Colebrook-White Equation can be used. An implicit equation that requires numerical solutions to be solved. The equation is defined as:

$$\frac{1}{\sqrt{f}} = 1.14 - 2 \log_{10} \cdot \left( \frac{e}{d} + \frac{9.35}{Re \sqrt{f}} \right) \quad (3.16)$$

Valid for flow with  $Re > 4000$ .  $\frac{e}{d}$  is the relative roughness of the material, where  $e$  is the typical surface roughness, and  $d$  is the diameter. In table 3.1 one can find values for roughness over different materials.

**Table 3.1:** Typical surface roughness on different materials. [15]

Material	Nature of Material	Roughness [mm]
Steel	Drawn, new	0.02 - 0.1
-	Welded, new	0.05 - 0.1
-	galvanized, new	0.15
-	Used, cleand	0.15 - 0.2
-	Lightly corroded	0.1 - 0.4
-	Severly corroded	0.4 - 3
-	Light scaling	1 - 1.5
-	Heavily scaling	1.5 - 4
-	Bitumed coated	0.05
Cast - Iron pipe	New	0.25 - 1
-	Corroded	1 - 2
-	With scaling	1 - 4
Concrete pipe	Smooth finish	0.3 - 1
-	Rough	1 - 3
Sheet steel	Smooth	0.07
Glass,lead,copper,brass	-	0.0001 - 0.0015

When the relative roughness and Reynold's number are known the friction factor can also be found in a Moody diagram, presented in figure 3.3.

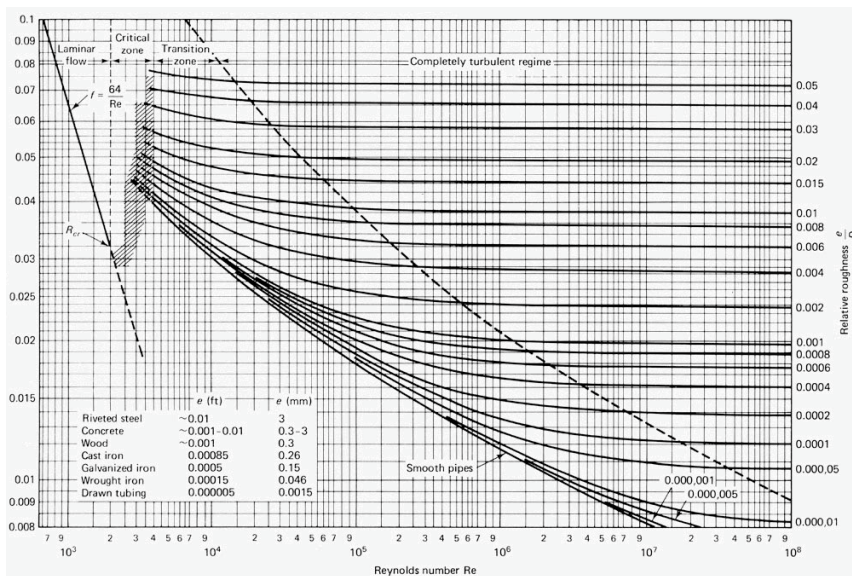


**Figure 3.3:** The moody diagram, used to obtain friction factor  $f$  [10]

Friction losses can also be found using Manning's formula which is often used to calculate friction losses in blasted shafts [5].

$$h_f = \frac{L \cdot v |v|}{M^2 \cdot R_h^{\frac{4}{3}}} \quad (3.17)$$

Where  $L$  = tunnel length,  $v$  = fluid velocity,  $M$  = Mannings number,  $R_h$  = hydraulic radius. Manning's number varies with tunnel area and the roughness of the tunnel surface. For blasted shafts, Maning's number is around 34, but are assumed lower in newer shafts as the roughness has increased over the years. For concrete Manning's number are found to be around 80. The hydraulic radius can be known from the formula:

$$D_h = \frac{4A}{p} \quad (3.18)$$

Where  $A$  is the area of the duct, and  $p$  is the wetted perimeter of the cross-section. Hydraulic radius is then defined as the ratio of area and wetted perimeter:

$$R_h = \frac{A}{p} \quad (3.19)$$

Cross section of the inlet tunnel can be seen in figure 3.4

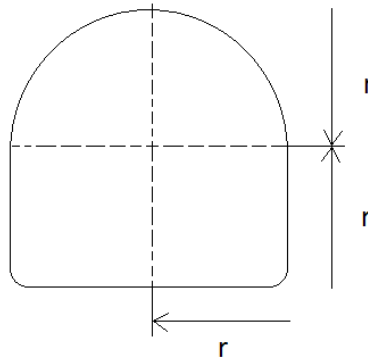


**Figure 3.4:** Cross section of the inlet tunnel

For the given cross section the wet perimeter is found by:

$$p = (4 + \pi)r \quad (3.20)$$

This gives leads to a general equation for the tunnelshape in figure3.4 :



$$D_h = \sqrt{\frac{8 \cdot A}{4 + \pi}} \quad (3.21)$$

and for the radius:

$$R_h = \frac{A}{(4 + \pi)r} \quad (3.22)$$

For typical hydro power plants, the friction coefficient is set to 0.05 for the head race tunnel and 0.01 for the penstock [21]. These are the values that are used in the power system. Friction factors for the test rig are calculated using Colebrook-White Equation 7.1. This is due to the requirements of preciseness for the friction loss when comparing simulation to real life tests.

### 3.4 Surge shaft

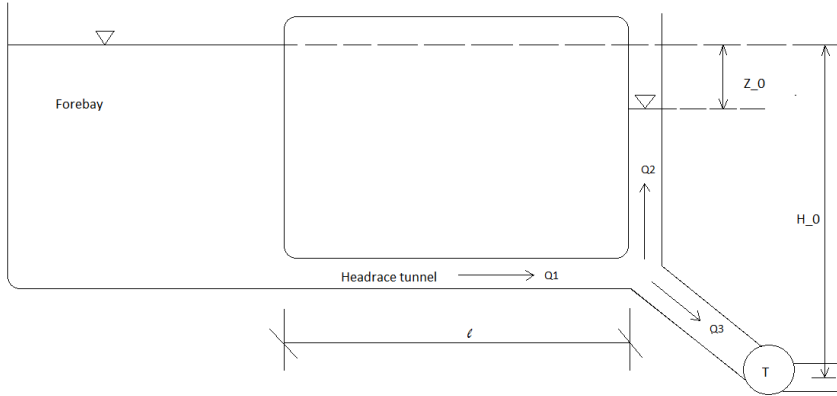


**Figure 3.5:** Cross section sketch of the conduit system at the surge shaft and the forebay.

During steady state operation  $Z_0$  represents height losses due to frictional forces in the headrace tunnel. If a change in the fluid mass flow occurs the system equilibrium ceases, resulting in oscillations for  $Z_0$ .

#### 3.4.1 Surge shaft Oscillations

Since the oscillations in the surge shaft appear to be slow, the water within the surge shaft considers being inelastic. This simplifies the equations regarding mass oscillations of water in the surge shaft. The force which creates an unbalanced fluid level in a U-pipe is defined as:

$$F = \rho g A \cdot 2z \quad (3.23)$$

Amount of mass to be accelerated:

$$m = \rho A l \quad (3.24)$$

Where  $l$  = fluid column length [ $m$ ]. For an ideal fluid with and neglecting friction we have:

$$F = ma = m \frac{dv}{dt} \quad (3.25)$$

Where  $v$  = fluid flow speed [ $\frac{m}{s}$ ]. Inserting 10.6 into 10.7:

$$\rho g A \cdot 2z = \rho A l \frac{dv}{dt} \quad (3.26)$$

Introducing fluctuations in away from the level of reference, where:

$$v = -\frac{dz}{dt} \quad (3.27)$$

This gives the harmonic swing equation, given in a differential form.:

$$\frac{d^2z}{dt^2} + \frac{2g}{l}z = 0 \quad (3.28)$$

The swing equation has the following solution:

$$z = k \cdot \cos(\omega t + \phi) \quad (3.29)$$

The angular velocity are described as inversely proportional to the swing time constant  $T$ :

$$\omega = \sqrt{\frac{2g}{l}} = \frac{2\pi}{T} \quad (3.30)$$

Identical to a physical pendulum with length  $l/2$

$$T = 2\pi\sqrt{\frac{l}{2g}} \quad (3.31)$$

### 3.4.2 Surge Shaft Transfer Function

The surge tank can be derived from the equation of continuity, and in this case, the losses are neglected. The equation for the changes in the surge shaft is given below 3.32. The changes of water level inside the surge shaft are dependent on the mass flow in the pipe system:

$$\frac{AH_r}{Q_r} \cdot \frac{dz}{dt} = Q_2 = Q_1 - Q_3 \quad (3.32)$$

With the equation linearized and Laplace transformed gives the following equation:

$$s \cdot z = \frac{1}{A_s} (Q1 - Q3) \cdot Q_r \quad (3.33)$$

where  $z_s$  is the head level inside the surge shaft and  $Q1 - Q3 = dQ$  gives the transfer function for a change in the head due to a change in flow:

$$\frac{dH}{dQ} = \frac{Q_r}{h \cdot A_s} \frac{1}{s} \quad (3.34)$$

Surge shaft filling time is there fore expressed as:

$$T_s = \frac{AH_r}{Q_r} \quad (3.35)$$

Giving the final transfer function for the surge shaft component:

$$\frac{dH}{dQ} = \frac{1}{T_s \cdot s} \quad (3.36)$$

## 3.5 Penstock and Tunnels

In this section, the principles for modelling the different penstock types are given. There are used three different methods in this thesis to model both penstocks and tunnels. The first pipe or tunnel is described as the head race tunnel, and it utilizes the simplified penstock model for a static pipe with no water elasticity.

Later in the hydraulic system comes the penstock. For the hydro power system simulations, there are only used two different types. The dynamic pen stock model and the penstock model from the electrical equivalent circuit. At last the draft tube is modelled with the same model as the head race. This was chosen due to its short length and slow speed.

For the surge shaft verification model, there are only used simplified penstock model due to the short pipe length of 11 m.

### 3.5.1 Dynamic penstock

The model shown in this section is described in literature such as Modelling and Controlling Hydropower plants, [12]. The transfer function for a penstock given as a dynamic system with compressible water effect and dynamic pipe walls are provided by the following equation:

$$\frac{\Delta H(s)}{\Delta Q(s)} = Z_p \cdot \tanh(s \cdot T_e + h_f) \quad (3.37)$$

Where the hydraulic surge impedance of the penstock,  $Z_p$  is given by:

$$Z_p = \frac{T_w}{T_e} \quad (3.38)$$

Where  $T_w$  is the water starting time in the penstock. This parameter describes the time for the water masses to accelerate up from  $Q = 0$  to  $Q = Q_r$  [22]. The value is given by:

$$T_w = \frac{L_p}{A_p \cdot g} \cdot \frac{Q_r}{H_r} \quad (3.39)$$

### 3.5.2 Approximation of Tanh

The model is deduced from the equations of continuity and motion which lead to the following relationship:

The hyperbolic tangent function can be written as:

$$\frac{e^x - e^{-x}}{e^x + e^{-x}} = \frac{\sinh(x)}{\cosh(x)} = \tanh(x) \quad (3.40)$$

Due to complications when solving for a irrational terms in transfer functions, the tanh function is rather used. By inserting  $x = T_e \cdot s$  gives the finite approximation for tanh function with the use of Maclaurin series [14]:

$$\tanh(T_e \cdot s) = \frac{s \cdot T_e \prod_{n=1}^{\infty} \left[ 1 + \left( \frac{s \cdot T_e}{n \cdot \pi} \right)^2 \right]}{\prod_{n=1}^{\infty} \left[ 1 + \left( \frac{2s \cdot T_e}{(2n-1)\pi} \right)^2 \right]} \quad (3.41)$$

For approximations  $n=0, 1$  and  $2$ , tanh function becomes:

$$\tanh(T_e \cdot s) |_{n=0} \approx s \cdot T_e \quad (3.42)$$

$$\tanh(T_e \cdot s) |_{n=1} \approx \frac{s \cdot T_e \cdot \left( 1 + \left( \frac{s \cdot T_e}{\pi} \right)^2 \right)}{\left( 1 + \left( \frac{2 \cdot s \cdot T_e}{\pi} \right)^2 \right)} \quad (3.43)$$

$$\tanh(T_e \cdot s) |_{n=2} \approx \frac{s \cdot T_e \cdot \left( 1 + \left( \frac{s \cdot T_e}{\pi} \right)^2 \right) \cdot \left( 1 + \left( \frac{s \cdot T_e}{2 \cdot \pi} \right)^2 \right)}{\left( 1 + \left( \frac{2 \cdot s \cdot T_e}{\pi} \right)^2 \right) \cdot \left( 1 + \left( \frac{2 \cdot s \cdot T_e}{3 \cdot \pi} \right)^2 \right)} \quad (3.44)$$

This approximation is necessary when modelling the system in block diagrams. Due to solver issues and iteration problems when directly inserted as a simple timedelay in form of a trigonometric function "tanh" or as a time delay block represented as  $e^{-timedelay[s]}$ .

### 3.5.3 RLC Penstock Model

The RLC model also called "Penstock Model From Electrical Equivalent Circuit" are using electrical analogy to represent a dynamic hydraulic line. The constants and simulation results are only valid during water hammer simulation and under severe pressure changes within the system.

The electric RLC equivalent circuit for a hydraulic pipeline can be described using the momentum and mass conservation equations. The equations are in advanced linearized around an operating point at  $H_r$  and  $Q_r$ . The model is used in literature such as [6] and

[18].

$$\frac{\partial \Delta H}{\partial x} = \frac{r_h}{A} \cdot \Delta Q + \frac{1}{g \cdot A} \cdot \frac{\partial \Delta Q}{\partial t} \quad (3.45)$$

$$\frac{\partial \Delta Q}{\partial x} = \frac{Ag}{a^2} \cdot \frac{\partial \Delta H}{\partial t} \quad (3.46)$$

Where  $A$  = pipe cross section,  $r_h$  = hydraulic resistance,  $g$ = acceleration of gravity,  $D$  = pipe diameter. The equation for pressure wave velocity, "a" can be found under section 3.2.1. Hydraulic resistance is define as:

$$r_h = A \cdot 2K_r \cdot Q_r \quad (3.47)$$

and

$$K_r = \frac{\partial H_0}{\partial x \cdot Q_r^2} \quad (3.48)$$

A constant level of head and  $dx = L$  gives:

$$K_r = \frac{H}{L \cdot Q_r} \quad (3.49)$$

The electrical equivalent circuit can be seen in figure 3.6.

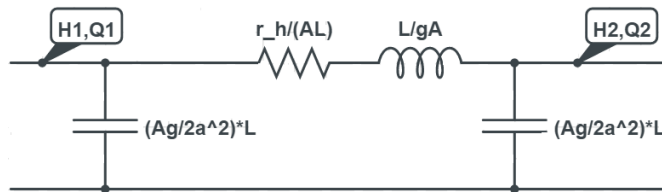


**Figure 3.6:** A penstock with length  $L$  can be represented with this equivalent circuit schematic

The components are defined as:

Introducing the Thevenin equivalent impedance  $Z_2$  for the circuit in figure 3.2 gives the impedance seen from the turbine. This value is defined by the transferfunction 3.52.

**Table 3.2:** RLC component description

Component	Definition	Formula
Resistor	$Z_R$	$\frac{r_h}{AL}$
Capacitor	$Z_C$	$\frac{AgL}{2a^2}$
Inductor	$Z_L$	$\frac{L}{gA}$

$$\frac{\Delta H_2}{\Delta Q_2}(s) = -Z_2(s) \quad (3.50)$$

Where  $Z_2$  is can be found form parallel component theory:

$$Z_2(s) = \frac{Z_C(s) \cdot (Z_L + Z_R)(s)}{Z_C(s) + (Z_L + Z_R)(s)} \quad (3.51)$$

This gives:

$$Z_2(s) = \frac{s \cdot (2 \cdot L \cdot a^2) + 2 \cdot a^2 \cdot r_h \cdot L \cdot g}{s^2 \cdot (L^2 Ag) + s \cdot r_h \cdot A(g \cdot L)^2 + 2a^2 \cdot g \cdot A} \quad (3.52)$$

### 3.5.4 Static Tunnel Model

The static model is based on the dynamic penstock model found in section 3.5.1, seen in equation 5.1

$$\frac{H(S)}{Q(S)} = -\frac{T_w}{T_e} \cdot \tanh(T_e \cdot S + h_f) \quad (3.53)$$

When assuming incompressible fluid with the conduit system defined as rigid and short, the time-traveling effect is negligible and elasticity is insignificant. The equation 5.1 is reduced to [12]:

$$\frac{H(S)}{Q(S)} = -T_w \cdot s - h_f \quad (3.54)$$





# Chapter 4

## Modelling and Simulation Tools

In this thesis, there are used two different computer programs to generate and simulate the hydropower system. At first, a MATLAB clone called Scilab is used to create the block diagram of the system. Then a program created in LabVIEW called LVTrans is used to verify and compare the block diagram. Another programme from now called "hill chart TN" is used to deduce turbine transfer coefficients, implemented in the Francis, turbine model. Other programs such as Excel and MATLAB are utilised during the thesis to handle simulation data and generate graphs but are not included in this chapter. The thesis is written in an online latex client called sharelatex.

## 4.1 Scilab

To create block diagrams, a program handling this feature is used. MATLAB were considered but Scilab is preferred due to its implementation in the industry and that it interfaces with LabVIEW. Xcos, a built-in feature is used to create the system, which is suitable for generating block diagrams and numeric system simulation.

The program interface is similar to Simulink, but it is free to use, open source software which makes it easy for programmers to access source codes and further develop the program. Figure 4.1 shows the main interface of scilab to the right. Top left is Xcos programming window. Blocks can be added from the palette browser (bottom left) by drag and drop. [19]

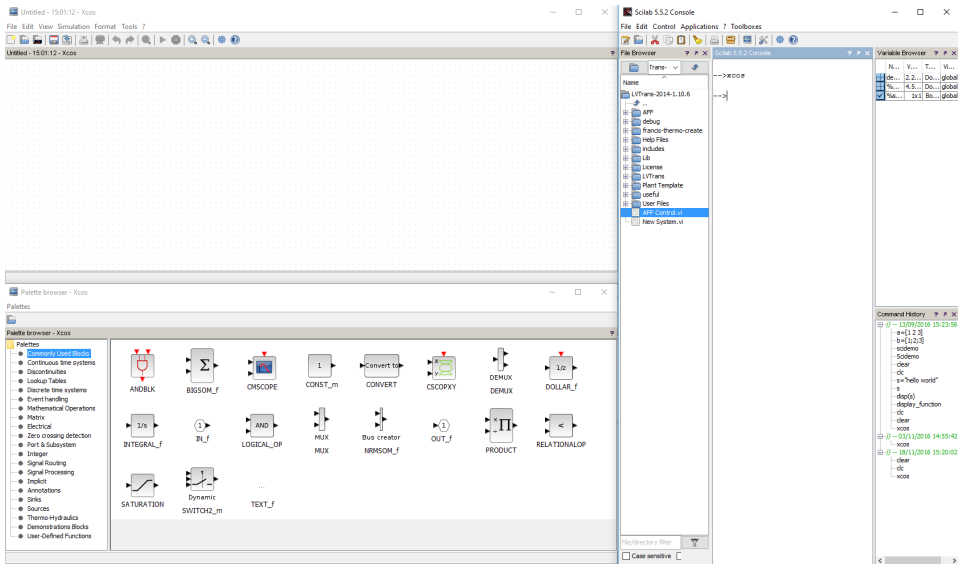


Figure 4.1: Interface of scilab

## 4.2 LVTrans

LVTrans is a program made in the LabVIEW environment, created to give high usability when it comes to modelling and simulating hydropower plants. The power system is built up of pre-made blocks representing pipes, draft tubes, turbines, PID regulators and valves. It is possible to run the simulation in real time and make adjustments at the same time, which makes the program quite versatile.

In this thesis, the program will be used to compare the model made in Scilab. Due to LVTrans preciseness, a fair comparison and model evaluation is achievable. Figure 4.2 shows the interface and how the system is build up from blocks. The left window shows the simulation settings, such as time steps and simulation speed. The window to the right is the programming schematics of the power plant. A closer view of the system can be found in section 10

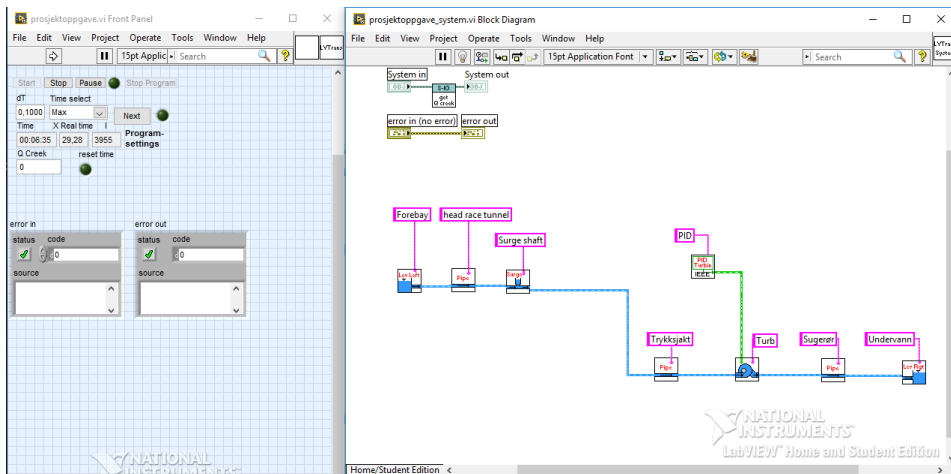
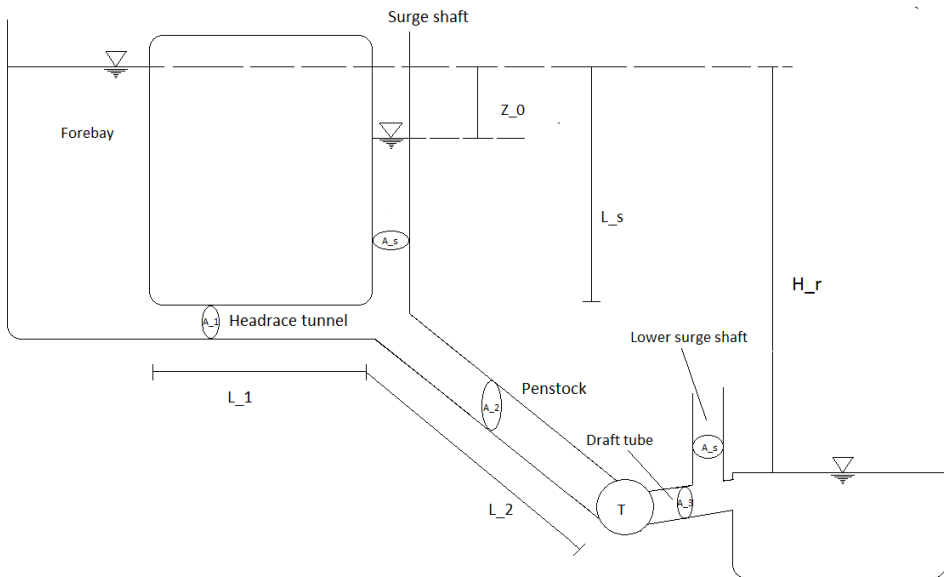


Figure 4.2: Interface of LVTrans



# Chapter 5

## Hydropower Modelling



**Figure 5.1:** Cross section of the system.

The modelled system is a self-designed power plant based on a typical Norwegian layout and can be seen in figure 5.1. Starting from the left, a fore-bay giving a constant head to the system which leads to the head-race tunnel. There are not taken account for any losses at the inlet gate.

The head race tunnel is given the length  $L_1$ , and leads to the penstock and the surge shaft,

with respective lengths  $L_2$  and  $L_s$ . At the end of the penstock lies the turbine, placed below the lower reservoir to avoid air getting sucked into the system. Pipe areas for head race tunnel, penstock the surge shaft and the draft tube are  $A_1$ ,  $A_2$ ,  $A_s$  and  $A_3$ . The draft tube is in this case simplified and not designed or specially designed. The cross section is chosen out from try and failure.

Frictional forces are taken account for in the tunnel penstock, and draft tube and they are calculated by the use of Darcy-Weisbach friction equation. Calculations for the tunnel system are found in Appendix A and is summarised in table 5.1.

**Table 5.1:** Hydraulic system parameter values.

<b>Part</b>	<b>Description</b>	<b>Value</b>	<b>Unit</b>
$L_1$	Head-race length	2000	$m$
$L_2$	Penstock length	250	$m$
$L_3$	Draft tube length	25	$m$
$D_{h1}$	Hydraulic diameter $L_1$	5.292	$m$
$D_{h2}$	Hydraulic diameter $L_2$	3.910	$m$
$D_{h3}$	Hydraulic diameter $L_3$	3.9	$m$
$D_{hs1}$	Hydraulic diameter, surge shaft	7.137	$m$
$D_{hs2}$	Hydraulic diameter, Lower surge shaft	3	$m$
$A_1$	Head-race tunnel area	25	$m^2$
$A_2$	Penstock area	12	$m^2$
$A_3$	Draft tube area	12	$m^2$
$A_{th1}$	Thoma area	26.48	$m^2$
$A_{th2}$	Thoma area, lower surge shaft	7.08	$m^2$
$A_{s1}$	Surge shaft area	40	$m^2$
$A_{s2}$	Lower Surge shaft area	11	$m^2$
$f_{D1}$	Head race friction factor	0.05	-
$f_{D2}$	Penstock friction factor	0.01	-
$f_{D3}$	Draft tube friction factor	0.05	-
$h_{f1}$	Head race loss	3.91	$m$
$h_{f2}$	Penstock loss	0.57	$m$
$h_{f2}$	Draft tube loss	0.28	$m$
$H_r$	Rated head	200	$m$
$Q_r$	Rated flow	50	$\frac{m^3}{s}$
$T_{w1}$	Water mass response time $L_1$	2.04	$s$
$T_{w2}$	Water mass response time $L_2$	0.53	$s$
$T_{w3}$	Water mass response time $L_3$	0.05	$s$
$T_w^{total}$	Water mass response time $L_{tot}$	2.62	$s$
$T_{s1}$	Surge shaft time constants(higher)	160	$s$
$T_{s2}$	Surge shaft time constants(lower)	28	$s$

## 5.1 Modeling scenarios

In figure 5.2, a general representation of the hydro power system with frequency regulation in a isolated grid with one machine is shown. The governor in this master thesis is in both systems (frequency and power regulated plants) based on a single PID regulator but blocks for pilot servo are also included in some simulations scenario. This will be specified during the analysis part. The system layout can be found in [13].

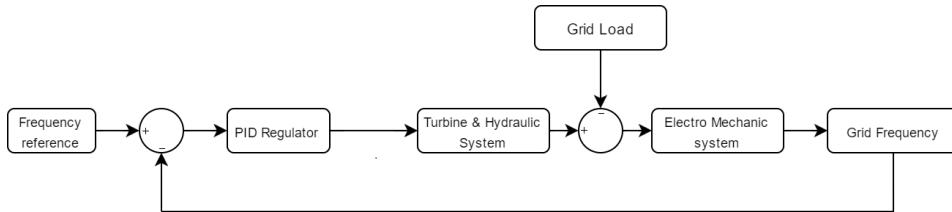


**Figure 5.2:** General layout for the system in grid mode with frequency regulation.

The system connected to a stiff grid in power regulation mode can be seen in figure 5.3. Inputs such as power reference and grid frequency are given in this model. The feedback loop is taken from generated power from the system to a summation point. From there the deviation signal is controlled by a permanent droop gain given by the size and specifications of the plant. The permanent droop controls the given amount of change in machine power output due to a certain amount of change in frequency.

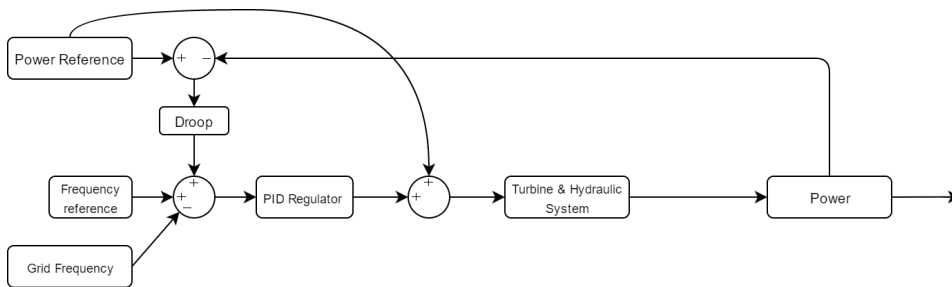


**Figure 5.3:** General layout for the system in stiff network mode with power regulation.



## 5.2 Hydraulic System

The hydraulic system is divided into three different parts. The head race tunnel that leads water from the reservoir or fore bay to the penstock. The penstock is the last piping between the head race tunnel and the turbine spiral casing. The surge shaft is included in the model since not all of the hydropower plants have one implemented. The upper surge shaft lowers the wave pressure reflection time which could lead to better stability, and regulation performance. This is important due to flexibility and maintaining good production quality. System requirements and suggestions due to plant regulation and stability can be found in section 6.2.

As seen in figure 5.4 the dynamics are dependent of all the three transfer functions. The functions are deduced from the the equation of continuity and equation of momentum. The hydraulic system are designed to give an realistic representation of the water column transients from the fore bay to the turbine via an surge shaft. Typical outputs from the hydraulic system that are useful designing a hydro power plant are the forces applied in transient state due to water-hammer effect, such as pressure pulsations. The head pressure dynamics also directly impacts the torque delivered by the turbine which influences its speed. The values inserted in the models are calculated in Appendix A. A full overview of the scilab hydraulic system is found in appendix D.

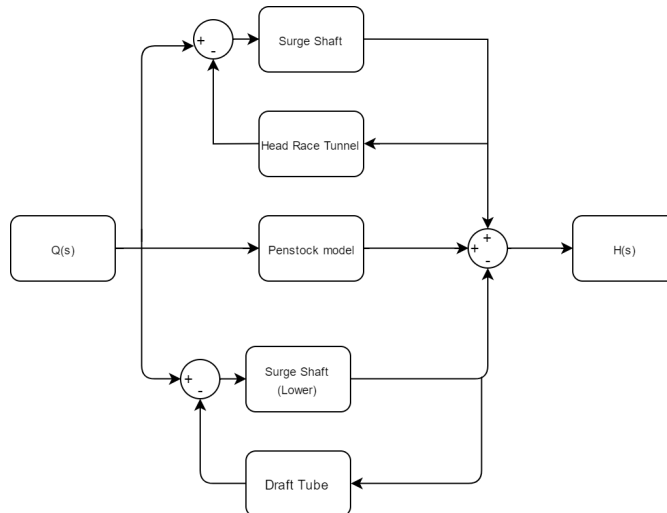


**Figure 5.4:** General layout for the hydraulic system used in the simulations with scilab.

### 5.2.1 Penstock

The penstock model used in the simulations is called the hyperbolic model. Due to the surge shaft and head race tunnel layout, the RLC model could not be integrated into the

hydraulic system. The model is however included as a part of the theory since it can be used in simulations isolated from surge shaft and tunnels.

### 5.2.1.1 Hyperbolic Model

The transfer function representing the elastic water column model is given in equation 5.1 and is found in Hernandez, [12]:

$$\frac{H(S)}{Q(S)} = -\frac{T_w}{T_e} \cdot \tanh(T_e \cdot S + h_f) \quad (5.1)$$

where elasticity time constant is given by assuming wave velocity during transients are  $1388 \frac{m}{s}$ . This value is a little high for elastic wave simulation and should be corrected during later simulations. A suggestion for a new value of  $T_e$  is given in Appendix A-6

$$T_e = \frac{l}{a} = \frac{250m}{1388 \frac{m}{s}} = 0.18s \quad (5.2)$$

During the simulations Due to complications starting the iterations when using tanh function directly in xcos the series expansion of tanh is used. Expanding to  $n = 2$  is done to get a higher order function, giving a realistic penstock behaviour:

$$\tanh(T_e \cdot s) \Big|_{n=2} \approx \frac{s \cdot T_e \cdot (1 + (\frac{s \cdot T_e}{\pi})^2) \cdot (1 + (\frac{s \cdot T_e}{2 \cdot \pi})^2)}{(1 + (\frac{2(s \cdot T_e)}{\pi})^2) \cdot (1 + (\frac{2(s \cdot T_e)}{3 \cdot \pi})^2)} \quad (5.3)$$

Inserting values for the penstock seen in table 5.1 gives the total block diagram for the penstock seen in figure 5.5

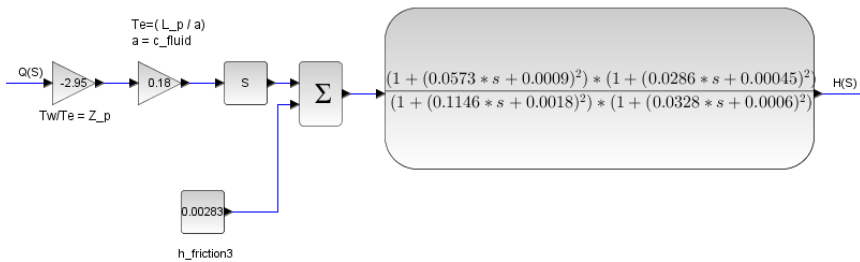


**Figure 5.5:** Block diagram from scilab describing the penstock used in the simulations.

### 5.2.1.2 Penstock Model From Electrical Equivalent Circuit

Transfer function for the electrical equivalent model is given by equation 5.4 and is deduced in section 3.5.3.

$$\frac{\Delta H_2}{\Delta Q_2}(s) = -Z_2(s) \quad (5.4)$$

Where  $Z_2$  is can be found form parallel component theory:

$$Z_2(s) = \frac{Z_C(s) \cdot (Z_L + Z_R)(s)}{Z_C(s) + (Z_L + Z_R)(s)} \quad (5.5)$$

This gives:

$$Z_2(s) = \frac{s \cdot (2 \cdot L \cdot a^2) + 2 \cdot a^2 \cdot r_h \cdot L \cdot g}{s^2 \cdot (L^2 A g) + s \cdot r_h \cdot A (g \cdot L)^2 + 2a^2 \cdot g \cdot A} \quad (5.6)$$

Inserting the respective system values from table 5.1 gives the following function used in simulations:

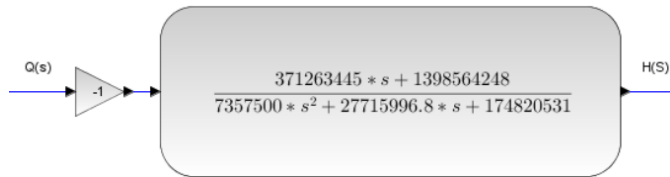


**Figure 5.6:** Transfer function block representing the RLC penstock model

## 5.2.2 Head Race Tunnel and Draft Tube

When assuming incompressible fluid and a rigid pipe, the time-traveling effect is negligible, and elasticity is insignificant [12]. The equation 5.1 is reduced to:

$$\frac{H(S)}{Q(S)} = -T_w \cdot s - h_f \quad (5.7)$$

Which gives the transfer function used in the model, where the output is needed to be a fluid flow:

$$\frac{Q(S)}{H(S)} = -\frac{1}{T_w \cdot s + h_f} \quad (5.8)$$

In figure 5.7 the block used in the simulations are found values inserted.

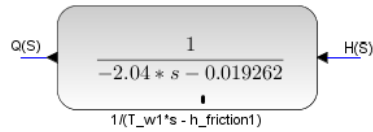


**Figure 5.7:** Transfer function block from scilab describing the head-race tunnel used in the simulations.

The same model is used for the simplified draft tube. The transfer function block can be seen in figure 5.8

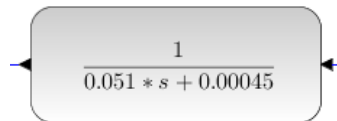


**Figure 5.8:** Transfer function block from scilab describing the draft tube tunnel used in the simulations.

### 5.3 Surge Shaft

The transfer function describing the surge shaft water level height is deduced in subsection 3.4.2. The surge shaft filling time is given by:

$$T_s = \frac{A_s \cdot H_0}{Q_0} \quad (5.9)$$

And the surge shaft transfer function is:

$$\frac{dH}{dQ} = \frac{1}{T_s \cdot s} \quad (5.10)$$

The block used in simulations is found in figure 5.9. The values are presented in Table 5.1 and are based on the calculations presented in Appendix A.

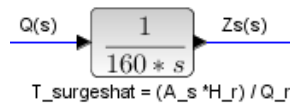


**Figure 5.9:** Transfer function block from scilab describing the surge shaft used in the simulations.

## 5.4 Surgeshaft validation model

This model is including an input representing a reservoir providing a particular flow to the system. It also includes a pipe between the tank and the surge shaft and the surge shaft itself. The model can be seen in figure 5.10

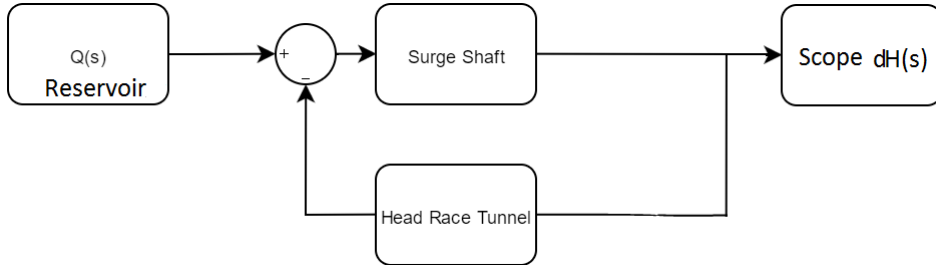


**Figure 5.10:** Block diagram for simulation of the test rig at the laboratory.

During the simulations the head race tunnel from section 5.2.2 is used. A step function is set from one to zero [pu] in the reservoir. The pressure or level of head will then oscillate due to the system dynamics from the head race tunnel and the surge shaft. The signal can then be seen in the scope. Adding the head pressure gives the scope output the correct pressure to total pressure. There is no need for multiplying inside the the lode with the head base since the head is 1m. This means that the change in head also is given in [m], as well as [pu]. In figure 5.11 the scilab model from the surge shaft validation can be seen:

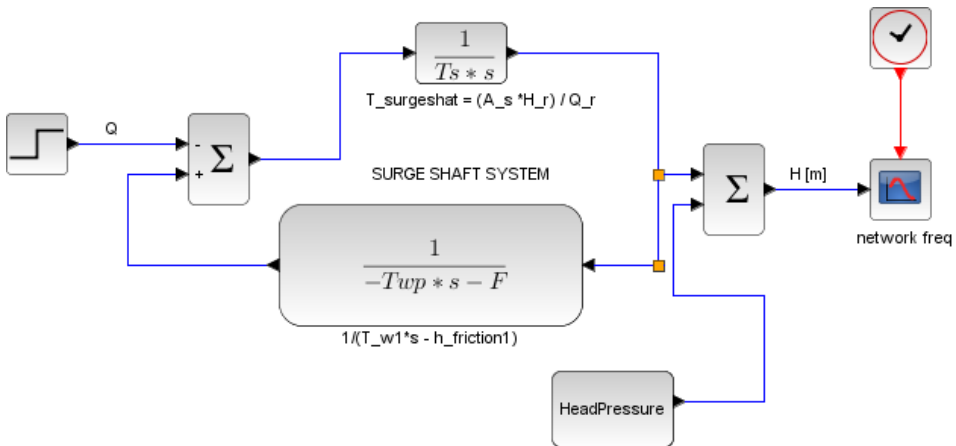


**Figure 5.11:** The model for surge shaft validation with scilab

## 5.5 Turbine

The Francis turbine model used in the simulations is based on the linearized turbine model. By linearizing the turbine characteristics around an operating point gives a detailed representation of the turbine model, but its accuracy is constricted around that specific point. Equation 5.13 and 5.14 is found and used in literature such as: [12], [4] and [7]. The dynamic characteristics for a Francis hydro-turbine can be described as:

$$q = q(h, n, G) \quad (5.11)$$

$$m_t = m_t(h, n, G) \quad (5.12)$$

Where  $m$  is the mechanical torque and  $q$  is the water flow through the turbine.  $h, n$  and  $G$  is respectively turbine head, turbine speed and the guide-vane opening. By utilizing first order Taylor expansion of Eq: 5.11 and 5.12 the dynamic expressions of the Francis turbine is obtained [12]:

$$\Delta q = \frac{\partial q}{\partial h} \Delta h + \frac{\partial q}{\partial n} \Delta n + \frac{\partial q}{\partial G} \Delta G \quad (5.13)$$

$$\Delta m_t = \frac{\partial m_t}{\partial h} \Delta h + \frac{\partial m_t}{\partial n} \Delta n + \frac{\partial m_t}{\partial G} \Delta G \quad (5.14)$$

Turbine transfer coefficients are described as partial deviates of flow and torque with respect to head, speed and guide vane position, where all variables are in per unit. For optimal performance the transfer coefficients should be deduced at the specific operating point of the turbine. In this thesis the operating point is set to BEP, and it is deduced by a program based on Euler's turbine equations. The program is programmed in labVIEW and is made by Bjørnar Svingen. The layout can be seen in Figure 5.12.





all the turbine transfer coefficients in a simple manner by the use of output variable from the program. The calculations and outputs can be found in appendix C. The transfer coefficients were calculated to be:

$$\frac{\partial m_t}{\partial G} = 1.01 \quad \frac{\partial m_t}{\partial h} = 0.503 \quad \frac{\partial m_t}{\partial n} = -0.97 \quad \frac{\partial q}{\partial G} = 1.005 \quad \frac{\partial q}{\partial h} = 0.5 \quad \frac{\partial q}{\partial n} = -0.966$$

In figure 5.13 the model is given in a block diagram form. Calculations done for the particular turbine used in the thesis can be found in Appendix B, and table 5.2 summarise up the different parameters of the turbine.

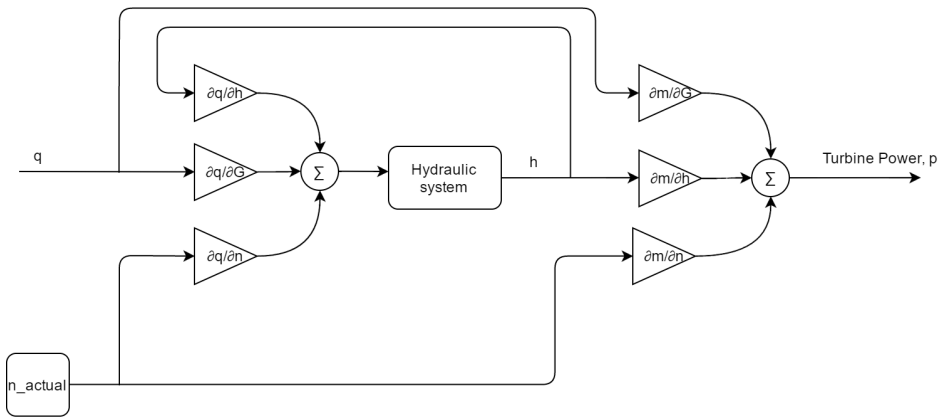


**Figure 5.13:** Transfer function block from scilab describing the surge shaft used in the simulations.

**Table 5.2:** Turbine specifications

Unit	Description	Value
Q <sub>bep</sub>	Best efficiency point flow [ $\frac{m^3}{s}$ ]	50
H <sub>bep</sub>	Best efficiency head [m]	200
N <sub>bep</sub>	Best efficiency speed [rpm]	333.33
T <sub>bep</sub>	Best efficiency torque [Nm]	2700694
$\eta_{bep}$	Efficiency at best point [-]	0.96
a <sub>1bep</sub>	Guide vane angle [°]	15
b <sub>1bep</sub>	Angle of the rotor blade, (absolutt angle)[°]	67.7
r <sub>1</sub>	Inlet runner radius [m]	1.311
r <sub>2</sub>	Outlet runner radius [m]	1.146
R <sub>q</sub>	Constant for RPT [-]	0
R <sub>m</sub>	Angular velocity damping constant [-]	0.04
R <sub>d</sub>	Design constant koeffisient [-]	0.03
R <sub>f</sub>	-	0.015

## 5.6 PID - Regulator

The PID regulator in this thesis regulates the active power production in response to the variation of power demand, hence frequency in the grid, see equation 5.18. The frequency and load variation has a relationship as follow [8]

$$\frac{\Delta f}{f_n} = -\rho \cdot \frac{\Delta P_g}{P_d} \quad (5.18)$$

Where  $\Delta f$  is the change in frequency,  $f_n$  is the nominal frequency in the grid,  $\Delta P_g$  is the change in active generated power, while  $P_d$  is power demand, and  $\rho$  is the static droop of the turbine governor characteristic.

By regulating the guiding unit of the Francis wheel, the power regulation is made possible. This chapter details mathematical modelling of the electro-hydraulic turbine governing system PID regulator (proportional, integrating derivating), that will function as a governor for the hydropower system.

As far as the literature describes the controller there is two ways of modelling. The one which is ideal, includes Kp into the derivative and integral part deducing new constants called integral and derivation gains. The model used in this thesis, is generated directly out from the Laplace transformed equation 5.23. This is done to ease the tuning, where tuning methods often are based directly on adjusting the time constants  $T_i$  and  $T_d$ .

The I-block or  $(\frac{1}{T_i \cdot s})$  is the part where stationary deviation the eliminated. D part ( $T_d \cdot s$ ) is reducing the dynamic deviation and counteracts on oscillations in the process value, an important part when running in island mode. [16] This leads to less wear on the water guiding device, and less time to reach stationary speed.  $K_p$  is simply a proportional gain, making sure that the gain is proportional to the deviation.

The mathematical relationships between the input and output for the PID regulator is as follow [9] :

$$u = K_p \cdot \left( \epsilon + \frac{1}{T_i} \int_0^t \epsilon dt + T_d \cdot \frac{d\epsilon}{dt} \right) + u_0 \quad (5.19)$$

Where  $\epsilon$  =deviation from reference input of what there is to be regulated. U is the output signal where

$$u = u_P + u_I + u_D + u_0 \quad (5.20)$$

In other words  $u$  is a function of the different contributions from the proportional, integral, derivative, and nominal states given as:

$$u_P = K_P \epsilon \tag{5.21}$$

$$u_I = \frac{K_P}{T_i} \int_0^t \epsilon \cdot dt \tag{5.22}$$

$$u_D = K_P \cdot T_d \cdot \frac{d\epsilon}{dt} \tag{5.23}$$

Introducing Laplace transformation to 5.19 gives

$$u(s) = K_P \cdot \epsilon(s) \left( 1 + \frac{1}{T_i \cdot s} + T_d \cdot s \right) + \frac{u_0}{s} \tag{5.24}$$

$$\frac{u(s)}{\epsilon(s)} = K_P \left( 1 + \frac{1}{T_i \cdot s} + T_d \cdot s \right) \tag{5.25}$$

Equation 5.25 gives the following block diagram, as seen in figure 5.14

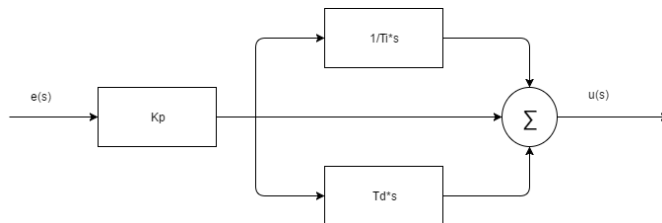


**Figure 5.14:** PID regulator for speed regulation and power regulation, as modelled in scilab. [17]

## 5.7 Servo System

The servo system in his thesis are only used in the water hammer simulations. It is a part of the mechanical system, making the system damp the water hammer, forces that may occur. By the use of a rate limiter closing time of the guide vanes can be limited and set to greater than the reflection time. The closing time is set to 10s during LVTrans simulations, so did the scilab model during the simulations. This should be enough as the reflection time in the system is less than 2s. Based on earlier experiences, if a pipeline of 1000m is filled up with water and the closing time is 10s, the pressure transients will appear as mildly [12]. In figure 5.15 the block used as rate limiter can be seen.

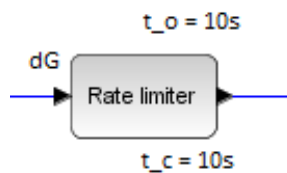


**Figure 5.15:** The ratelimiter block used for waterhammer simulations.

## 5.8 PID Tuning

### 5.8.1 Method 1

PID tuning can be done in many ways based on the type of system and its criteria for system stability. In this thesis two different methods are reviewed. The first one is called "Method 1" in the guide book of LVTrans [21], and it is the one used in this thesis. The procedure steps can be seen in the list below:

1. Set the PID in island mode running at 85% til 100% load.
2. Set  $P = 1$ ,  $T_i = 10$ ,  $T_d = 0$
3. Wait until the system is stable.
4. Set  $T_i = 10^{10}$  (or as high as possible)
5. Apply steps in the reference value of frequency of 10%
6. Increase P until a overshoot of 15% is observed in the frequency process value (PV) compared to the step in reference.
7. Decrease  $T_i$  until the overshoot in PV is 30%
8. At last decrease P until the overshoot is acceptable. Typical 5% til 20%
9. For PID, increase  $T_d$  until the overshoot is acceptable. Typical 5% til 20%

This methods is applied to the system in LVTrans and has been the reference thought the system simulations done in chapter 6. As the regulator only has been working as a PI regulator, the D parameter has been set to 0. The values are found to be:

- $P = 3$
- $I = T_i = 7s$

## 5.8.2 PID tuning by frequency analysis

When tuning the system in the frequency plane from the start a frequency response of the system without the regulator is done. This transfer function is called  $h_0^*$ . By following the five stages in the list below, PI settings for the controller can be found.

1. Choose the type of regulator PI, PD, or PID.
2. Achieve Bode plot for the open loop transfer function without the regulator. This is given by  $h_0^*(s)$
3. Decide the amplitude cross frequency  $\omega_{\phi c}$
4. Decide the regulator parameters. A proposal for this is found in table 5.3
5. Control the gain margin and perhaps adjust  $K_p$

**Table 5.3:** Proposal for PID tuning by frequency analysis [9]

-	P	PI	PD	PID (product)	PID (sum)
$\angle h_0^*(j\omega_{\phi c})$ = <i>ang</i>	$-180^\circ$ $+\Delta\Phi$	$-160^\circ$ $+\Delta\Phi$	$-220^\circ$ $+\Delta\Phi$	$-200^\circ$ $+\Delta\Phi$	$-210^\circ$ $+\Delta\Phi$
$T_i$		$\frac{2.8}{\omega_{\phi c}}$		$\frac{2.8}{\omega_{\phi c}}$	$\frac{2.8}{\omega_{\phi c}}$
$T_d$			$\frac{1}{\omega_{\phi c}}$	$\frac{1}{\omega_{\phi c}}$	$\frac{1}{\omega_{\phi c}}$
$[K_p]_{dB}$	$- ang _{dB}$	$- ang _{dB}$ $-1dB$	$- ang _{dB}$ $-3dB$	$- ang _{dB}$ $-4dB$	$- ang _{dB}$ $-2dB$

In table 5.3, the different variables are:  $\angle h_0^*(j\omega_{\phi c})$  which is the phase angle that decides the amplitude cross frequency. This is just called *ang* further in the table, and the  $\Delta\Phi$  is the phase margin for the given system. Once the frequency is found both  $T_i$  and  $T_d$  can be found. At last the gain called  $K_p$  can be found. This is done by taking the gain at the calculated amplitude cross frequency and subtracting the right amount of dB given for the specified regulator (P, PI, PD, or PID). The PID on sum or product is only a mathematical preference where most of the new micro controller based regulators are on the sum form. The product form is defined as:

$$h_{pid}^{prod}(s) = K_p \cdot \frac{1 + T_i \cdot s}{T_i \cdot s} \cdot \frac{1 + T_d \cdot s}{1 + \frac{T_d}{n} \cdot s}$$

And the sum form of the PID regulator is given by:

$$h_{pid}^{sum}(s) = K_p \left( 1 + \frac{1}{T_i \cdot s} + \frac{T_d \cdot s}{1 + \frac{T_d}{n} \cdot s} \right) \quad (5.26)$$

PI constants are then analyzed and can be modified with frequency analysis to the system. This, is done in section 6.3. In order to perform the frequency analysis an extra package in the scilab program is installed. The package is called CPGE and makes it possible to generate both bode plots and Nyquist diagrams directly from the block diagram interface.

The margins from the response in figure 6.10 in the frequency analysis chapter 6.3 are well within limits, when looking at the general criteria for a stable system where the phase and gain margins both are positive. Figure 5.16 illustrates two examples of a stable and unstable system. The stable system is marked with the red line, while the blue is unstable.

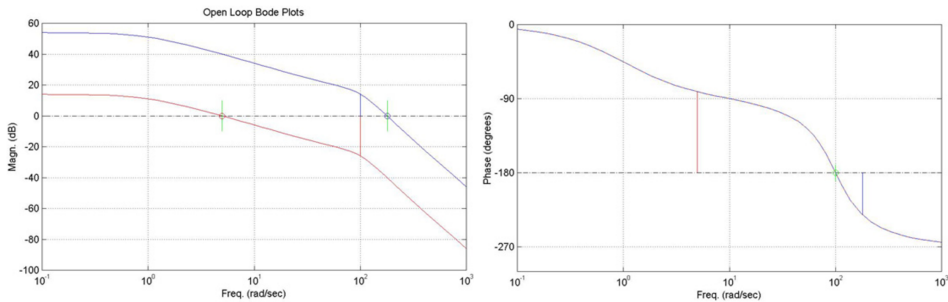


**Figure 5.16:** Examples of unstable and stable systems based on phase and gain margin [11].

and the system is found to be stable during any external influences such as load rejections and frequency variations the system are not adjusted any more than it is from the original settings. This is a subject that could be taken further, and a proper PID analysis in the frequency plane could be performed as future work for the system.

# Chapter 6

## Simulation and Analysis

In this chapter, the analysis and simulations results are shown. The content involved in this chapter is:

- System setup overview, p48.
- Functional requirements for hydropower generation and control in Norway p56.
- Stability analysis for Scilab model, p57.
- Evaluation of the hydraulic system in Scilab, p60.
- Model validation with LVTrans, p64.

The laboratory work can be found in chapter 7 page 71. The chapter contains surge shaft model verification with the u-pipe test rig.



## 6.1 System Setup

In this section models from the block diagrams are shown and explained. There are four block diagrams from the Scilab program that is shown:

- Frequency regulation in island model
- Power regulation in a stiff network
- Analytic island model
- Analytic Island model with variable time dependant friction settings, used in water hammer and mass oscillation simulations.

Each model is saved in individual xcos files, and can be opened by Scilab.exe. The program has a "write to CSV" block which logs the given input signal to a given time interval. The log is saved as a text file and can easily get imported to Excel, MATLAB or similar programs.

LVTrans is programmed into a more compressed simulation tool which makes the amount of work programming the system minimal. By an advanced PID regulator, both island and stiff network simulations can be switched by a button. Also, simulations for the water hammer is done by the regulator by turning a switch.

### 6.1.1 Scilab Setup

#### Frequency regulation in island mode

The model in figure 6.1 is frequency regulated turbine in island mode. It is a single machine, single load environment and it is much used in stability analysis on the hydraulic part as the stiffness from a normal stiff network is absent. PID parameters are also set in this configuration, and for Norwegian power plants, the settings should also be fully functional during turbine power regulation with stiff loads.

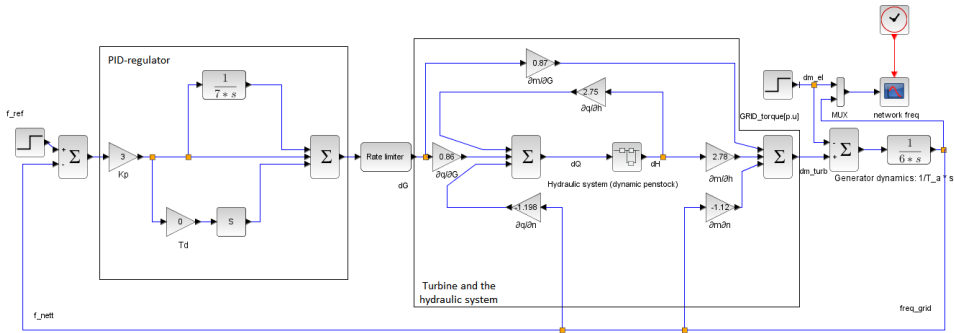


**Figure 6.1:** Layout of the block diagram for frequency regulation in island mode.

Power regulation in a stiff network

Next system is the block diagram for a power regulated turbine connected to a stiff network or load seen in figure 6.2. The system is based on the first model but has some changes made to it. With this model, grid frequency is set as an input, as well are power and speed references to the turbine too. The simulations are done with a step in grid frequency.

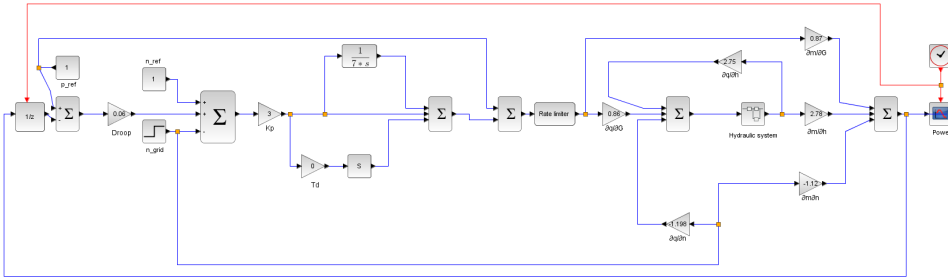


Figure 6.2: Layout of the block diagram for load regulation connected to a stiff load.

It is a single machine stiff load environment, with an implemented droop function which decides how much the guide apparatus shall act during a change in load. Figure 6.3 illustrates the effect of different droop settings:

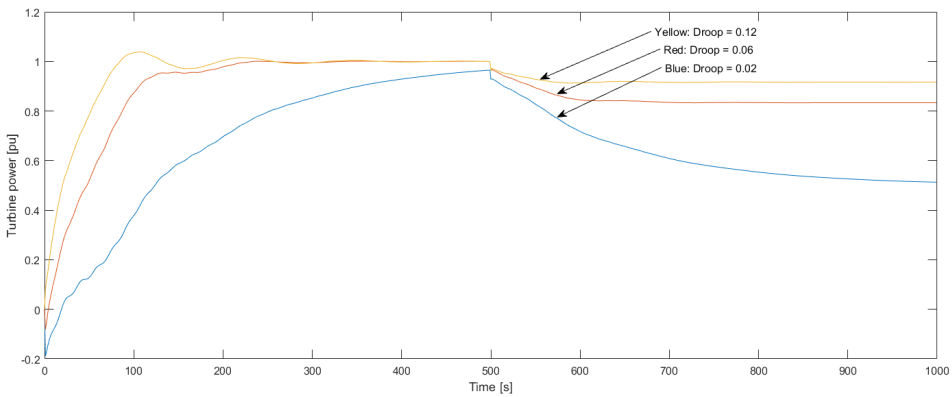


Figure 6.3: The effect of three different droop settings

As the droop get lower, the more will the turbine react to a change in frequency. In the example, a drop of 0.5Hz is done at t=500. For the drop of 0.02, almost half of the machine power gets reduced, compared to the droop of 0.12, where only 10% of the power gets reduced. During the simulations, a droop of 0.06 is set.

## Analytic Island model.

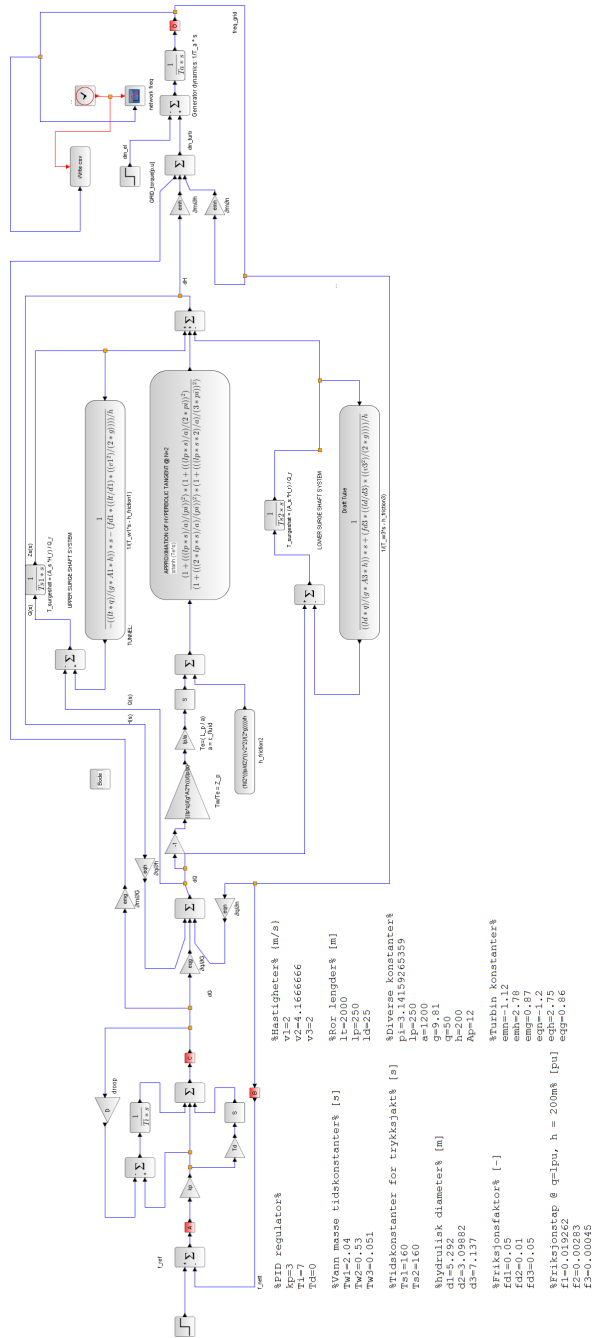


Figure 6.4: The hydraulic system used in the simulations.

The analytic model in figure 6.4 is made to perform stability analyses and system parameter analysis. By using the "set context" function in Scilab makes it possible to give the parameters names and values. By inserting the different equations for PID parameters, turbine parameters and hydraulic equations into the blocks, the program calculates the transfer functions after what is defined in the context file.

By using the block: "PARAM VAR", different inputs can be simulated in one go. This provides an effective way to perform parameter analysis to the system. The small red blocks with letters in sets the reference point to where the program shall calculate the transfer function. For a closed loop, frequency analysis between point A and B is inserted in the BODE function block as start and end points.

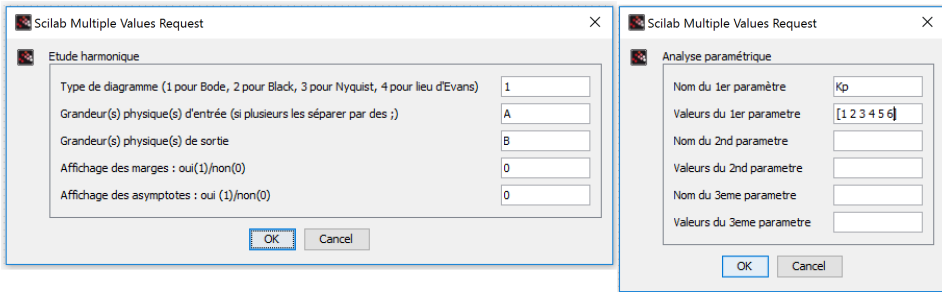
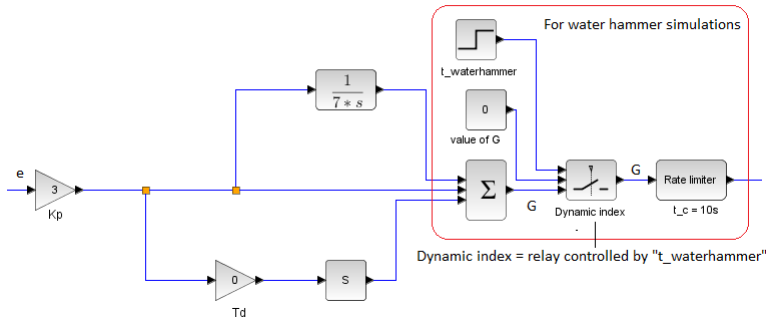


Figure 6.5: Analytic functions for scilab model

In figure 6.5 the context for bode plot is set in the box to the left. In the box to the right, settings for multiple variable simulations are done. In the figure,  $K_p$  is simulated for the values 1 to 9.

### Waterhammer Simulations

To perform the simulations correctly, the guide vane closing time must be limited to about 10s, and the power from the grid must fall to zero. The guide vane must in the same time be kept constant at zero. With the basis of the island mode diagram, modifications to the governor and block infrastructure is done, see figure 6.6:



**Figure 6.6:** Changes in the infrastructure due to water hammer simulations.

After performing simulations with the setup from figure 6.6 in combination with the system in figure 6.1, some more modifications had to be done to make corrections for the friction factors as the flow changes states and value.

The friction still stays static during the event, but new values in the form of friction factor can be changed with the system setup in figure 6.8. By use of relays and new blocks describing the tunnels with new friction factors, the changes can be done in the time of the valve closure. New friction settings are defined in the "set context" function under simulation settings see figure 6.7.

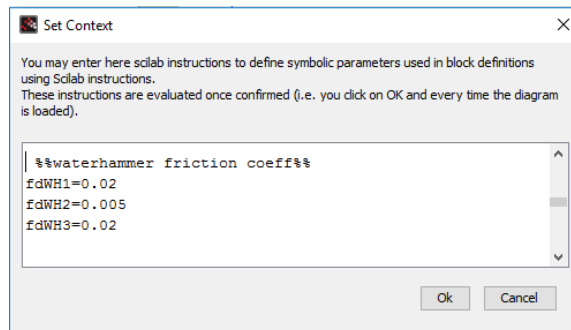


**Figure 6.7:** set context tool to inset system variables.

Analytic Island model with variable time-dependent friction settings

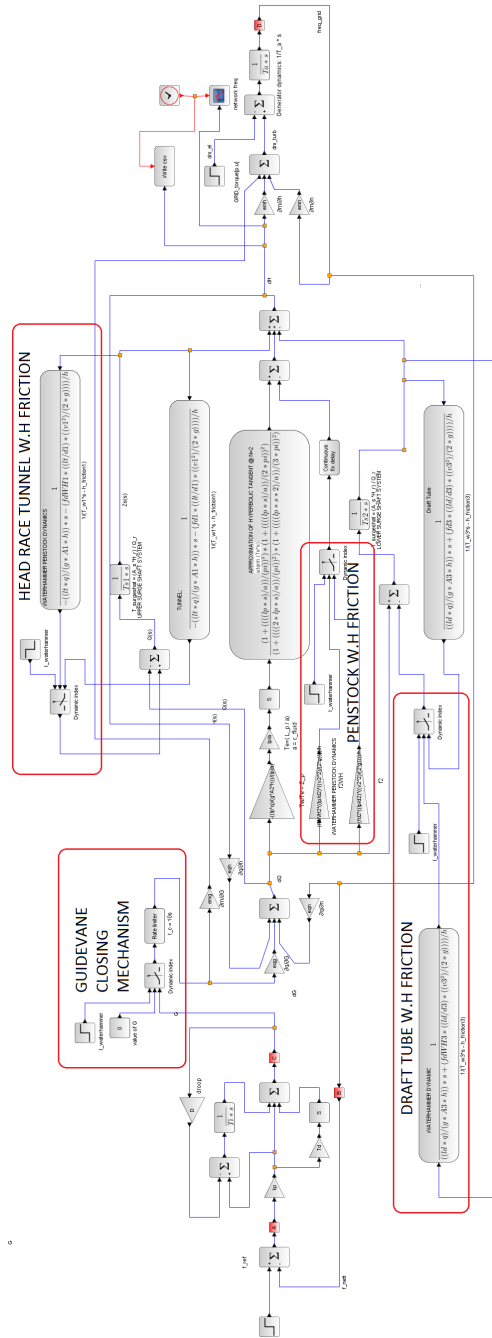
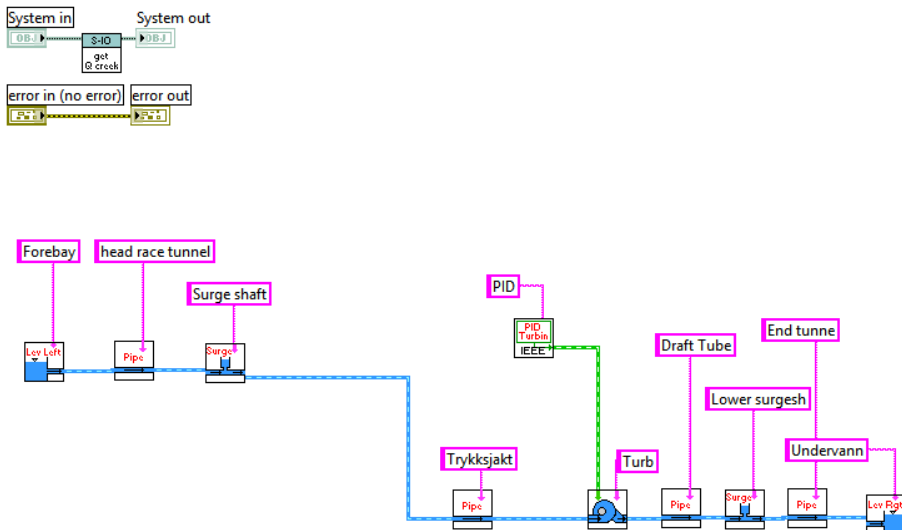


Figure 6.8: Analytic model with water hammer sim and friction modification.

## 6.1.2 LVTrans Setup

The model in LVTrans can be seen in figure 6.9. It is programmed through using premade blocks in the programme. After starting the program, each block can be defined in the system specifications. In Appendix E, The parameters utilised in the simulations can be found.



**Figure 6.9:** System in LVTrans

The setup is modelled as closely to the scilab model as possible. There are some smaller deviations in the model such as the end tunnel and the servo implemented in the PID regulator. By choosing a small length of the end tunnel (1m), and implementing a rate limiter in the most transient simulations the deviations got minimised. The program has a good implementation of logging functions and generates plots via MATLAB is easily done. The program comes with a guide book as well, which makes it easy to get started and ready to use.



## 6.2 Functional Requirement

The Norwegian power system administrator, Statnett is responsible for the operation of the main grid in Norway. Through their book of guidelines (FIKS) [20], information on how to operate energy production facilities are set, and different criterion for system stability are given. Some of them are listed down below, and the simulations are to some degree evaluated towards them.

### General functional requirements

- Frequency regulation with a positioning feedback loop, with separate load adjustments.
- Power regulation mode, measuring the generator power production. A droop should also be implemented in the controller.
- Resolution of frequency measurements should not be less than 0.01% when operating in the area of 90% to 110% of the nominal frequency.
- Time constant  $T_y$  in the servo system should not be more than 0.4s This regards Francis turbines as well as Pelton. The time constant the based on an opening of 100%.
- The permanent droop should be adjustable between 2% and 8%.
- For island operation: During a 10% change in load while running at 85% power production, no more 6% frequency transient should occur.

### Power response during destabilisation

- Unbalance between power production and and power consumption results in a change in frequency. The turbine regulator should then compensate by regulating depended on the measured frequency.
- The correction in production will vary based on the systems permanent droop.
- Stability analysis for an existing power station is identified by frequency analysis.
- Criteria for system stability is that the phase margins is in the interval between  $25^\circ$   $35^\circ$  and the frequency margin is between 3dB til 5dB at full load and a constant voltage level.
- One should aim the regulation parameters by these margins for the best system stability possible.

## 6.3 Stability Analysis

The stability analysis is based on frequency response and a step response of the system. It is performed bode plot from the system in open loop in the figures below. To perform the frequency analysis, an extra package in the Scilab program is installed. The package is called CPGE and makes it possible to generate both Bode plots and Nyquist diagrams directly from the block diagram interface. The PI parameters are set to  $K_p = 3$  and  $T_i = 7$  during all the plots. Due to the many derivative blocks in the system, a delay in the gain signal is implemented. This is necessary for the program to include the dynamics of the turbine and penstock.

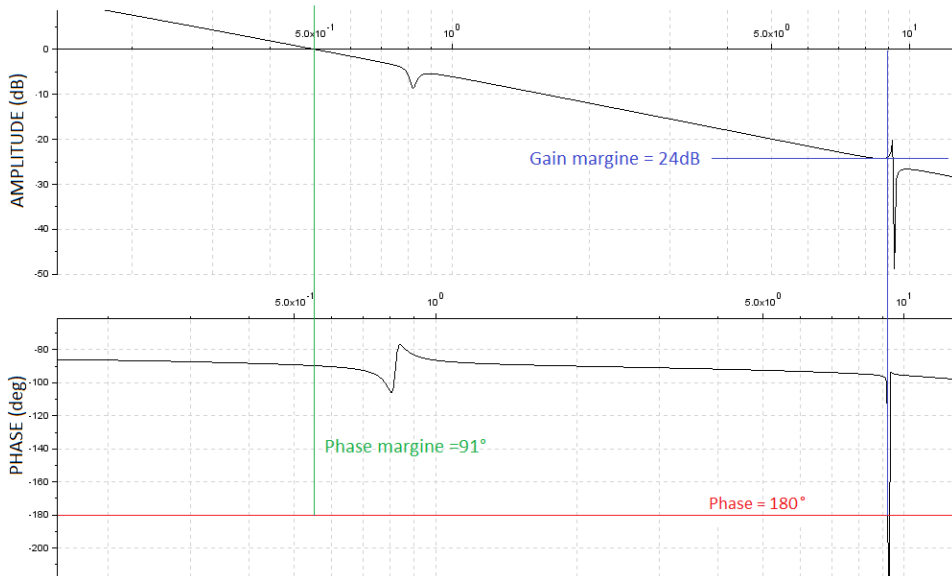


**Figure 6.10:** Bode plot for the open loop transfer function.  $K_p = 3$ ,  $T_i = 7$  and time delay = 0.01s

In figure 6.10 bode plot for the open loop including the PI regulator is made. A time delay of 0.01s has been included in front of the turbine model, and the  $K_p$  and  $T_i$  settings are 3 and 7. This leads to a gain and phase margins of  $24dB$  and  $91^\circ$ .

The tuning can be done by adjusting  $T_i$  and  $K_p$  to change the gain and phase margins. See figure 6.11 where the cross frequency changes as  $K_p$  changes from 1 to 9:

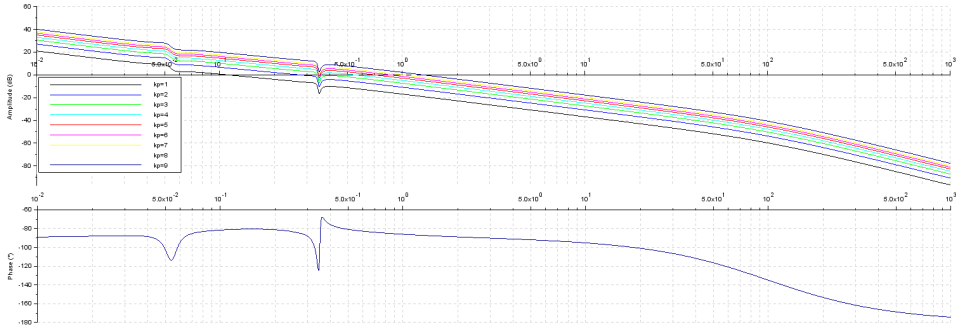


**Figure 6.11:** Gain and phase response due to changes in  $K_p$

In figure 6.12 the response for changing  $T_i$  from 1 to 9 as  $K_p$  is kept constant at three can be seen. Choosing a lower  $T_i$  results in a lower phase angle at a frequency of  $0.02 \frac{rad}{s}$  to  $10 \frac{rad}{s}$ . Doing so also increases the cross frequency which may result in a higher phase margins. So there is a balance that must be set for the gain and the integral time.

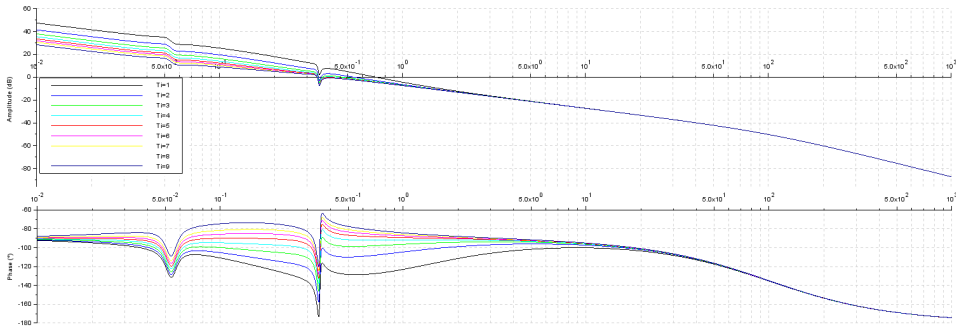


**Figure 6.12:** Gain and phase response due to changes in  $T_i$

The results from the frequency analysis show promising stability characteristics for the system. With both positive phase and gain margins, the general stability criteria for a dynamic system are set. The criteria set by statkraft is not fulfilled, and should be aimed when systems shall be used for simulating with new plant data, or used for dimensioning a new full-scale power plant.

Stability analysis are also done with a step response in load demand, simulating grid frequency over a period of 2000s. The step occurs at  $t = 1000s$  with a negative magnitude of  $0.5pu$ . The simulations are done in island mode with a simple machine, single load.

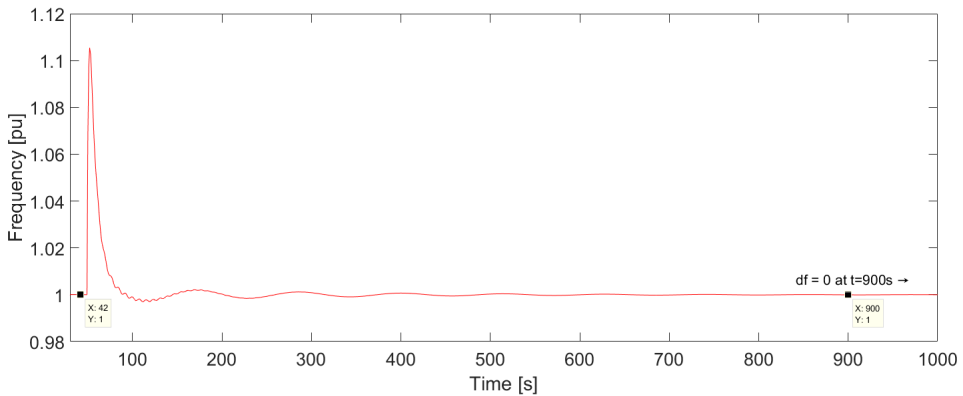


**Figure 6.13:** Frequency response for a load drop of 50%

Figure 6.13 shows the governor action in the form of PI regulation. As the drop in load demand occurs, the governor stabilises the energy produced by the turbine, by closing the guide vanes from fully open with and process value of 1.962 to 1.462 as seen in figure 6.14. The governor then slowly stabilizes the frequency by decelerating the turbine by applying less amount of inlet flow, which corresponds well according to the mechanical torque equation where the shaft torque is a function of fluid flow:  $M_t = \rho Q(r_{in} \cdot c_{u,in} - r_{out} c_{u,out})$  and where the turbine power is a function of torque and angular speed, the torque must decrease in order to maintain the speed as the load decreases, seen in equation:  $P_t = M_t \cdot \omega_t$ . This must be, in order to keep the general stability and production criteria where the energy demand and energy production must be equal:  $P_l = P_t$ .

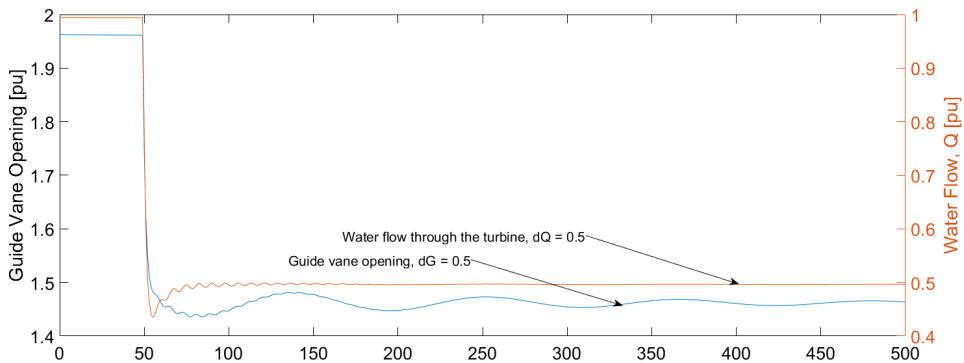


**Figure 6.14:** Gate opening, responding to a drop in load demand of 50%

## 6.4 Evaluation of Hydraulic Systems in Scilab

Evaluation of the dynamic penstock is done by comparing it to the classical, static model. This is done to confirm the impact, which the dynamic model brings to the system. The draft tube and lower surge shaft are not included in the model in the first simulations. First off a comparison between the static and the dynamic penstock are done to see the impact of frequency dynamics on the grid under a load change of  $-10\%$ . The second comparison is in water head level a larger load change. Last penstock model comparison is simulations done with penstock as the only pipe in the system. Simulations of pressure pulsations with different penstock lengths are also done to see the impact of pressure transients when extending the penstock. Til last, the effect of adding a draft tube and a lower surge shaft are being investigated.

### 6.4.1 Comparing Dynamic and Static Penstock

In the figure, 6.15 a comparison of the static and dynamic penstock model with surge shaft dynamics is made. The blue line is simplified static penstock model, and the red line is dynamic penstock model.

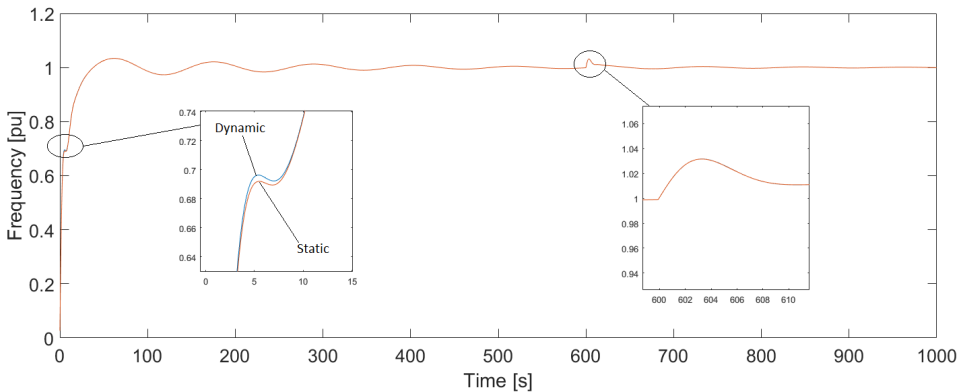


**Figure 6.15:** Comparing the frequency dynamics of two penstock models, when simulating a drop in load of 10 % in island-mode.

The differences between the two penstock models are not visible during the decrease in load, as seen in the right figure inside figure 6.15. A Small deviation in the start-up dynamics can be viewed in the figure to the left. The little difference could be because of the short penstock length. This makes the effect of elastic water string small and almost neglectable. As seen in section 6.18 the penstock of 500m has more effect on the system than the shorter one of 250m.

Simulations for the pressure in front of the turbine can be seen in figure 6.16. It is the same setup as in the simulations from figure 6.15, but with a larger load drop of 50%.

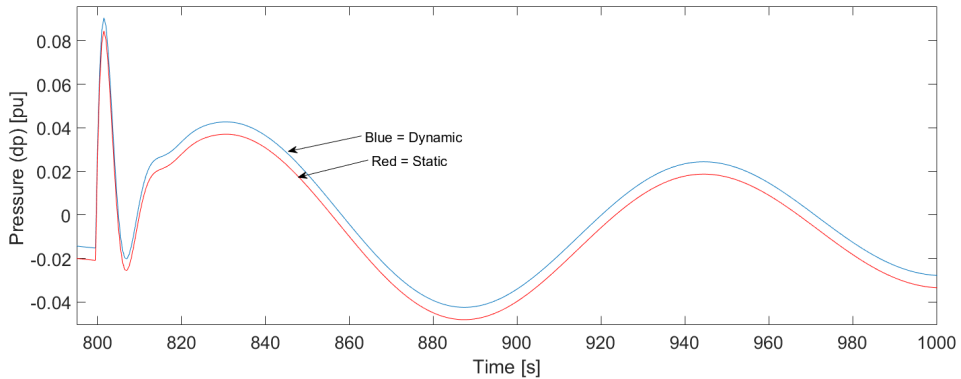


**Figure 6.16:** Comparing the pressure dynamics in front of the turbine when simulating a drop in load of 50 % in island-mode.

The deviation from the load drop can be seen in figure 6.16 with a pressure difference of  $0.006pu$  which in the  $200m$  head base system is  $1.2m$ . Due to deviation in friction, the head in the dynamic penstock is some higher than the other. The models seem to behave very similarly, and the penstock effect is obviously small in the system. Due to its short length, the dynamic effect is almost neglectable from the view of pressure pulsations. New simulations with only the penstock connected to the system gave better results for comparison, see figure 6.17

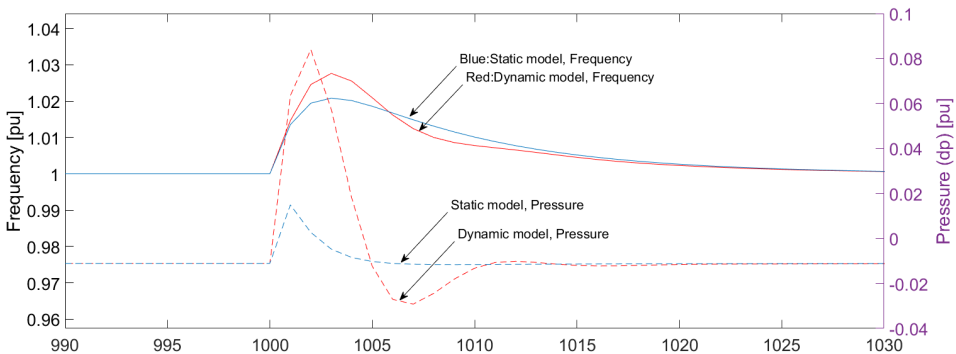


**Figure 6.17:** Simulation of pressure and frequency, comparing the penstock models isolated.

By isolating the penstock in the simulations, differences became clearer. In the figure, 6.17 head pressure and frequency are plotted as a function of time. The simulations are performed in island mode, with a load drop from 85% to 75% at  $t=1000$ . As seen the dynamic model has a much larger influence in the form of increased pressure in front of

the turbine. There are also some deviations in the frequency dynamics as well. See table 6.1 for comparing figure values:

**Table 6.1:** Values from comparing dynamic and static penstock

Model	$p_{tot}$ [m]	$\Delta p$ [m]	$\Delta f$ [pu]
Dynamic	216.8	19	0.028
Static	203	5.2	0.021

### 6.4.2 The Effect of Extending Penstock Length

To investigate the effect of penstock length, the change in head pressure in front of the turbine is measured. It is simulated during a drop in load from 0.85 pu to 0.75pu, seen in figure 6.18. The simulations are done with the analytic model, running in island mode.

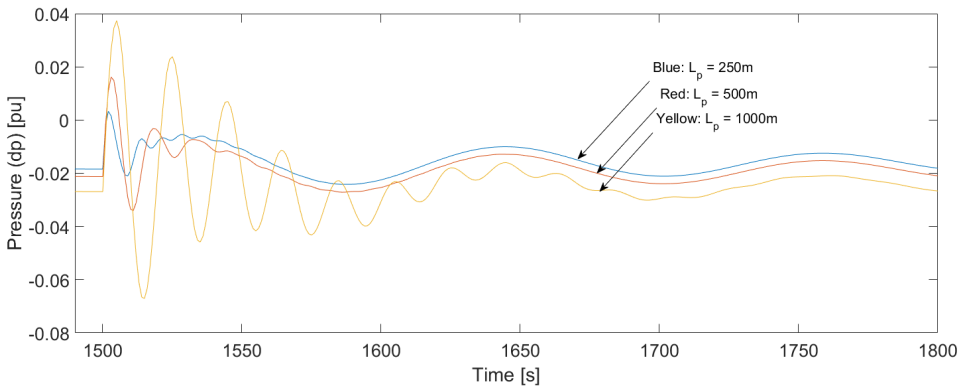


**Figure 6.18:** Pressure pulsation effect for different penstock lengths

As the length increases so do the head pressure as a result of flow change due to a change in load demand. More oscillations can be seen in the longer penstock as the elasticity time constant is increasing, where:

$$T_e = \frac{l_p}{a}$$

The deviation in total friction loss and pressure at the first transient are measured and can be seen in table 6.2 The pressure  $\Delta p_t$  is measured from steady state head to the first transient. The head loss is measured directly from steady state head. Values from the graph are in per unit, and converted in the table to m.

**Table 6.2:** Values inserted in the scilab model during the simulations

Penstock length $l$ [m]	Friction loss $\Delta h_f^{tot}$ [m]	Change in pressure $\Delta p_t$ [m]
250	-3.86	4.34
500	-4.25	7.48
1000	-5.38	12.85

### 6.4.3 The effect of adding a draft tube and lower surge shaft

The effect of implementing a draft tube and a lower surge shaft can be seen in figure 6.19. The figure shows pressure changes in front of the turbine given in pu. The simulations are performed in island mode with a drop in load from 1pu to 0.9. It is done with a draft tube with the same area as the penstock and the lower surge shaft dimensioned after the size of the draft tube.

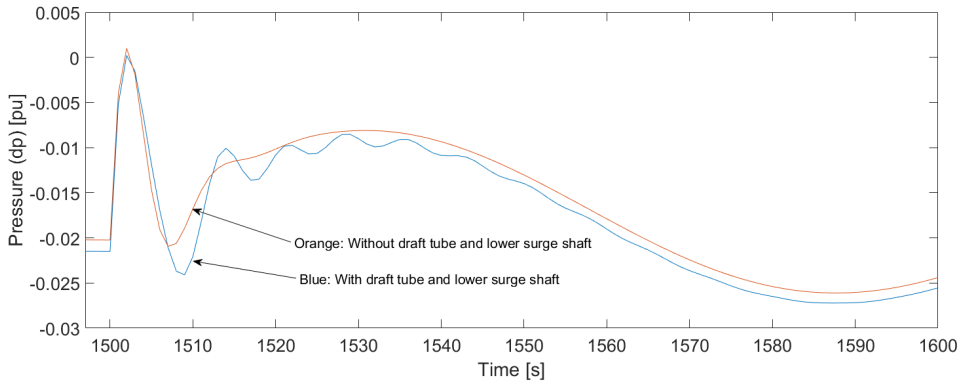


**Figure 6.19:** Frequency response of system start up and during a load rejection of 10% during full load.

The implementation provides more friction which leads to a lower static head. A more oscillatory behaviour during changes in flow can be observed with a higher pressure transient. Friction loss with draft tube and lower surge shaft implemented are at 4.302m and without them, 4.048m. Both models provide a pressure increase til around 200m head, which makes the model with the implantation some higher.



## 6.5 Model Validation with LVTrans

In this section the block diagram made in scilab is validated up against LVTrans. There are performed three types of simulation:

- Frequency regulation in island mode
- Power Regulation in Stiff Grid Mode.
- Water Hammer Simulation

By comparing the two programs, an idea of how the Scilab model performs compared to the physical model can be achieved. Since LVTrans has proven to be very accurate and used in the industry as a standard simulation tool this program is used a validation method.

By using step response in both frequency and electric load, the model characteristics are compared up against each other. The simulations are done with a step in load demand for island operation and with steps in frequency for the power-regulated model. Since the turbine and piping models have such large impact on how the responses are to pressure pulsations and turbine speeds, a good system evaluation is possible to achieve by the step responses.

Water hammer simulations are performed at the end of the chapter. This shows more clearly how the Scilab model performs in the form of pressure pulsations and mass oscillation simulation.

### 6.5.1 Frequency regulation in island mode.

Changes in grid frequency occur constantly, but since the load system is so substantial, the frequency variation often appears to be small. Larger deviations in frequency occur typically during line faults, and large load connect and disconnections. To provide good quality and high reliability in the electrical power supply, governing in the production units are necessary. This due to keep frequency and voltage fluctuations as low as possible and maintain stability in a complex dynamic system. [8] In the simulations the systems are stressed with frequency drops of 10% and a worse case of 50% load rejection.

In the figure below 6.20 a drop of 50% in load demand is applied to the systems. The Scilab simulation was far off the LVTrans simulation during the heavy drop. It is a frequency deviation of 4Hz, and the Scilab simulation is slower to reach steady state.

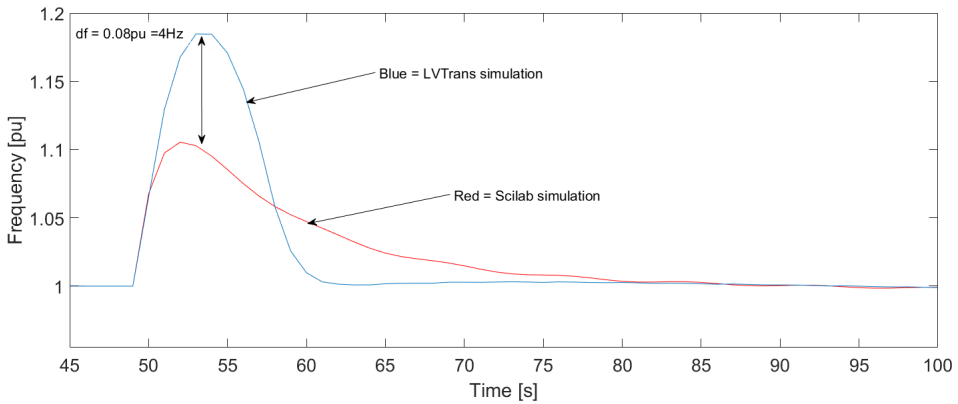


**Figure 6.20:** Frequency regulation during a drop from 100% to 50% in load demand

Figure 6.21 shows that the stability criteria is proven to be within the limits when running in island mode. Acceptable results from both simulations in LVTrans and Scilab can be seen as it is under a 6% transient peak during a 10% drop in load from 85% of BEP. The LVTrans model had a peak of 1.026 pu while the Scilab simulation peaked at 1.021 pu, as seen in the figure, deviation in frequency between the models are at 0.25Hz.

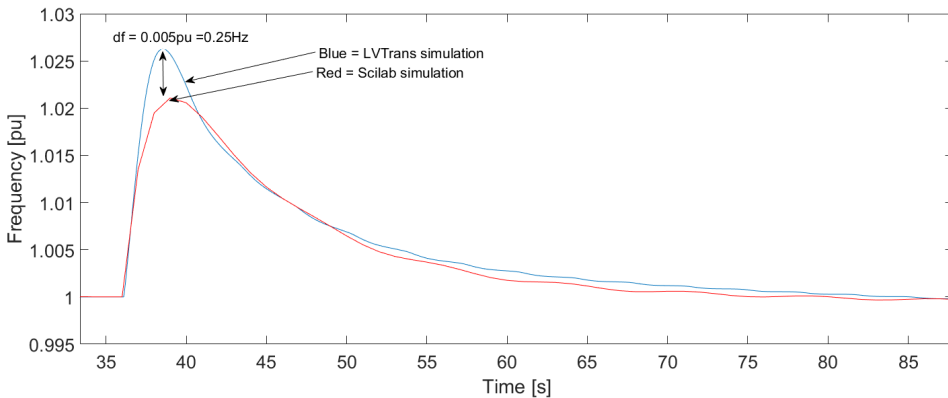


**Figure 6.21:** Frequency regulation during a drop from 85% to 75% in load.

## 6.5.2 Power Regulation in Stiff Grid Mode.

Simulations of Turbine power regulation connected to a stiff network is shown in this section. In both simulations figure 6.22 and 6.23 the droop is set to:  $\rho = 0.06$ . The first simulation can be seen in figure 6.22 and it is done with a drop in grid frequency if 0.5Hz.

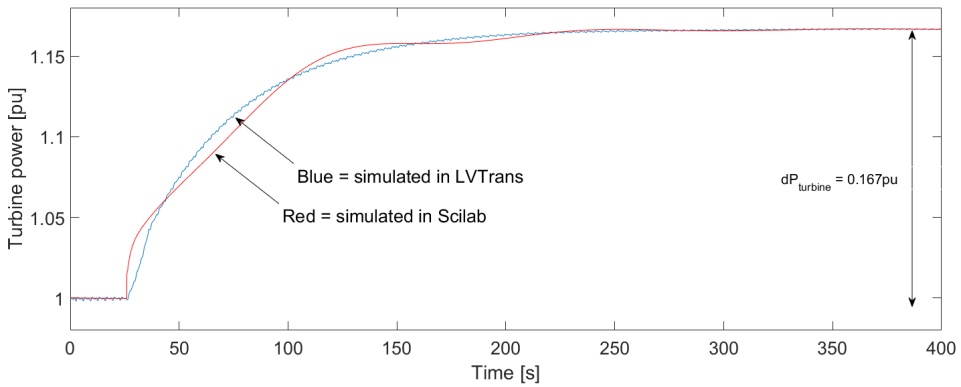


**Figure 6.22:** Power regulation in stiff grid mode with a drop of 0.01% in grid frequency

The result is an increase in power production of 0.167 pu, equivalent to 15.74MW with the rated turbine power of 94.27MW. The value corresponds well to theory. Equation 6.1 found in, [8] shows the mathematical relationship between changes in generated power as a function of change in frequency:

$$\Delta P_g = \frac{P_d \cdot \Delta f}{f_n \cdot -\rho} = \frac{1pu \cdot -0.01pu}{1pu \cdot -0.06} = 0.167pu \quad (6.1)$$

In figure 6.23 simulations are done with an increase in the frequency of 0.5Hz.

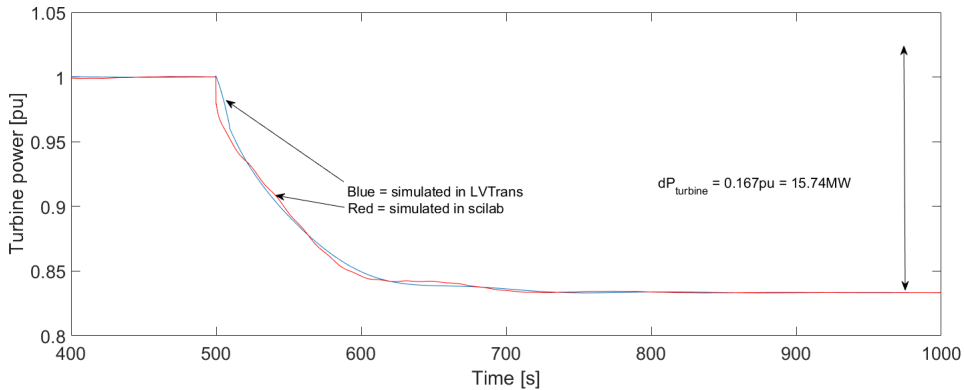


**Figure 6.23:** Power regulation in stiff grid mode with an increase of 0.01% in grid frequency

Simulations show the same  $\Delta P_t$  as in figure 6.22, but oppositely. This naturally results in a lower power production from the aggregate, and the turbine power output decreases from 1pu to 0.833, a drop of 15.27MW.

### 6.5.3 Water Hammer and Mass Oscillations

The water hammer simulations are performed during BEP conditions of  $H = 200\text{m}$  and  $Q = 50\frac{\text{m}^3}{\text{s}}$ . By using the modifications in the Scilab program, full closure of the guide vane is done over a period of 10s. Full load rejection from the grid is done at the same time, which makes the flow stop completely. Due to the full stop, pressure pulsations and mass oscillations are generated by the hydraulic dynamics that can be seen in the figures 6.24 and 6.25 below.

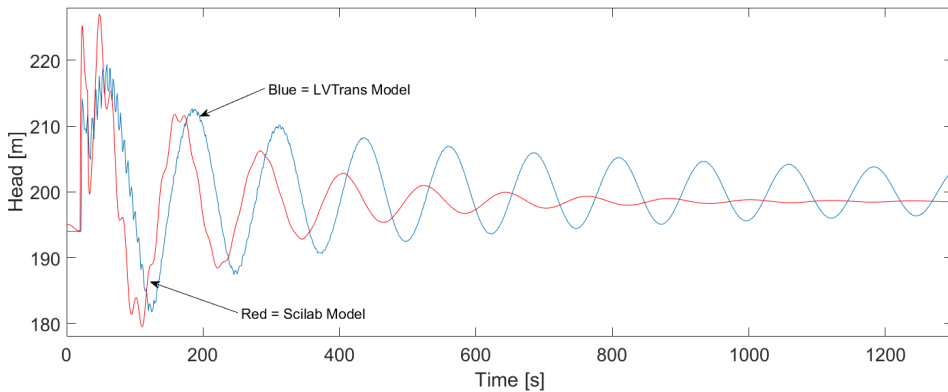


**Figure 6.24:** Water hammer simulations done in scilab and LVTrans

As seen in the simulations, some clearly deviations of the response are present. Higher transients in the first 50s of the simulations for the scilab model. The mass wave will then decrease fast in amplitude for the scilab model while the LVTrans model is slower and keeps on oscillate for the rest of the simulation time over 1200s.

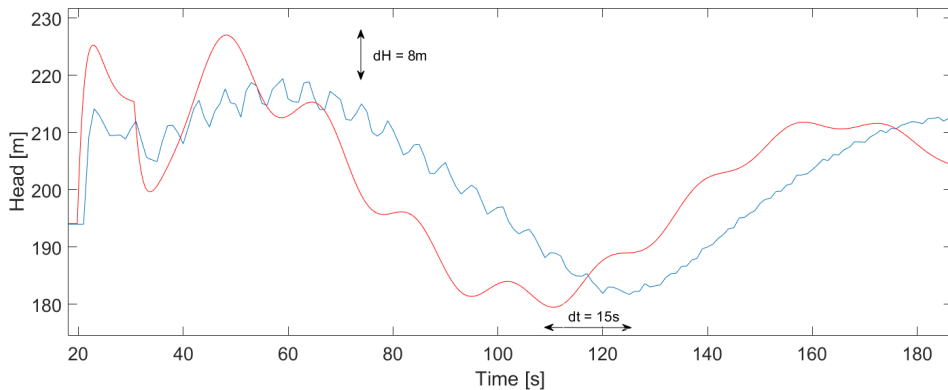


**Figure 6.25:** A close look at the first transient from figure 6.24.

The first transients have a deviation of 8m in pressure and get close to identical in the second one. LVTrans model catches up the smaller pressure oscillations in the first 100s after the closure, while the Scilab model doesn't perceive the fast pulsations.

Much of the results deviations are assumed to be due to system friction. In LVTrans the friction varies as the flow changes. Due to this, a modification in the Scilab block diagram is implemented to investigate the effect of a change in friction as the flow changes. The friction factors are not variable during the simulations, but are changed to a lower static value after the flow goes close to zero. The new friction factors count after 78s, 40s after the guide vane starts to close. This delay is set to ensure that the flow has decreased adequately. The new friction factors are set to the following:

- $f_{D1} = 0.02$
- $f_{D2} = 0.005$
- $f_{D3} = 0.02$

In figure 6.26 , the results of this simulation can be seen:

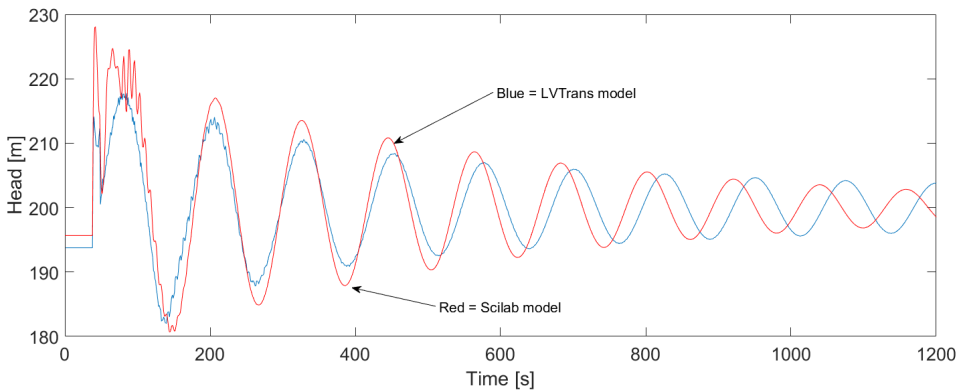


**Figure 6.26:** Simulation of a full system stop, with changes in the internal friction factors in the scilab model.

As seen in figure 6.26 the results are much closer, but the Scilab model is reaching steady state after around 3000s, while the LVTrans model keeps on oscillating. Simulations to around 40000s are done with LVTrans, and the oscillations are still going but with a small amplitude.

As the friction factor of each part is changed, they all had their characteristic influence on the system. When decreasing the friction factor for the head race tunnel, a much higher amplitude is achieved. This factor has the biggest influence for how the mass oscillations behave. The penstock has a minimal impact. The outcome when changing the friction

factor in this region is close to zero. Changing friction factor for the draft tube has a much larger influence again. It seems to induce much more oscillations during the transient stage of the simulations. As seen, the first 250s are in the last simulations much more oscillatory than the first one in figure 6.24.



# Chapter 7

## Laboratory Work



**Figure 7.1:** Picture of the rig.



In this section, information and results from the laboratory work are presented. The test rig is made to investigate harmonic oscillating flow which involves creating pressure transients in a u-pipe rig. The rig is made by a co-student named Isak Bergset and the rig-results presented in this section are done in cooperation with him.

The purpose of the testing is to perform verification of the surge shaft model that is implemented in the modelled hydro power plant, see section 5.4. By using the rigs facility data and perform simulations with the surge shaft model in xcos, it is possible to achieve some knowledge of how the model performs to real physical behaviour.

In figure 7.1 the end of the test rig can be seen. Pressure gauges are located on the left side. To create the water hammer, the flow is stopped by manually turning the valve in the middle of the picture. Up in the left corner, the tank can be seen. The pump is located on the floor below.

## 7.1 Laboratory Setup

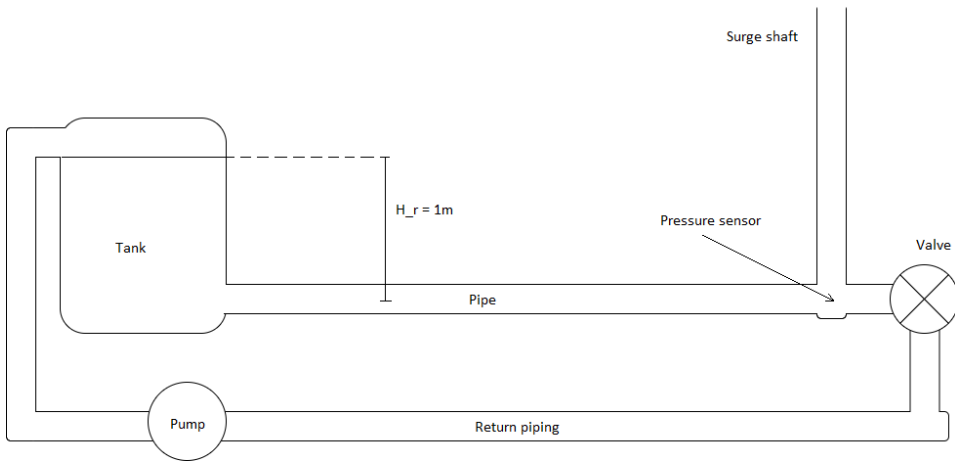


**Figure 7.2:** A sketch of the test ring at the laboratory

In figure 7.2 the cross section of the test rig at the laboratory can be seen. It is designed with an overflow function so that the head level can not exceed 1m. The piping diameter is 150mm and the pipe length between the tank and the surge shaft is 11m. After the surge shaft an valve which is operated manually. The flow can then go in return to a pump which keeps the steady level of head to the system. The roughness of the piping is assumed to be 0.02mm and can be found in table 3.1. Summarized, the system setup has the following settings:

- $H_0 = 1m$
- $d_{pipe} = 150mm$
- $e = \text{roughness} = 0.02mm$
- $L_{pipe} = 11m$
- $f_t = \text{Steel thickness} = 3.3mm$
- $\mu_{H_2O}^{20^\circ C} = 1.002 \cdot 10^{-3}$

There is performed three different tests on the rig, each with different steady state flow rates before the valve closes. The first test is with a flow of  $0.016 \frac{m^3}{s}$ , the second is with a flow of  $0.01389 \frac{m^3}{s}$  and the 3rd with  $0.007 \frac{m^3}{s}$ .

Calculations of the friction factor will be performed with the Colebrook-White equation:

$$\frac{1}{\sqrt{f}} = 1.14 - 2 \log_{10} \cdot \left( \frac{e}{d} + \frac{9.35}{Re \sqrt{f}} \right)$$

While the friction loss is calculated with Darcy-Weisbach equation.

$$h_f = f_D \cdot \frac{L}{D} \cdot \frac{V^2}{2g}$$

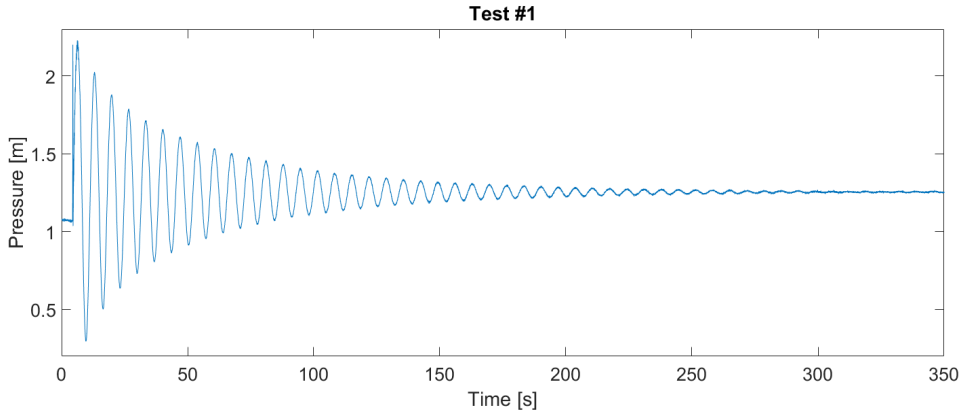
The different losses in the pipe can be seen in table 7.1

**Table 7.1:** Losses in the test pipe under different flow scenarios.

Test Number [#]	Q [ $\frac{m^3}{s}$ ]	Re [-]	Friction factor $f$ [-]	Friction loss [ $m$ ]
1	0.0160	135539	0.0177	0.0521
2	0.0139	117751.5	0.0182	0.0420
3	0.0070	59296.4	0.0206	0.0121

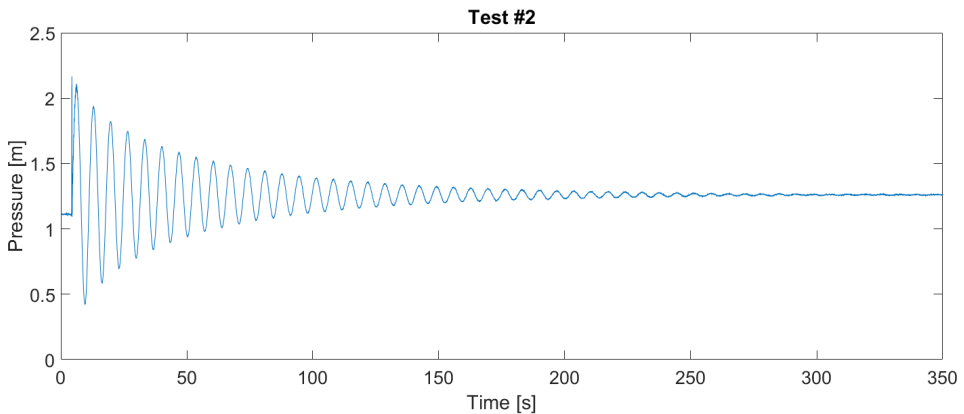
## 7.2 Results From the Rig

The results are plotted with a time step of 0.0002 ( $5000 \frac{\text{points}}{\text{s}}$ ) and have been averaged every 500 points. The test results can be seen in figures 7.3 to 7.6 below. Notice that the y-axis is scaled in all the figure. For comparison see figure 7.6.



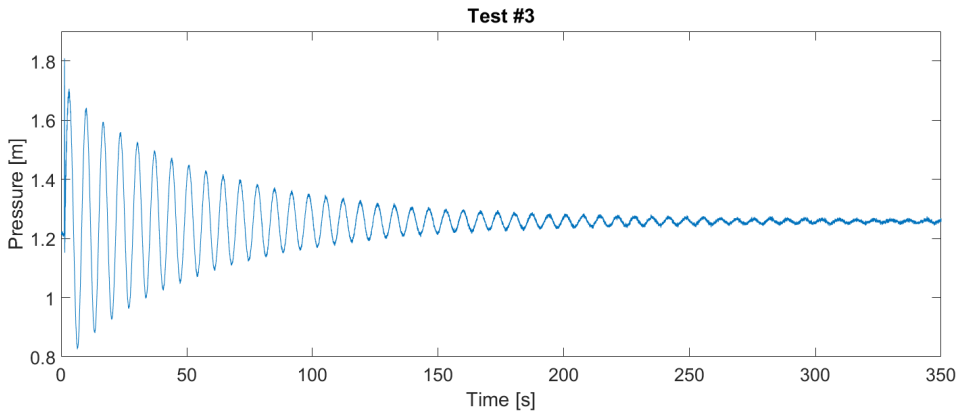
**Figure 7.3:** Rig test result #1

Figure 7.3 shows the results from test one where the transient reaches 2.228 m in pressure. This gives  $dH = 1.136m$ . Due to some deviation in the level of head from 1m, the transient is not precisely 1.228m.



**Figure 7.4:** Rig test result #2

In figure 7.4 show the results from test number two where the transient reaches 2.11m of pressure with an  $dH = 1m$ . Some smaller than test1 which is expected due to less flow.



**Figure 7.5:** Rig test result #3

Figure 7.5 shows the results from test three where the transient reaches 1.8m of pressure, giving a pressure differential of  $dH = 0.586m$ . Again some smaller transient than the other tests above due to flow reduction.

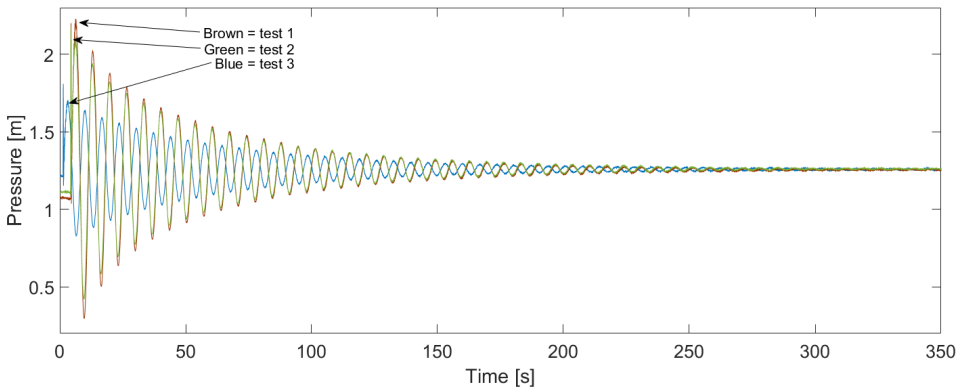


**Figure 7.6:** Comparison of all three test results from the rig.

In figure 7.6 all three tests are compared to each other. Note that test 3 is some offset in the time of the event. This results in an offset phase in the oscillations. The transients are clearly decreasing as the flow rate decrease, which was expected from equation 3.11, as seen below:

$$\Delta h = \frac{c\Delta v}{g} \cdot \frac{T_r}{T_c} = 2 \cdot \frac{\Delta Q}{T_c} \cdot \frac{L}{gA}$$

### 7.3 Rig results V.S Scilab model

When comparing the rig tests to the model in xcos, some of the modelling constants changes as the flow changes throughout the tests. The changes in flow results in changes to the water starting time, the surge shaft time constant and the friction losses. The different parameters can be seen in table 7.2

**Table 7.2:** Values inserted in the scilab model during the simulations

Test Number [#]	$T_w$ [s]	$T_s$ [s]	Re [-]	Friction loss [ $m$ ]
1	1.0152	1.1045	135539	0.0521
2	0.8820	1.2713	117751.5	0.0420
3	0.4442	2.5245	59296.4	0.0121

Compering the simulations done in xcos with a static pipe model to the laboratory tests are done as shown in the figures below.

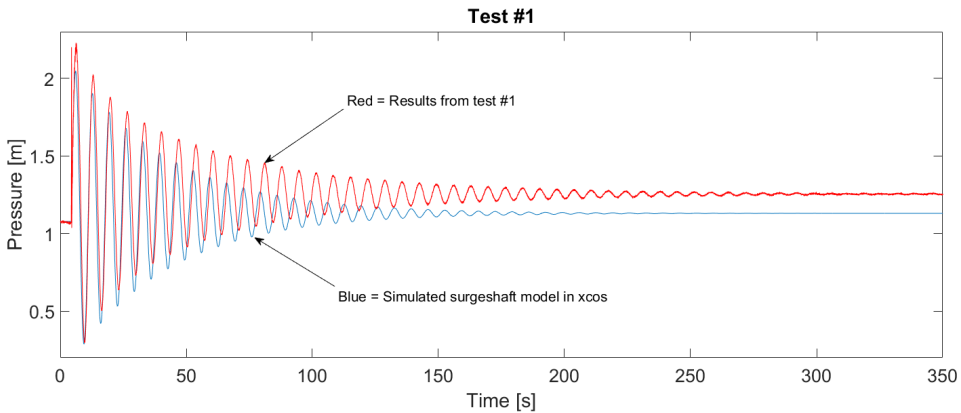


**Figure 7.7:** Comparing test 1 with the scilab model

In the figure, 7.7 the deviation in pressure is  $0.2m$  from the first pressure transient. The pressure from the laboratory test will then increase over time due to less friction as it reaches steady state. This was not possible to simulate, as the friction model for the scilab simulations where to simple. The friction stays the same throughout the whole time and does not variate with the changes in flow.

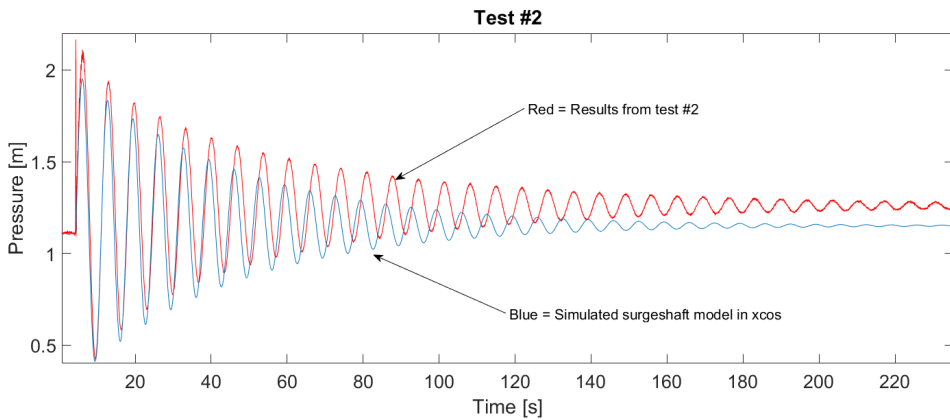


**Figure 7.8:** Comparing test 2 with the scilab model

In figure 7.8 the deviation is smaller with a deviation in pressure of 0.15m. The same friction effect is visible in this simulation. The steady state pressure is not shown in the figure here, but the pressure is levelling out at 300s, about the same as in figure 7.7

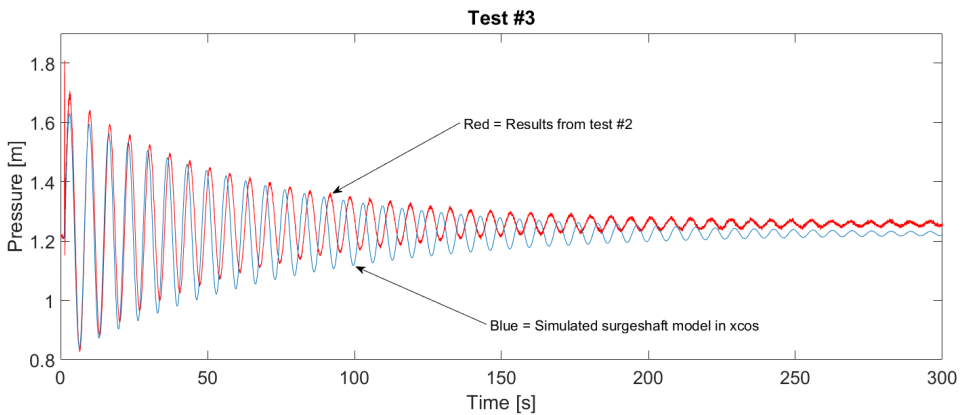


**Figure 7.9:** Comparing test 3 with the scilab model

The last comparison is with the smallest flow, gives the best results in the comparison tests. The pressure deviation between the simulated and real values are 0.08m. The oscillations stay in phase for almost a minute, and due to the low friction, the steady state value is also similar.



# Chapter 8

## Discussion

The discussion part is divided into three main parts.

- Model validation
- Scilab model performance compared to LVTrans
- Surge shaft verification from the laboratory test rig

An analytic description of the simulation results and modelling aspects will be presented in this chapter. The surge shaft verification will also be discussed and evaluated up against the rig results. The primary emphasis is the comparison of the Scilab and LVTrans results. This has been the main aim for the analysis part and is weighted accordingly.



## 8.1 Model Validation

The goal of the model verification chapter is to analyse the effect on the different hydraulic components in the system. Simulations of the frequency and pressure were done comparing two different penstock models seen in figure 6.15 to 6.16. This was done in island operation, with a step in a local load. The results show small deviations between the models and in this case with a penstock of 250m the simplified model would be sufficient. Simulations with only a penstock in the hydraulic system show different results. Figure 6.17 displays pressure and frequency simulations for both penstock models during a decrease in load from 85% to 75%. The pressure transient is clearly much higher with the dynamic model as seen in the figure and is over three times greater than the static one. The dynamic model also has an impact on frequency regulation characteristics and shows some higher transient frequency than the static model.

To show the impact of penstock lengths, simulations were done with three different lengths, 250, 500 and 1000 meters. The simulations show that the more length added to the penstock the higher change in pressure and more oscillations occurs due to a change in flow. The water elasticity effect and the water starting time is influenced by the changes in length, resulting in a more unstable system. From table 6.2 the results from the different penstock lengths are shown. It indicates that when doubling the penstock length, the pressure transients increases close to twice the value. The friction loss for the different penstock lengths is visually shown, as the graphs move down the pressure axis for the longer penstocks. This was expected behaviour, due to the increase in water masses added to the pipeline. More masses increases the force as a result of flow deceleration ( $F = ma$ ).

The effect of implementing draft tube and surge shaft are also investigated. The purpose of the draft tube is to transform kinetic energy from the runner to pressure energy. By decelerate the water from the turbine, a higher head on the backside of the turbine can be achieved. This prevents less wear on the turbine runner during changes in speed and flows [3].

The simulations seen in figure 6.19 shows a more unstable and oscillatory behaviour with this extra tunnel and surge shaft. In theory, there should be fewer pulsations and a more stable head due to flow changes. The diagram show some tendencies of back pressure as the first slope for the blue line in figure 6.19 is some deeper than the red one, representing the system without the lower surge shaft and draft tube. Reasons for this misbehaviour is the dimensions for the lower hydraulic parts. The draft tube in most cases has a characteristic cone shape and a variable area along its length. This is not taken account for, making the area dimensions for the draft tube to small. A consequence for this is an undersized lower surge shaft. This may cause a negative effect on the stability and provide small pressure pulsations. Averaging a new draft tube area could improve the performance. Transfer functions for geometry such as a special designed cone shaped pipe may be possible, but it is not done or researched during the thesis. From the study of draft tube designs in "Hydraulic Turbines" by Brekke [3] it is stated that: "The dynamic behaviour of the flow in a real draft tube with bend and a rectangular outlet is not fully understood today". So

modelling a draft tube to behave like a real life model could be very difficult.

## 8.2 Model Stability

The stability is analysed through frequency analysis, and step responses. The frequency analysis is based on bode plot of the open loop transfer function. The plot shows the system gain and phase response over a span of different frequencies. By looking at the margins of phase and gain the system stability is characterised. The step response shows the system stability physically. By causing changes in the external signals of the system, such as the connected load, system stability can be evaluated.

The Bode plot for the system in figure 6.10 shows a stable system with both positive phase and gain margins of  $91^\circ$  and  $24dB$ . Running tests with changes in  $T_i$  and  $K_p$  shows normal behaviour in the form of how the margins and cross-frequency moves. An increase in  $K_p$  gives a higher cross frequency, lifting the gain at lower frequencies. Increasing  $T_i$  results in a decrease in cross frequency, and lifting the phase up over a span of  $0.02\text{Rad/s}$  to  $10$ .

Testing the system stability from a change in load demand shows good stability characteristics for the system. In figure 6.13 a significant drop is impacting the system. 50% of the load demand is cut off at  $t=1000\text{s}$ , and the governor immediately responds to decrease gate opening seen in figure 6.14. The drop results in an increase of approx  $0.1\text{pu}$  in frequency. Due to PI action, the system regulates the frequency down to a reference value, and the frequency is stabilised at  $1\text{pu}$  or  $50\text{Hz}$ . The regulator in the system works good, and the stability of the system is within the limits of what statkraft recommend which is a transient frequency of no more than 6% during a 10% change in load while running at 85% of aggregate performance. This simulation of performance can be seen in section 6.5.1, figure 6.21. It shows a transient in the frequency of 2.1% in Scilab and 2.6% in LVTrans.

The system is found to be stable during any external influences such as load rejections and frequency variations, (see figure 6.22 and 6.23). The system is not adjusted anymore from the original settings. This is a subject that could be taken further, and a proper PID tuning analysis in the frequency plane could be performed as future work for the system.

## 8.3 Scilab VS LVTrans

### 8.3.1 Frequency regulation in Island mode

The models responded as expected from theory. When the load demand drops, an increase in frequency and machine speed occurs. Both systems responded by changing the guide vane opening (G), and reducing the hydraulic force to the turbine wheel. By doing so, the system speed is getting regulated back to its point of reference, as system speed is proportional to the power-system frequency:  $n = \frac{f \cdot 60}{Z_p}$ .

The response can be linked to system frequency as well as turbine and generator speed. This tendency of regulation can be seen in all the simulations done in island mode with frequency control.

Two simulations are done with drops in load from 1pu to 0.5, and 0.85 to 0.75pu as seen in figure 6.20 and 6.21. The models behave as expected. They gave different results in both of the events of frequency regulations during load drops. Since the Scilab model is linearized around the point of 1pu, a much larger drop away from 1pu should give a larger error in the simulation. This could explain the large error in transient frequency seen in figure 6.20 with 0.5pu load drop.

The whole event is much more similar in shape and governing action in the simulation with a drop from 0.85 to 0.75pu, and with a smaller deviation in frequency transient between the models. During the first simulation with 0.5pu load-drop gives a frequency difference of 4Hz or 0.08pu in frequency. In the second simulation, only 0.25Hz deviates between the models and the regulators respond synchronised after some time and bring the system back to steady state simultaneously 50s after the event.

### 8.3.2 Power regulation in Stiff Grid Mode

Simulations performed in a stiff grid can be seen in the figures 6.22 and 6.23. Both simulations show power regulation as the frequency drops and increase 0.01 pu. The regulator performs as it supposed to, and increases the production as the frequency drops and decreases power output as the frequency increases.

Comparing the two models, they both behave very similar in the form of production rate during governing action, and final steady state values. The models behave accordingly to theory, and it seems that the scilab model gives a good representation of such simulation scenario.

Some more oscillatory behaviour is observed in the scilab model during the guide vane regulation, and this could be due to the linearization issues as the turbine operation point is changed during the governing. Simplifications in the linearized model such as system

friction and governing servos are simplified in the scilab model which has an adverse impact on the behaviour of the system, leading to deviations between the models.

### 8.3.3 Mass oscillation and water hammer simulations

Simulations of water hammer, pressure transients and mass oscillations can be seen in figure 6.24 to 6.26. The first Scilab simulation is done with the simple water hammer simulation model that only utilises the standard island operation model but with the extra guide vane closure implementations seen in figure 6.6. The simulations differ in several ways. The first pressure transient deviates approximately 8m. The Scilab model simulates a pressure increase of a 30m while LVTrans simulations reach about 22m. The mass oscillations from Scilab model leads with 15s during the first periods, and pressure pulsations on top of the mass oscillations in LVTrans are much more visible.

There are reasons to believe that that due to simplification, especially the friction model causes these deviations. In the case of a fully closed guide vane, the friction is no longer constant, but it varies as the flow stops in and the pressure pulsations force water masses to pulsate for and backwards in the conduits. By keeping a constant friction such as it is done in the scilab model, the simulation accuracy decreases and the simulation results in a situation with too much friction and a pressure behaviour that decreases too fast and reaches steady state too early. The water elasticity time constant  $T_e$  has been too low during the simulations, and as a consequence the simulations shows a little lower pressure transients. Not a big influence overall, but it should be mentioned and corrected for further work with the model. In appendix A-6 a suggestion for a more accurate elastic water time constant is given.

This was later corrected in the next simulation seen in figure 6.26. By the use of the system seen in figure 6.8, the friction in the conduits can be automatically changed at a given time, e.g., at the moment of guide vane closure. In the simulation, new values of friction coefficients are chosen to give a better pressure behaviour. As seen the results are much better and the mass oscillations are almost in phase and at the same amplitude for the first 600s of simulation. After 600s the friction has changed even more in LVTrans, and larger deviations between the model are observed.

The electrical equivalent model or RLC model could improve the simulation, which is used in the paper by Mishra [18]. By dividing the penstock into many sections a more accurate simulation of the pressure pulsations can be achieved. In doing so, the whole conduit system must be modelled in the same type of modelling. The RLC model only gave worse results when trying to simulate water hammer and comparing with the test rig.

It adds up to the following conclusion regarding scilab model performance after multiple tests and simulations comparing the two models. Scilab model simulates frequency regulation well around its operating point, but it is not thrust worthy when the external influences get too large. Simulations with turbine power regulation in a stiff grid environment give the best results. Almost no error compared to LVTrans simulations in both scenarios of

frequency increase and drop. The model is not suited for accurate dynamic pressure simulations. It gives indications on how the masses oscillates and the first pressure transients during the first few second after a full plant shutdown. Scilab model is also showing some higher results compared to the LVTrans model here, so least it's not underrating the forces induced by the gate closure, which is a good thing regarding using the model to do plant designs.

## 8.4 Surgeshaft Verification With Test Rig

The verification of the surge shaft model is found in section 7. Results comparing the tests against the simulations are found in the figures 7.7 to 7.9. As seen in the figures the simulations show reasonably good results compared to the rig test, but the friction model causes errors inn the scilab model. Figure 7.7 indicates that the steady state head decreases as the mass oscillations are damped out by pipe friction while the scilab head pressure is the same even tho the water has no velocity in the pipe.

Another reason for deviations is that there is no rate limiter implemented in the scilab model during the simulations. This causes a lead in the mass oscillations compared to the test rig. The manometer in the test rig flushes with the pipe wall, which means that the velocity pressure in the system is not included in the total sum of pressure measurements. This could lead to minor errors during the tests, but are almost neglectable as the dynamic velocity pressure is calculated to  $0.041pa = 4.26 \cdot 10^{-6}mWC$  at a velocity of  $0.9\frac{m}{s}$  during the highest flow rate of  $0.0160\frac{m^3}{s}$ . This amounts to approximately 0.0004%.

Overall the surge shaft model provides to some extent a precise representation of the dynamics during a sudden stop in the system flow. The comparison between the scilab model and the rig gives the model itself more heft and quality, knowing that the surge shaft is accurate regarding mass oscillations and pressure transients.

# Chapter 9

## Conclusion

The master thesis has seven points that should be completed within the deadline. The seven points are:

1. Add a surge shaft and an inlet tunnel to the existing model
2. Verify the surge shaft with experiments in the laboratory
3. Research the opportunities to add an elastic penstock model to the system
4. Theoretical deduction of the partial derivatives for use in the xcos model, based on Torbjørn Nielsen's turbine model
5. Simulate the system with both an isolated and stiff grid
6. Look for possibilities to do a frequency response analysis
7. A short paper shall be written and presented at the 7th International Symposium on Current Research in Hydraulic Turbines (CRHT-VII) at Katmandu University, April 2017
8. Write a report

1. The surge shaft and inlet tunnel were implemented in the existing model. In addition to this, a draft tube and a lower end surge shaft were also applied to improve the hydraulic accuracy. These implementations resulted in a more dynamic water path, hence a hydraulic system influencing the regulation of power and frequency as seen in the simulations. Improvements for the draft tube model should be made in future work with the system.
2. The surge shaft model is verified with a test rig at the laboratory. The results show good performance for the scilab model, it giving a good representation of mass and pressure behaviour during transient states. A new way of implementing a dynamic friction model which varies with the changes in flow automatically would improve the results.
3. An elastic penstock is implemented to the system. By the use of Maclaurin series expansion of the hyperbolic function  $\tanh(T_e \cdot s)$ , the implementation could be done without iteration issues. During the system evaluation, the dynamic effect proved to be small and neglectable for small penstock lengths.
4. The theoretical deduction of the partial derivatives was performed in the form of using a hill chart generator which is based on Torbjørn Nielsen's turbine equations. By doing so, the transfer coefficients could be calculated by the output values given by the program.
5. Simulations were done in both isolated operations with a single machine and single load and Stiff grid with a single machine. The simulations were compared up against simulations done in LVTrans. The frequency simulations in island mode indicate that the scilab model has a restricted area of operation. Performing simulations way off its operating point give larger errors in the simulation, as seen in the simulation with a drop of 50% drop in load. Simulations around the operating point give much better results, and the two models give a very similar response in governing action and transient values. Power simulations done in stiff grid operation shows good results and the two models acts very similar during events of smaller frequency variations. These simulations gave the best results for the scilab model.
6. A frequency response of the system is made, and a bode plot is generated automatically from the open loop system transfer function with the use of an ad-don to the scilab program called CPGE. The results show system stability with both positive phase and gain margins. System stability is also analysed in the form of step responses in the electrical load. Good stability is shown as the frequency transient does not exceed 6% during a load drop from 85% to 75%.
7. A paper is delivered in the event of the 7th International Symposium on Current Research in Hydraulic Turbines, and it can be found in Appendix G. During the symposium a presentation of the thesis was performed.
8. A report has been written, accordingly to the university standards.

# Chapter 10

## Further Work

During the process of developing the system, several marks on how to improve the system have been noted. The draft tube should be redesigned, and new values which are representing an average diameter must be calculated. By doing so, changes in the characteristics of the lower surge shaft has to be done. The use of RLC equivalent hydraulic system model during pressure transient simulations would be interesting. In theory, this should give better results for such simulations. Also improving the friction model to get the friction loss to variate simultaneously with the rate of flow would give the model, overall a better performance.

In form of system layout, a better representation in the block schematics should be done. Creating "superblocks" to improve the design and to get a better overview of the system could improve the usability.





# Bibliography

- [1] Hermod Brekke. *Transient Characteristics of High Head Francis Turbines*. Doktor engineer thesis, Trondheim, NTH, 1990.
- [2] Hermod Brekke. *Konstruksjon av Pumper og Turbiner*. NTNU, 1998.
- [3] Hermod Brekke. *Hydraulic Turbines, design, erection, and operation*. 2001.
- [4] Wang.C. Goa.H. Effect of detailed hydro turbine models on power system analysis. *Zhejiang University, Hangzhou IEEE 2006*, 2006.
- [5] Odd Guttormsen. *Vassdragsteknikk II*. Akademika forlag, 2014.
- [6] Kartein J. Olsen Hans M. faanes, Arne T. Holten. Stabilitet for kraftsystemer og motordrifter. pages 45–50, 1990.
- [7] Nkosinathi Dlakavu Hongqing Fang, Long Chen and Zuyi Shen. Basic modeling and simulation tool for analysis og hydraulic transients in hydroelectric power plants. *IEEE. Transactions on energy conversjon*, Vol. 23(NO. 3):p.834–841, 2008.
- [8] James R. Bumby Jan Machowski, Janusz W. Bialek. *Power System Dynamics: Stability and Control, Sec. edition*. Wiley, 2012.
- [9] Per Hveem Kåre Bjørvik. *Reguleringsteknikk*. Kybernesis, 2012.
- [10] L.F.Moody. Trans. asme. Volume 66, 1944.
- [11] MIT. Stability criteria in bode plot. [http://www.mit.edu/afs.new/athena/course/2/2.010/www\\_f00/psets/hw3\\_dir/tutor3\\_dir/tut3\\_g.html](http://www.mit.edu/afs.new/athena/course/2/2.010/www_f00/psets/hw3_dir/tutor3_dir/tut3_g.html), 29 september 2000. [Online; accessed 21-May-2017].
- [12] German Ardul Munoz-Hernandez. *Modelling and Controlling Hydropower Plants*. Springer, 2013.
- [13] Torbjørn Nielsen. *Dynamic Dimensioning Of Hydrop Power Plants*. NTNU, Vannkraftlaboratoriet.

- 
- [14] J. Riera O. Quiroga and C. Batlle. Identification of partially known models of the susqueda hydroelectric power plant. *Lat. Am. appl. res.*, Volume 33(Number 4), 2003.
- [15] The Engineering Page. Roughness of different materials. [http://www.the-engineering-page.com/forms/dp/typ\\_eps.html](http://www.the-engineering-page.com/forms/dp/typ_eps.html), 2017. [Online; accessed 10-May-2017].
- [16] B Vahidi R.A. Naghizadeh, S. Jazebi. Modeling hydro power plants and tuning hydro governors as an educational guideline. *International Review on modelling and simulations*, Vol. 5(NO. 4), 2012.
- [17] Erik Rognaldsen. *Project Work: Comparison of Blockdiagrams for Hydropower Plants*. NTNU, 2016.
- [18] D.K. Khatod Sachin Mishra, S.K Singal. Effect of variation of penstock parameter on mechanical power. *International Journal og Energy Science*, Volume 2(Number 3):110–114, 2012.
- [19] Scilab Enterprises S.A.S. <https://www.scilab.org/scilab/about>. 2017.
- [20] Statnett. *Funksjonskrav i kraftsystemet (FIKS)*. Statnett, 2012.
- [21] Bjørnar Svingen. *LVTrans Manual*. 2016.
- [22] Nielsen T. *Dynamisk dimensjonering av vannkraftverk*. Trondheim, Sintef, 1990.

---

# Appendix

---

# A

## Dimensioning Conduit Parameters

Friction losses in a conduit is found by Dracy Weisbach's equation:

$$h_f = f_D \cdot \frac{L}{D_h} \cdot \frac{V^2}{2g} \quad (10.1)$$

For the headrace tunnel the following constants are set as:

**Table 10.1:** Parameter values for the head race tunnel

Parameter	Description	Value	Unit
$A_1$	Area	25	$m^2$
$v_1$	Velocity @ $Q_r$	2	$m^2$
$L_1$	Length	2000	$m$
$f_{D1}$	Friction factor	0.05	—

To calculate the hydraulic diameter, the tunnel geometry must be decided. Typical geometry used in Nowegian hydropower plants are the one introduced in the theory chapter:

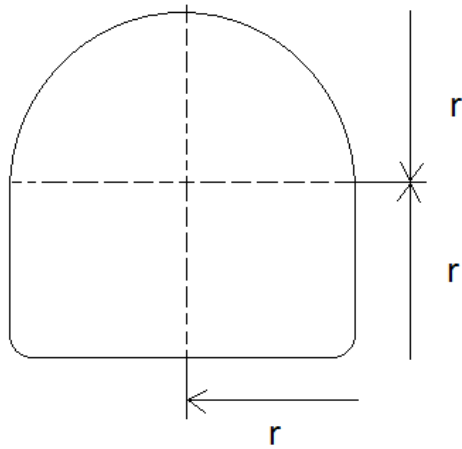


**Figure 10.1:** Cross section of the head race tunnel

Hydraulic diameter is defined as:

$$D_h = \frac{4 \cdot A}{p} \quad (10.2)$$

For the given geometry, this can be deduced down to:

$$D_h = \sqrt{\frac{8 \cdot A}{4 + \pi}} \quad (10.3)$$

This gives the tunnel a hydraulic diameter of:

$$D_h = \sqrt{\frac{8 \cdot 25}{4 + \pi}} = 5.292m \quad (10.4)$$

The friction loss can now be calculated:

$$h_{f1} = 0.05 \cdot \frac{2000m}{5.292m} \cdot \frac{(2 \frac{m}{s})^2}{2 \cdot 9.81 \frac{m}{s^2}} = 3.85m \quad (10.5)$$

For the penstock the following parameters are set as in table

---

**Table 10.2:** Parameter values for the penstock

Parameter	Description	Value	Unit
$A_2$	Area	12	$m^2$
$v_2$	Velocity @ $Q_r$	4.167	$m^2$
$L_2$	Length	250	$m$
$f_{D2}$	Friction factor	0.01	—

The penstock has a round geometry, as seen in figure 10.2.

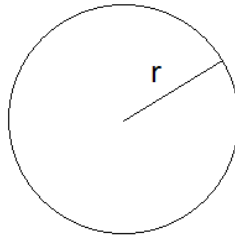


**Figure 10.2:** Cross section of the penstock

For such geometry with the pipe completely filled with water, the hydraulic diameter is the same as its diameter.

$$D_h = \frac{4 \cdot A}{p} = \frac{4 \cdot \pi \cdot r^2}{2 \cdot \pi \cdot r} = 2 \cdot r = D \quad (10.6)$$

This gives the following hydraulic radius:

$$D_h = \frac{4 \cdot 12m^2}{2 \cdot \sqrt{\frac{12m^2}{\pi}}} = 3.91m \quad (10.7)$$

This gives the head loss:

$$h_{f2} = 0.01 \cdot \frac{250m}{3.91m} \cdot \frac{(4.167 \frac{m}{s})^2}{2 \cdot 9.81 \frac{m}{s^2}} = 0.57m \quad (10.8)$$

And for the Draft tube:

---


$$h_{f3} = 0.05 \cdot \frac{25m}{3.91m} \cdot \frac{(4.167 \frac{m}{s})^2}{2 \cdot 9.81 \frac{m}{s^2}} = 0.053mm \quad (10.9)$$

Water mass starting time are given by:

$$T_w = \frac{L_p}{A_p \cdot g} \cdot \frac{Q_{base}}{H_{base}} \quad (10.10)$$

Timeconstant for headrace are:

$$T_{w1} = \frac{2000m}{25m^2 \cdot 9.81 \frac{m}{s^2}} \cdot \frac{50 \frac{m^3}{s}}{200m} = 2.04s \quad (10.11)$$

and for the penstock:

$$T_{w2} = \frac{250m}{12m^2 \cdot 9.81 \frac{m}{s^2}} \cdot \frac{50 \frac{m^3}{s}}{200m} = 0.53s \quad (10.12)$$

The draft tube is assumed to be the same dimensions and form as the penstock, but with a length of 25m. The water starting time is therefore:

$$T_{w3} = \frac{25m}{12m^2 \cdot 9.81 \frac{m}{s^2}} \cdot \frac{50 \frac{m^3}{s}}{200m} = 0.053s \quad (10.13)$$

When designing the surge shaft, the area in the canal is given by the Thoma area. Typical approach is to set the surge shaft area  $A_s = 1.5 \cdot A_{thoma} = 1.5 \cdot A_{th}$ . Where:

$$A_{th} = \frac{L \cdot A_1 \cdot v_1^2}{2 \cdot h_{f1} \cdot g \cdot H_0} \quad (10.14)$$

This gives an value of:

$$A_{th1} = \frac{2000m \cdot 25m^2 \cdot (2 \frac{m}{s})^2}{2 \cdot 3.85m \cdot 9.81 \frac{m}{s^2} \cdot 200m} = 26.5m^2 \quad (10.15)$$

So the surge shaft area becomes:



---


$$A_{s1} = 1.5 \cdot A_{th} = 1.5 \cdot 26.5m^2 = 39.7m^2 \approx 40m^2 \quad (10.16)$$

Surge shaft time constant can now be calculated:

$$T_{s1} = \frac{A_s \cdot H_r}{Q_r} = \frac{40m^2 \cdot 200m}{50 \frac{m^3}{s}} = 160s \quad (10.17)$$

Surge shaft swing limits are given by:

$$\Delta Z = v \cdot \sqrt{\frac{L \cdot A_t}{g \cdot A_s}} \quad (10.18)$$

$$\Delta Z = 2 \frac{m}{s} \cdot \sqrt{\frac{2000m \cdot 25m^2}{9.81 \frac{m}{s^2} \cdot 40m^2}} = 22.58m \quad (10.19)$$

Calculations for the lower surge shaft are shown below. It uses the same equations and procedure as the one higher up:

$$A_{th2} = \frac{25m \cdot 12m^2 \cdot (4.16 \frac{m}{s})^2}{2 \cdot 0.283m \cdot 9.81 \frac{m}{s^2} \cdot 200m} = 4.68m^2 \quad (10.20)$$

$$A_{s2} = 1.5 \cdot A_{th} = 1.5 \cdot 4.68m^2 = 7.02m^2 \approx 7m^2 \quad (10.21)$$

Surge shaft time constant can now be calculated:

$$T_{s2} = \frac{A_s \cdot H_r}{Q_r} = \frac{7m^2 \cdot 200m}{50 \frac{m^3}{s}} = 28s \quad (10.22)$$

The wave velocity calculations is based on rigid water conduits and the simplified velocity equation is used:

$$a = \sqrt{\frac{K}{\rho}} = \sqrt{\frac{2.2 \cdot 10^9 pa}{1 \cdot 10^3 \frac{kg}{m^3}}} = 1483 \frac{m}{s} \quad (10.23)$$

---

Suggestion of elasticity water time constant for future simulations:

A new value for the elasticity constant for future simulations are found here. At first the wall thickness is calculated, then a new wave velocity for elastic water string is deduced.

The wall thickness is based on a general rule of a stress limit of  $\sigma = 100\text{Mpa} = 100 \frac{\text{N}}{\text{mm}^2}$

The maximum force acting on the penstock are at the very end, with a head pressure of 100mwc. In Pa this is:

$$P = \rho \cdot g \cdot h = 1000 \frac{\text{kg}}{\text{m}^3} = 1962000\text{Pa} \quad (10.24)$$

Forces acting on half a pipe wall with diameter of 3.91m over a length of 1mm gives:

$$F = P \cdot A = P \cdot D \cdot 1\text{mm} = 1962000\text{Pa} \cdot 3.91\text{m} \cdot 0.001\text{m} = 7671.42\text{N} \quad (10.25)$$

And the pipe thickness is given by:

$$F = 2 \cdot \sigma \cdot A = 2 \cdot \sigma \cdot t \cdot 1\text{mm} \quad (10.26)$$

This gives a thickness of:

$$t = \frac{F}{2 \cdot \sigma} = \frac{7671.42\text{N}}{2 \cdot 100 \frac{\text{N}}{\text{mm}^2}} = 38.36\text{mm} \quad (10.27)$$

New velocity based on the pipe thickness is then calculated:

$$a = \sqrt{\frac{K}{\rho(1 + \frac{D \cdot K}{f \cdot E})}} = \sqrt{\frac{2.2 \cdot 10^9 \frac{\text{N}}{\text{m}^2}}{1000 \frac{\text{kg}}{\text{m}^3} (1 + \frac{3.91\text{m} \cdot 2.2 \cdot 10^9 \frac{\text{N}}{\text{m}^2}}{0.038\text{m} \cdot 2.22 \cdot 10^{11} \frac{\text{N}}{\text{m}^2})}} = 1043.7 \frac{\text{m}}{\text{s}} \quad (10.28)$$

The elasticity time constant  $T_e$  for the penstock then becomes:

$$T_e = \frac{l}{a} = \frac{250\text{m}}{1043.7 \frac{\text{m}}{\text{s}}} = 0.239\text{s} \approx 0.24\text{s} \quad (10.29)$$

---

# B

## Dimensioning Francis Turbine Wheel

Calculations done in this chapter is based on theory from the book "pumper og turbiner", made by Hermod Brekke [2]. The picture below in figure 10.5 is from the same book, and defines the velocity components at the entrance and the end of the turbine wheel.

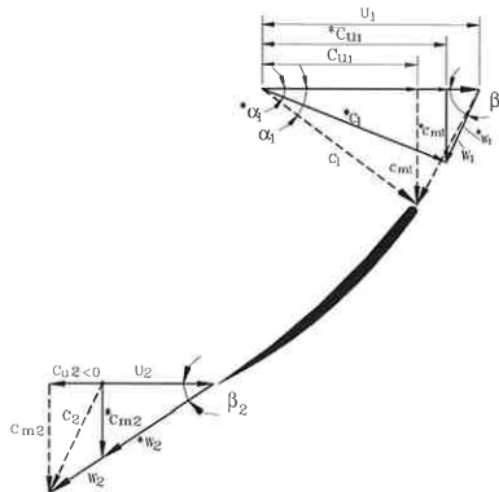


**Figure 10.3:** Velocity triangles for a Francis turbine. [2]

Where:

----- = Performance over BEP (Best efficiency point)

\* = BEP

---

## General equations

NPSH (Net Positive Suction Head) is used as a starting point when designing Francis turbine wheel. The value of NPSH gives the pressure that the turbine wheel must withstand without starting to cavitate.

**Table 10.3:** Values for the parameters, a and b based on earlier experiences.

Parameter	Tubines	Pumps
a	$1.05 < a < 1.15$	$1.6 < a < 2.0$
b	$0.05 < b < 0.15$	$0.2 < a < 0.25$

The relationship between NPSH and the velocities for the outflow is described as:

$$NPSH_t = a \frac{c_{m2}^2}{2g} + b \frac{u_2^2}{2g} \quad (10.30)$$

Also the following criteria must be fulfilled.

$$NPSH_t < \frac{c^2}{2g} - j = -H_s + h_b h_{vp} \quad (10.31)$$

Where  $h_b$  is barometer pressure and  $h_{vp}$  is water vaporizing pressure.  $H_s$  is negative for turbines with an negative head due to the lower reservoir. And also:

$$NPSH = \frac{a(u_2 \cdot \tan \beta_2)^2 + bu_2^2}{2g} \quad (10.32)$$

Typical angles for  $\beta_2$  are based on empiric values of  $13^\circ$  and  $19^\circ$ . Also typical velocities of  $u_2$  is between 35 and  $43 \frac{m}{s}$ .

Further the relationships between  $c_m$  and the outflow diameter  $D_2$  is given by:

$$c_{m2} = \frac{4 \cdot Q^*}{\pi D_2^2} \quad (10.33)$$

where  $Q^*$  is dimensional flow rate.

The relationship between  $u_2$  and the parameters of  $D_2$  and  $n$ :

---


$$u_2 = \frac{\pi D_2 n}{60} \quad (10.34)$$

where  $n$  is the synchronous speed of the wheel in relation of the grid frequency (50Hz in Norway):

$$n = \frac{f \cdot 60}{Z_p} = \frac{3000}{Z_p} \quad (10.35)$$

where  $Z_p$  is number of pole pairs, and the value being an integer. So in order to keep the chosen vane angle, an correction for the wheel diameter is done to maintain the form of velocity triangle.

Based on that  $\beta$  remains constant and that  $c_u = 0$  gives the equation for correcting velocity  $c_m$

$$c_{m2} = \frac{4 \cdot Q^*}{\pi D_2^2} \rightarrow c_{m2corr} = \frac{4 \cdot Q^*}{\pi D_{2corr}^2} \quad (10.36)$$

This gives the following conditions:

$$\frac{c_{m2corr}}{c_{m2}} = \left(\frac{D_2}{D_{2corr}}\right)^2 = \frac{u_{2corr}}{u_2} \quad (10.37)$$

Further when  $\beta_2 = constant$  and  $c_{u2} = c_{u2corr} = 0$  gives:

$$\tan \beta_2 = \frac{c_{m2}}{u_2} = \frac{\frac{4Q^*}{\pi D_2^2}}{\frac{\pi \cdot n D_2}{60}} \quad (10.38)$$

and as  $\beta = constant$  the same relationship counts for corrected speed and diameter.

$$\tan \beta_2 = \frac{c_{m2corr}}{u_{2corr}} = \frac{\frac{4Q^*}{\pi D_{2corr}^2}}{\frac{\pi \cdot n D_{2corr}}{60}} \quad (10.39)$$

This gives:

$$n_{corr} D_{2corr}^3 = n D_2^3 \quad (10.40)$$

Finally  $D_{2corr}$  is found to be:

---


$$D_{2corr} = \left( \frac{D_2^3 n}{n_{corr}} \right)^{\frac{1}{3}} \quad (10.41)$$

It is possible to choose number of pole pairs at the beginning and directly find  $D_{2corr}$ , but then  $u_{2corr}$  must be found.

$$u_{2corr} = n_{corr} \pi \frac{D_{2corr}}{60} \quad (10.42)$$

further

$$c_{m2} = \frac{4 \cdot Q^*}{\pi D_{2corr}} \quad (10.43)$$

The turbine diving head must be checked by the equation 10.30 in order to make sure that cavitation does not occur. If NPSH becomes to large relative to the available head, a lower peripheral speed or a lower  $\beta_2$  will decrease the value.

The inner diameter is then found. The speed of  $c_{m1}$  is here found by keeping the flow constant through out a control volume:

where:

$$c_m = \rho_m = constant \quad (10.44)$$

Which gives

$$c_{m2} = \frac{c_{m1} \rho_1}{\rho_2} \quad (10.45)$$

And using control volume as a test:

$$\int_{r_{21}}^{r_{22}} c_m r dr = Q \quad (10.46)$$

There is also necessary to controll the full load flow where  $c_{u1} \neq 0$ . This is done til last, where margins of  $NPSH$  must be atleast  $0.5[mH_2O]$  v.s  $NPSH_t$ . Introducing Euler's pump and turbine equation the following relationship is given:

---


$$\eta_h = \frac{(u_1 c_{u1} - u_2 c_{u2})}{gH} = 2 \cdot (u_1 c_{u1} - u_2 c_{u2}) \quad (10.47)$$

Assuming  $\eta_h = 0.96$  and BEP with vertical outlet gives  $c_{u2} = 0$ . This leads to:

$$\eta_n = 2 \cdot (u_1 c_{u1}) = 0.96 \quad (10.48)$$

Choosing the relationship between  $u_1$  and  $c_{u1}$  in such way that the losses are reduced due to pressure variations as angle of the guide vanes vary. Typical values are,  $u_1 = 0.7 - 0.76$ . This gives an value for  $c_{u1}$  of:

$$c_{u1} = \frac{0.96}{2 \cdot 0.71} = 0.67 \quad (10.49)$$

Knowing  $c_{u1}$ ,  $D_1$  can be found by the following equation:

$$D_1 = \frac{2 \cdot u_1}{\omega} = \frac{2 \cdot u_1 \cdot \sqrt{2gH}}{\frac{n\pi}{30}} \quad (10.50)$$

Next is to get the dimensions for the height of the wheel, or the with. From equation of continuity we have:

$$c_{m1} A_1 = c_{m2} A_2 \quad \text{and} \quad c_{m2} = 1.1 c_{m1} \quad (10.51)$$

This gives:

$$B_1 D_1 \pi = \frac{1.1 \pi D_2^2}{4} \rightarrow B_1 = \frac{0.275 D_2^2}{D_1} \quad (10.52)$$

Knowing that,

$$c_{m1} = \frac{c_{m2}}{1.1} \quad \text{and} \quad u_1 = 0.72 \sqrt{2gH} \quad (10.53)$$

the entry angle  $\beta_1$  is found as:

$$\tan \beta_1 = \frac{c_{m1}}{(u_1 - c_{u2})} \quad (10.54)$$

---

## Dimensioning the turbine wheel

The main dimensions for the Francis turbine wheel is calculated here. The values may differ a little from the ones used in "test-hill" programme and "LVTrans". This is due to some values being rounded off, but they are based on the same facility data and are approximately the same.

Facility data:  $Q^* = 50 \frac{m^3}{s}$ ,  $\eta_h = 0.96$ ,  $H = 200m$ ,  $A = 8 \frac{m^3}{s}$ ,  $T_w = 0.95$

$$P = \eta \rho g Q H = 0.96 \cdot 1000 \frac{kg}{m^3} \cdot 9.81 \frac{m}{s^2} \cdot 50 \frac{m^3}{s} \cdot 200m \approx 94,176MW \quad (10.55)$$

$\beta_2$  and  $u_2$  are chosen to  $16^\circ$  and  $40 \frac{m}{s}$

$$\tan \beta_2 = \frac{c_{m2}}{u_2} \rightarrow c_{m2} = 11.47 \frac{m}{s} \quad (10.56)$$

$$D_2 = \sqrt{\frac{4 \cdot Q^*}{\pi \cdot c_{m2}}} = \sqrt{\frac{4 \cdot 50}{\pi \cdot 11.47}} = 2.35m \quad (10.57)$$

$$n = \frac{u_2 \cdot 60s}{\pi \cdot D_2} = \frac{40 \frac{m}{s} \cdot 60s}{\pi \cdot 2.35m} = 325rpm \quad (10.58)$$

Number of pole pair:

$$Z_p = \frac{3000}{n} = \frac{3000}{325} = 9.228 \quad (10.59)$$

Choosing  $Z_p = 9$  for this machine. This gives new dimensions:

$$n_{synch} = \frac{3000}{9} = 333.33 \quad (10.60)$$

$$D_{2corr} = \sqrt[3]{\frac{D_2^2 u_2 60}{\pi n_{synch}}} = \sqrt[3]{\frac{2.35^2 m \cdot 40 \frac{m}{s} \cdot 60s}{\pi \cdot 333.33rpm}} = 2.33m \quad (10.61)$$

$$u_{2corr} = \frac{n \pi D_{2corr}}{60s} = \frac{333.33rpm \cdot \pi \cdot 2.33m}{60s} = 40.66 \frac{m}{s} \quad (10.62)$$



---

Further, calculations for the inlet gives:

$$\underline{c}_{m1} = \frac{c_{m2}}{1.1} = \frac{c_{m2}}{1.1 \cdot \sqrt{2gH}} = \frac{11.47 \frac{m}{s}}{1.1 \cdot \sqrt{2 \cdot 9.81 \frac{m}{s^2} \cdot 200m}} = 0.166 \quad (10.63)$$

Calculations are based on  $\eta = 0.96$  and chosen value of  $\underline{c}_{u2} = 0.67$ :

$$\eta_h = 2\underline{u}_1 \underline{c}_{u1} \rightarrow \underline{u}_1 = \frac{0.96}{2 \cdot 0.67} = 0.716 \quad (10.64)$$

This gives the inlet diameter of the turbine:

$$D_1 = \frac{60u_1}{\pi n} = \frac{60s \cdot \sqrt{2gH} \underline{u}_1}{\pi n} = \frac{60 \cdot \sqrt{2 \cdot 9.81 \frac{m}{s^2} \cdot 200m} \cdot 0.716}{\pi \cdot 333.33rpm} = 2.57m \quad (10.65)$$

Now finding the height of the turbine:

$$B_1 = \frac{Q^*}{\pi D_1 c_{m1}} = \frac{Q^*}{\pi D_1 c_{m1} \sqrt{2gH}} = \frac{50 \frac{m^3}{s}}{\pi \cdot 2.57m \cdot 0.166 \cdot \sqrt{2 \cdot 9.81 \frac{m}{s^2} \cdot 200m}} = 0.6m \quad (10.66)$$

At last the inlet angles can be found:

$$\alpha_1 = \tan^{-1}\left(\frac{c_{m1}}{c_{u1}}\right) = \tan^{-1}\left(\frac{0.166}{0.67}\right) = 13.9^\circ \quad (10.67)$$

$$\beta_1 = \tan^{-1}\left(\frac{c_{m1}}{u_1 - c_{u1}}\right) = \tan^{-1}\left(\frac{0.166}{0.716 - 0.67}\right) = 74.51^\circ \quad (10.68)$$

---

# C

## Calculations of Turbine Transfer Coefficients

(Assuming Constant system head pressure of 200m.)

m (y,h,n) :

```
-#-#-#-#-#-#-#-#-#-#-#-#-#-#-#-#-#-#-#-#-#-#-#-#-#-#-#-#-#-#-#-#-#-#-
```

$$\text{kappa1} = 0.9999 \Rightarrow \text{mg1} = 0,999899$$

$$\text{kappa2} = 1.0001 \Rightarrow \text{mg2} = 1,000101$$

$$\text{dm/dy} = (\text{mg2} - \text{mg1}) / (\text{kappa2} - \text{kappa1}) = 1.01$$

```
-#-#-#-#-#-#-#-#-#-#-#-#-#-#-#-#-#-#-#-#-#-#-#-#-#-#-#-#-#-#-#-#-#-#-
```

$$\text{omega1} = 0.9999 \Rightarrow \text{mg1} = 1,000095$$

$$\text{omega2} = 1,0001 \Rightarrow \text{mg2} = 0,999901$$

$$\text{dm/dn} = -0.97$$

```
-#-#-#-#-#-#-#-#-#-#-#-#-#-#-#-#-#-#-#-#-#-#-#-#-#-#-#-#-#-#-#-#-#-#-
```

$$\text{dm/dh} = \text{dm/dq} * \text{dq/dh}$$

$$\text{q1} = 0.9999 \Rightarrow \text{mg1} = 0,999899$$

$$\text{q2} = 1.0001 \Rightarrow \text{mg2} = 1,000101$$

$$\text{dq/dm} = 0.995$$

$$\text{dq/dh} = 0.5$$

$$\text{dm/dh} = (\text{dm/dq}) / (\text{dh/dq}) = (1/0.995) / 2 = 0.5025$$

**Figure 10.4:** Calculations of transfer coefficients in reference to induced torque by the turbine



---

# D

Scilab Models

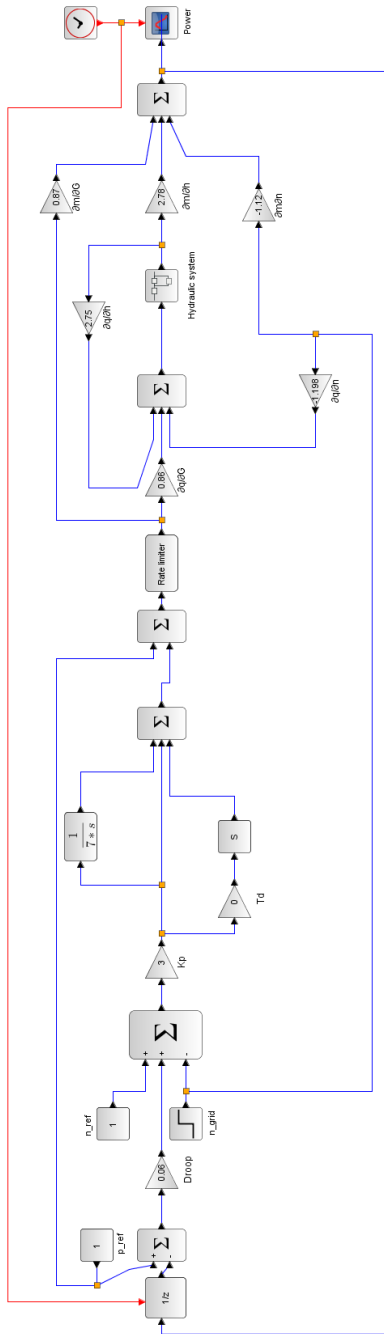


**Figure 10.6:** Power regulation in a stiff network.

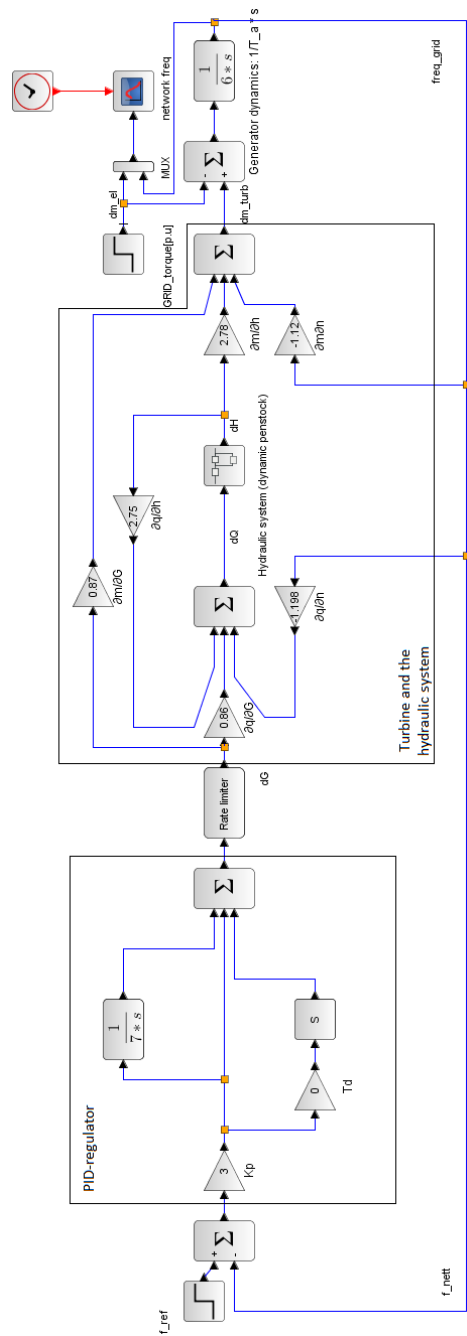


Figure 10.7: Frequency regulation in island mode.

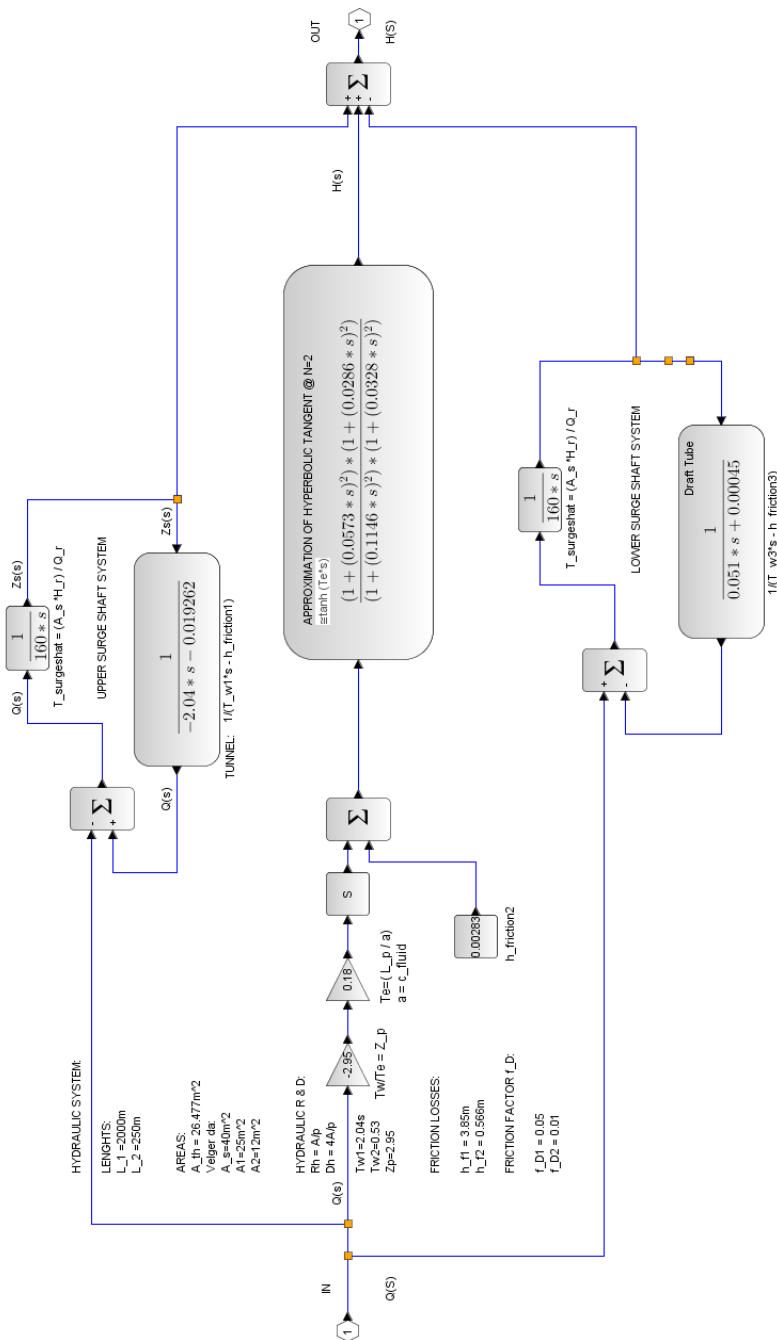


Figure 10.8: The hydraulic system used in the simulations.

---

# **E**

Parameters used in the LVTrans simulations



---

```

[Turb]
window_name = "Turb"
Qr = 50,000000E+0
Hr = 200,000000E+0
Hr_design = 200,000000E+0
Nr = 333.33,000000E+0
Tr = 2700,000000E+3
Er = 2700,000000E+3
alr(deg) = 15,800000E+0
blr(deg) = 67,700000E+0
r1 = 1311,000000E-3
r2 = 1146,000000E-3
Ta = 6,000000E+0
Twt = 100,000000E-3
Rq = 0,000000E+0
Rm = 40,000000E-3
Rd = 30,000000E-3
eta_h = 940,000000E-3
eta_r = 950,000000E-3
Nturb = 1,000000E+0
Poles = 18,000000E+0
D_grid = 0,000000E+0
delta_r = 785,400000E-3
F_grid = 50,000000E+0
eve_mod = 200,000000E-3
rt_data? = FALSE

[Draft tube]
window_name = "Draft tube"
L = 25,000000E+0
D = 3,91
f = 50,000000E-3
Lambda = 500,000000E+3
rho = 1,000000E+3
a = 1,200000E+3
DH? = FALSE
Areal = 0,0
P = 0,000000E+0
ZO = 0,000000E+0
Z1 = 0,000000E+0
QO = 50,000000E+0
HO = 0,000000E+0
rt_data? = FALSE
full_moody? = FALSE
epsilon[m] = 10,000000E-3
ny = 1,100000E-6
f_max = 10,000000E+0

[Forebay]
window_name = "Forebay"
HO = 200,000000E+0
Cvp = 100,000000E+3
Cvm = 100,000000E+3
rt_data? = FALSE
simp_calc? = FALSE

[head race tunnel]
window_name = "head race tunnel"
L = 2000,000000E+0
D = 5,292
f = 50,000000E-3
Lambda = 500,000000E+3
rho = 1,000000E+3
a = 1,200000E+3
DH? = FALSE
Areal = 0,0
P = 0,000000E+0
ZO = 0,000000E+0
Z1 = 0,000000E+0
QO = 50,000000E+0
HO = 200,000000E+0
rt_data? = FALSE
full_moody? = FALSE
epsilon[m] = 10,000000E-3
ny = 1,100000E-6
f_max = 10,000000E+0

[Surge shaft]
window_name = "Surge shaft"
HO = 200,000000E+0
D = 7,136
f = 50,000000E-3
Cvp = 100,000000E+3
Cvm = 100,000000E+3
rt_data? = FALSE
simp_calc = FALSE

[Lower Surgesh]
window_name = "Lower Surgesh"
HO = 0,000000E+0
D = 3
f = 50,000000E-3
Cvp = 100,000000E+3
Cvm = 100,000000E+3
rt_data? = FALSE
simp_calc = FALSE

[Endpipe]
window_name = "enderør"
L = 2,000000E+0
D = 5,642
f = 50,000000E-3
Lambda = 500,000000E+3
rho = 1,000000E+3
a = 1,200000E+3
DH? = FALSE
Areal = 0,0
P = 0,000000E+0
ZO = 0,000000E+0
Z1 = 0,000000E+0
QO = 50,000000E+0
HO = 0,000000E+0
rt_data? = FALSE
full_moody? = FALSE
epsilon[m] = 10,000000E-3
ny = 1,100000E-6
f_max = 10,000000E+0


[Penstock]
window_name = "Penstock"
L = 250
D = 3,91
f = 0,01
Lambda = 500,000000E+3
rho = 1,000000E+3
a = 1,200000E+3
DH? = FALSE
Areal = 0,0
P = 0,000000E+0
ZO = 0,000000E+0
Z1 = 0,000000E+0
QO = 50
HO = 200
rt_data? = FALSE
full_moody? = FALSE
epsilon[m] = 10,000000E-3
ny = 1,100000E-6
f_max = 10,000000E+0

```

**Figure 10.9:** Parameters used in the LVTrans simulations

NITNU		Hazardous activity identification process		Prepared by	Number	Date
HSE				HSE section	HMSRV2691E	09.01.2013
				Approved by		Replaces
				The factor		01.12.2006

**Unit:** (EPT)  
**Supervisor:** Bjørnar Svingen  
**Participants in the identification process** (including their function):-  
**Short description of the main activity/main process:** Master project for student, Erik Rogndalsen. Modelling and simulation of hydropower in SciLab. Some minor laboratory work has been done, but it has been purely theoretical.  
**Is the project work purely theoretical?** (YES)  
*Answer: "YES" implies that supervisor is assured that no activities requiring risk assessment are involved in the work. If YES, briefly describe the activities below. The risk assessment form need not be filled out.*

**Signatures:** Responsible supervisor: \_\_\_\_\_ Student: 

ID nr.	Activity/process	Responsible person	Existing documentation	Existing safety measures	Laws, regulations etc.	Comment
	Collect data from testing at the laboratory.	-	-	-	-	Only computer equipment where used

**Figure 10.10:** Risk assessment

---

# G

Paper Presented as the 7th International Symposium on Current Research  
in Hydraulic

,

## **Modeling and simulation of hydropower plant in Scilab**

**Erik Rognaldsen<sup>1\*</sup>**

*<sup>1</sup>Department of Energy and Process Engineering, Norwegian University of Science and Technology, Alfred Getz vei 4, Norway*

*\* Corresponding author ([erikrogn@stud.ntnu.no](mailto:erikrogn@stud.ntnu.no))*

---

### **Abstract**

A hydropower plant is modeled in a computer application called Scilab, an open source MATLAB clone with possibilities to create block diagrams and do system simulations. The system is designed to do both frequency regulation when running in island operation and power regulation in a stiff power network. The conduit system are set up with a dynamic penstock model, surge shaft and a rigid head-race tunnel. It is used a linear turbine model allowing the author to linearize turbine characteristics of a specified turbine to get a detailed description of the turbine directly in the model. The linearization are performed with a computer program based on modified Euler's turbine equations. The system are until now only implemented with a simple governor with a PID-regulator. A servo system may be implemented at a later point of the mater thesis process.

In both simulation scenarios (grid and island), peak and mean steady state values are similar, but there is clearly a more oscillatory behavior in simulations performed in LVTrans, compared to Scilab. In grid mode the frequency responded with an increase of 8.5Hz when performing a step in load of 50%. This happened in both programs, but the time to develop steady state are different where LVTrans where faster and more aggressive. Simulating in grid mode, performing a drop of 0.5Hz with a droop set to 0.06, an increase of 17% in power generation occurred in both programs. Also in this event LVTrans behaved more oscillatory.

:

**Keywords:** System modeling, Hydropower Simulaiton, Scilab, LVTrans, Model verification

---

# 1. Introduction

## 1.1. Context

During the spring 2016 the project work assignment at NTNU gave the thesis a start, providing the writer knowledge of system modeling and hydropower systems through a literature study. The models in this paper are found in different articles and books and are cited during the theory section. What there is provided to the field of subject are the use of computer software tools and the method of system verification. During literature study, a hydropower plant has not been found modeled in Scilab, xcos before and the thesis will give the program an evaluation of hydropower simulation performance with block diagrams. Later in the process, a model verification of the surge shaft will be performed with the u-pipe test rig at the laboratory at NTNU.

## 1.2. Motivation

Load variation on the grid or different events of faults causes changes on the grid frequency. In order to obtain the goals for stability, safety and supply, regulations of the aggregate units are necessary. Simulations of a hydro power plant in the transient states are therefore crucial to get predictability needed to build and maintain the system, but also to know the limits of plant design. [1]

The modeling and simulations are performed in two different contexts. The one being frequency regulation in island operation, with only a local load and a single machine see Figure 1. The other one is power regulation on a stiff power network, Figure 2

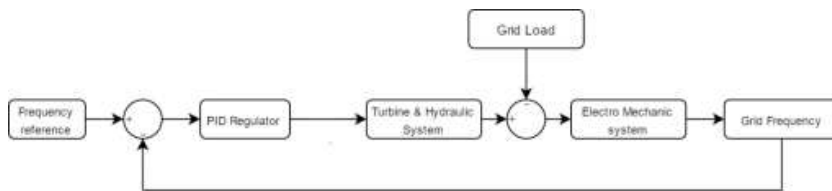


Figure 1: General block diagram for simulating frequency regulation in island operation.

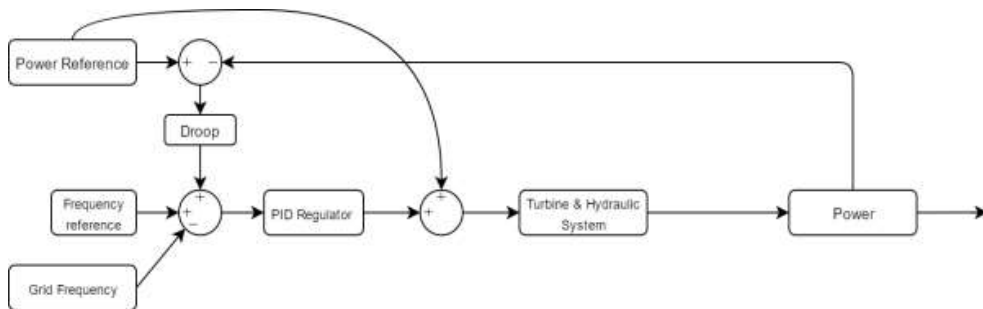
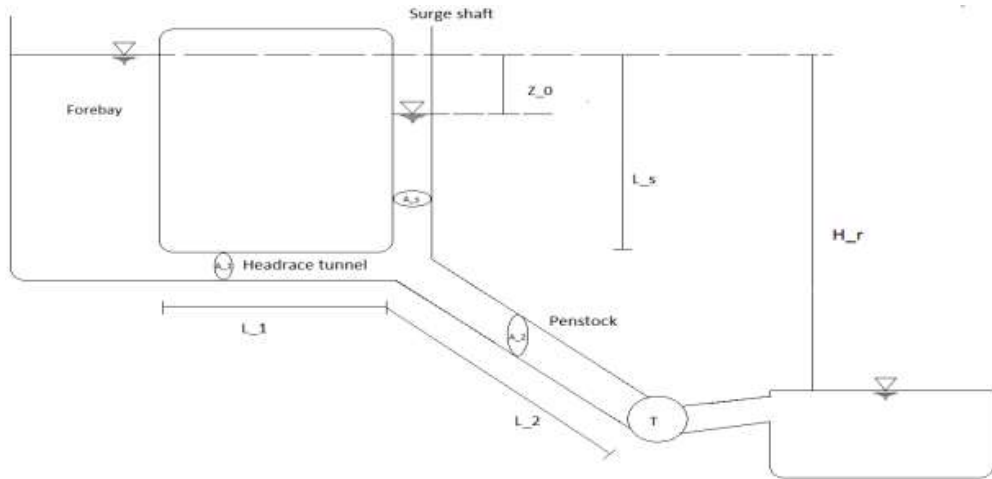


Figure 2: General block diagram for simulating power regulation in a stiff power network

## 2. System Modeling and Theory

### 2.1. Conduit system

The conduit design consists of a penstock, a surge shaft and a headrace tunnel as seen in Figure 3



**Figure 3: System layout.**

The level of  $H_r$  are considered constant in the model. The lengths  $L_1$  (2000m) and  $L_2$  (250m) are the headrace tunnel and the penstock, while  $L_s$  (25m) is the height of the surge shaft. Same subscripts accounts for areas and velocities in the model where  $A_1 = 25m^2$ ,  $A_2 = 12m^2$ ,  $A_s = 40m^2$ . System head base are 200m, rated fluid flow is set to  $50 \frac{m^3}{s}$  which gives base power at the runner 94MW. The dynamic penstock is modeled in articles such as: [2]

Basic mathematical models are derived from Newton's second law of motion, and conservation of mass law. For a fluid element inside a tube, transient flow is described as the differential equation 1.

$$\frac{\partial H}{\partial X} + \frac{1}{gA} \cdot \frac{\partial Q}{\partial t} + \frac{fQ|Q|}{2gDa^2} = 0 \quad (1)$$

See table 1.1 for parameter explanation:

**Table 1: List of parameters**

<i>Symbol</i>	<i>Description</i>
H	Water pressure [m]
X	Displacement [m]
Q	Flow rate [m <sup>3</sup> /s]
g	Gravity acceleration =9.81
A	Cross section area [m <sup>2</sup> ]
t	Time [s]
f	Friction coefficient [-]
D	Tube diameter [m]

Introducing conservation of mass law for a CV (control volume) gives the continuity equation. This takes account for water compressibility effect during transient periods, and tube elasticity:

$$\frac{\partial Q}{\partial X} + \frac{gA}{a^2} \cdot \frac{\partial H}{\partial t} = 0 \quad (2)$$

Where “a” is the velocity of the pressure wave in meters per second. After Laplace transformation, per unitizing and algebraic manipulation introducing the characteristic impedance  $Z_c$ , water starting time constant  $T_w$  and the elastic time constant  $T_e$  gives the following equation set in a matrix format:

$$\begin{bmatrix} h_U(s) \\ q_U(s) \end{bmatrix} = \begin{bmatrix} \cosh(zT_e) & -Z_c \sinh(zT_e) \\ -\frac{1}{Z_c} \sinh(zT_e) & \cosh(zT_e) \end{bmatrix} \cdot \begin{bmatrix} h_D(s) \\ q_D(s) \end{bmatrix} \quad (3)$$

This gives the classical wave solution as a transfer function, describing pressure and flowrate at each point of the conduit in a hyperbolic function:

$$\frac{h(s)}{q(s)} = -\frac{T_w}{T_e} \left(1 + \frac{fQ_0}{2DA \cdot s}\right)^{1/2} \tanh\left(\left(s^2 + s \frac{fQ_0}{2DA}\right)^{1/2} T_e\right) \quad (4)$$

This leads to the final function describing the dynamic penstock used in the simulations:

$$\frac{h(s)}{q(s)} = -\frac{T_w}{T_e} \tanh(sT_e) \quad (5)$$

For a rigid conduit without the elasticity taken account for, the transfer function is reduced to:

$$\frac{h(s)}{q(s)} = -T_w - h_f \quad (6)$$

Where  $T_w$ , is the water mass time constant given by:

$$T_w = \frac{Q_{base}}{g H_{base}} \sum \frac{L}{A} \quad (6)$$

The surge shaft is described as a change in surge shaft water level head  $Z$  over a change in the system flow  $Q$ , which are given by:

$$\frac{Z(s)}{Q(s)} = \frac{1}{T_s \cdot s} \quad (7)$$

Where  $T_s$  is the surge shaft time constant given by:

$$T_s = \frac{A_s H_0}{Q_0} \quad (8)$$

Total layout of the conduit system can be seen in Figure 4

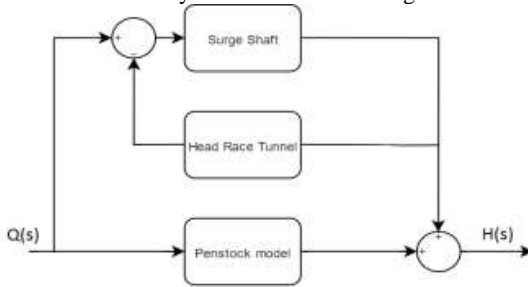


**Figure 4: Layout of the conduit system.**

## 2.2. Turbine model

The turbine model used in the simulations is referred as the linearized turbine model and can be found in literature such as: [3]. The model consists of two equation sets describing the changes in flow through the turbine,  $\Delta q$ , and the changes in momentum  $\Delta m$ .

$$\Delta q = \frac{\partial q}{\partial h} \Delta h + \frac{\partial q}{\partial n} \Delta n + \frac{\partial q}{\partial G} \Delta G \quad (9)$$

$$\Delta m = \frac{\partial m}{\partial h} \Delta h + \frac{\partial m}{\partial n} \Delta n + \frac{\partial m}{\partial G} \Delta G \quad (10)$$

Where “h” is head, “q” is flow and “G” is guide vane opening. The partial derives from now on called turbine transfer coefficients are found by different methods. Typical method is by calculations of Euler’s internal turbine equations. In the thesis modified Euler turbine equations are used, deduced by T. Nielsen at NTNU. By linearizing the equation around an operating point turbine transfer coefficients can be found.



Turbine used in the model can be seen in table 2:

**Table 2. Turbine parameters**

Parameter	Definition	Value
Qbep	Best efficiency point flow [ $\frac{m^3}{s}$ ]	50
Hbep	Best efficiency head [m]	200
Nbep	Best efficiency speed [rpm]	333.33
Tbep	Best efficiency torque [Nm]	2700694
n_bep	Efficiency at best point [-]	0.96
a1bep	Guide vane angle [°]	15
b1bep	Angle of the rotor blade [°]	67.7
r1	Inlet radius [m]	1.311
r2	Outlet radius [m]	1.146
Rq	Constant for RPT [-]	0
Rm	Angular velocity damping constant [-]	0.04
Rd	Design constant coefficient [-]	0.03
Rf	-	0.0015

This gives the following turbine transfer coefficients:

$$\frac{\partial q}{\partial h} = 2.75, \frac{\partial q}{\partial n} = -1.198, \frac{\partial q}{\partial G} = 0.86, \frac{\partial m}{\partial h} = 2.87, \frac{\partial m}{\partial n} = -1.12, \frac{\partial m}{\partial G} = 0.87$$

Block diagram describing the turbine model are given in figure 5. The conduit system are in this figure referred as: "Hydraulic system".

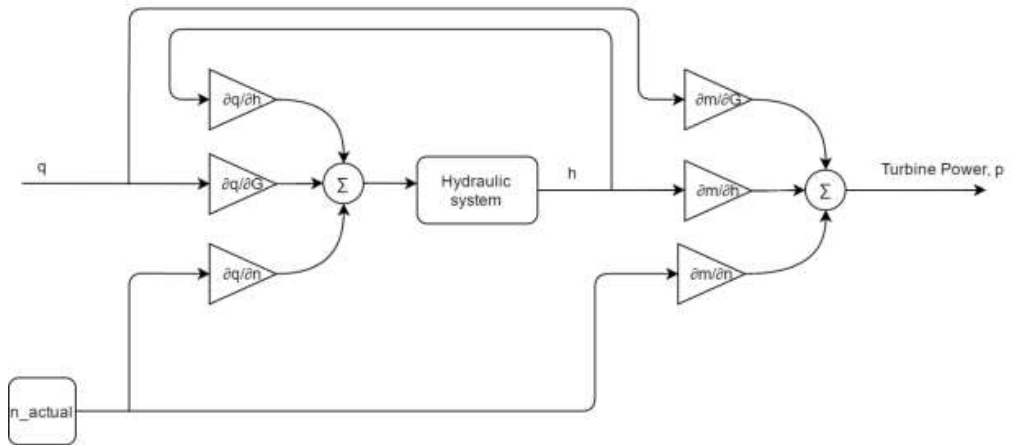


**Figure 5:** Turbine model used in the simulations

### 2.3. PID regulator

A classical PID regulator is used in the system. Equation 11 describes the regulator:

$$u = K_p \cdot \left( e + \frac{1}{T_i} \int_0^t e \cdot dt + T_d \cdot \frac{de}{dt} \right) + u_0 \quad (11)$$

Where “e” is the deviation from reference input value, and “u” is the output signal. The regulator is modeled as in figure 6.

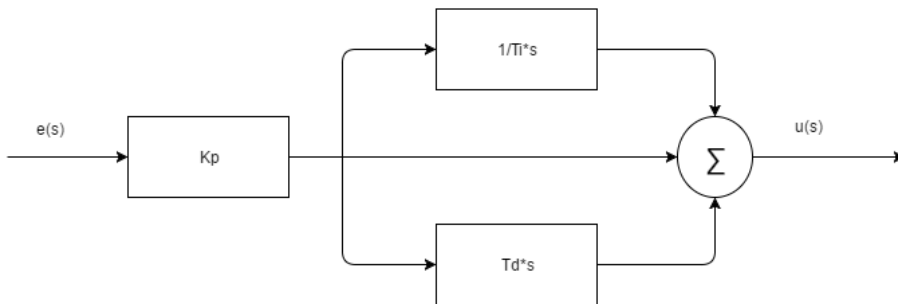


**Figure 6:** PID regulator

### 3. Results

Results from both Scilab and LVTrans are presented in this chapter. The system are modeled as similar as possible in both programs. All simulations are done with PID parameters set to:  $K_p=2.3$ ,  $T_i=8$  and  $T_d=0$ .

#### 3.1. Scilab simulations

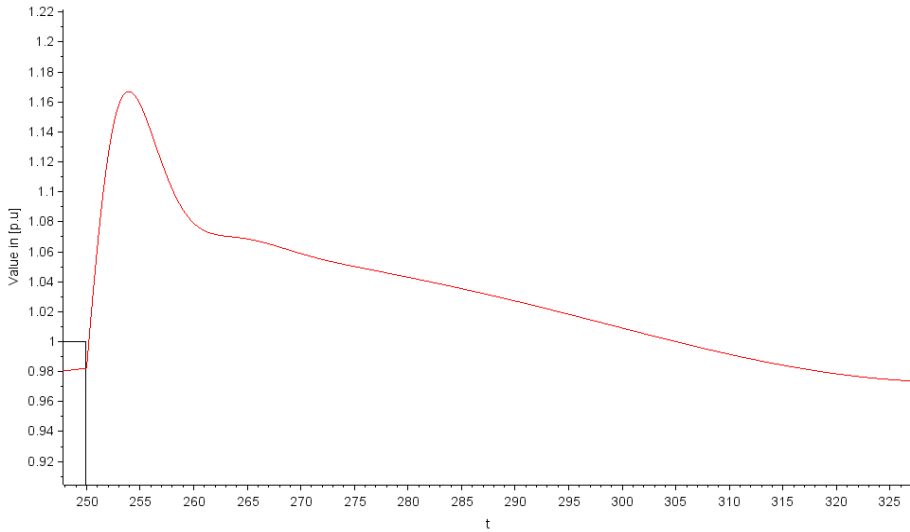


**Figure 7:** Running in island mode, simulating frequency response to a load drop of 50%.

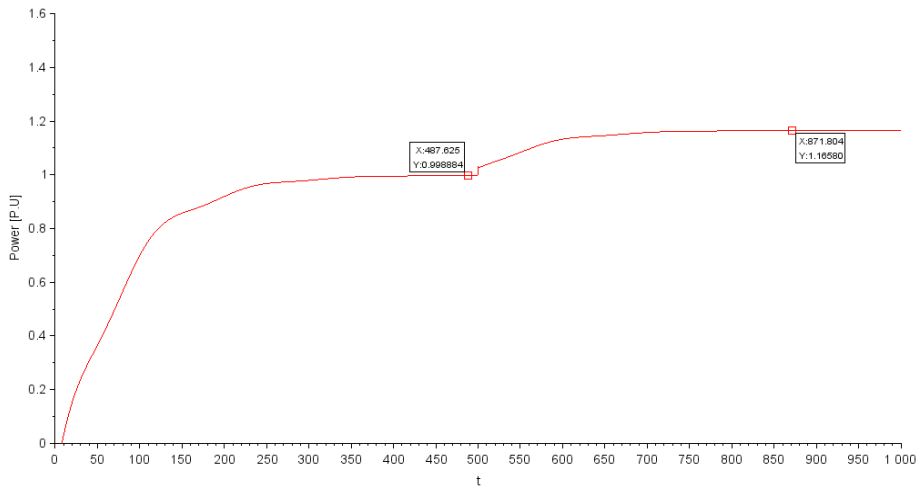


**Figure 8:** System in grid mode, with a change in grid frequency of 0.5 hz at  $t=500$ s.

### 3.2.LVTrans simulations

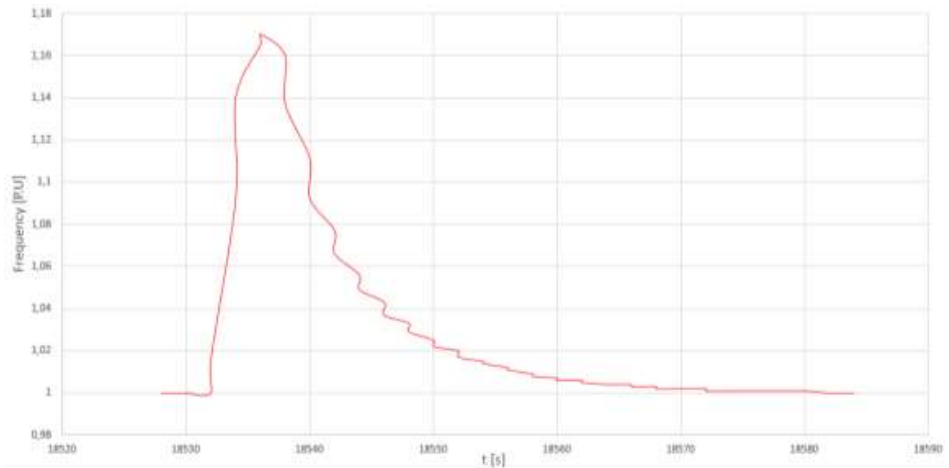


**Figure 9:** Simulation in island mode with a load drop of 50%

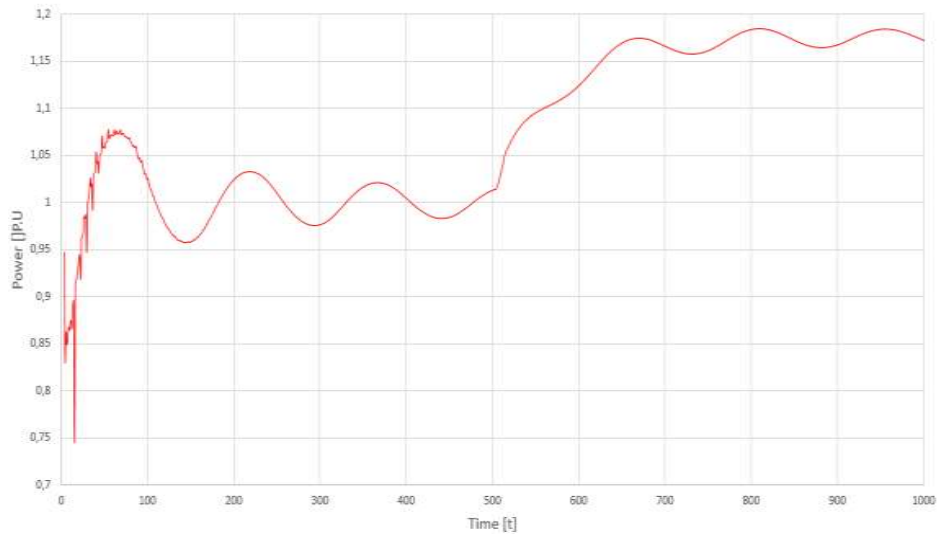


**Figure 10:** Simulation in grid mode with a drop of 0.5Hz in the grid frequency

## 4. Analysis

### 4.1. Discussion

Looking at the frequency response when the systems are running in island mode the peak value are comparable as the peak reaches 1.17 pu frequency giving a  $\Delta f = 0.17 \text{ pu}$  in both programs. This gives an increase of 8.5hz in a 50Hz base system. The dynamics of the transient effect are different comparing the two programs. Regulation in LVTrans performs more aggressive compared to Scilab, resulting in a more oscillating response. It is known that LVTrans utilizes a more advanced governing system with implemented hydraulics. This provides the system with a higher order transfer function which in this case results in a more detailed response.

The same behavior is observed in simulations in grid mode. Simulations done in LVTrans are more oscillatory but the mean values of energy production are similar. When simulating a drop in 0.5 Hz with a static droop at 0.06, gives an increase in power generation of approximately 17% which in a 94MW base system gives increase of 16MW in production.

### 4.2. Conclusion

The system modelled in Scilab gives to some degree, accuracy when performing simulations for dynamic response of frequency and power generation. The main differences in the two systems are the oscillatory effect, which can be explained by the differences in governing system. By implementing a more accurate governing and prime mover model for Scilab, this can be tested and evaluated once more, later in the master thesis process.

## 5. Future work

During the thesis, a more thorough analysis shall be performed. A modal and Bode plot analysis will be done during the spring. A more detailed model of the penstock shall also be made. By using an electrical RLC component equivalent model makes it is possible to perform realistic simulations of pressure propagation during water hammer.

Laboratory work with a u-pipe rig will be performed in near future, which will give an verification of the surge shaft model. This will be done hopefully the last days of March and hopefully some results are ready within 4.th of April .

## **References**

[1] Statnett "FIKS", 2012

[2] Working Group on prime mover and energy supply, "Hydraulic turbine and turbine control models for system dynamic studies", Transactions on power systems, Vol 7, No1, February 1992 p(167-179)

[3] Huimin. Gao, Chao. Wang, "Effect of detailed Hydro Turbine Model on Power System Analysis" PSCE 2006